Formation Evaluation of Interlava Volcaniclastic Rocks from the Faroe Islands and the Faroe-Shetland Basin

Óluva Ellingsgaard

Masters thesis in Geology at Lund University - Lithosphere and Biogeosphere Sciences, no. 255 (45 hskp/ECTS)

Geologiska institutionen
Centrum för GeoBiosfärsvetenskap
Lunds universitet
2009

Formation Evaluation of Interlava Volcaniclastic Rocks from the Faroe Islands and the Faroe-Shetland Basin

Master Thesis

Óluva Ellingsgaard

Department of Geology
Lund University
2009

Contents

Cover Picture: Volcaniclastic sandstone from the Faroe Islands.

Contents

Formation Evaluation of Interlava Volcaniclastic Rocks from the Faroe Islands and the Faroe-Shetland Basin

ÓLUVA ELLINGSGAARD

Ellingsgaard, Ó., 2009: Formation Evaluations of Interlava Volcaniclastic Rocks from the Faroe Islands and the Faroe-Shetland Basin. *Exam in Geology at Lunds University* No. 255, 78 pp. 45 ECTS points.

Abstract: Traditionally, volcaniclastic interbeds have been considered to have poor reservoir potential due to their volcanic components readily altering to various clay minerals, but published discoveries within lava successions in the Faroe-Shetland Basin may challenge this dogma. This study therefore, evaluates porosities and permeabilities for volcaniclastic interbeds from the Faroe Islands Basalt Group (FIBG), Faroe Islands.

70 volcaniclastic samples were taken from sedimentary horizons >0.2 m thick from 1 scientific, 8 geotechnical boreholes and additional field localities. 43 porosity and 30 permeability measurements were obtained from samples covering the Beinisvørð, Malinstindur, Sneis and Enni formations. The overall porosity average is 17% (range: 0.1-46.4%) and the permeability average is 0.86md (range: 0.02-6.04md).

For comparison wire-line derived porosities were obtained from the scientific Glyvursnes-1 borehole and the offshore Well 6005/15-1 located at the leading edge of the FIBG. The Glyvursnes-1 borehole was drilled to a depth of ~700 m through the basalt dominated Malinstindur and Enni Formations and encountered 23 volcaniclastic intervals ranging in thickness from ~1 cm to >5 m (average: 60 cm). Porosity and permeability measurements were obtained from 22 samples collected from the thickest intervals (i.e. > 0.4 m). These samples gave an average porosity of 18.1% (range: 9.1-46.4%) and permeability of 1.13 md (range: 0.12-6.04md).

Six volcaniclastic intervals, with measured porosity values, were selected from the Glyvursnes-1 borehole and compared to porosity values derived from the Neutron, Density and Sonic wire-line logs. The measured values for the three intervals from the Malinstindur Formation have a good correlation to the derived porosities (e.g. correlation coefficient (R^2) up to 0.85). Although the porosity values are different, the trend, or change in porosity across the interval, is replicated. The difference in R^2 for each interval is partly attributed to lithology, where the Malinstindur Formation interbeds are dominantly sandy whereas the thicker units, e.g. Argir Beds, show greater variability in grain size from clay-rich to granule-rich sections.

Well 6005/15-1 terminated at a depth of 4026 m in the Vaila Formation. The Well penetrated a number of volcaniclastic rocks containing degraded volcanic ash. These include most notably the Kettla Member but also three intervals in the underlying ~ 1241 meter thick Vaila Formation. Two of the sedimentary intervals (Section - I and - III) from the Vaila Formation have been classified as volcaniclastic sandstones by the onsite geologist while Section - II has been classified as a non-specific sandstone. From Section - II measured porosities data was available. The measured average porosity from this section was 10.1% (range: 6.0-15.0%) and has a correlation coefficient (R^2) of 0.36 when compared to wire-line derived values.

This study shows that although the volcaniclastic intervals may show low permeability properties, their measured porosity values suggest a reservoir potential for the intervals and if the volcaniclastic rocks should get mixed with siliciclastic material, which may be possible towards the edge of the lava field, this should only increase their reservoir potential.

Keywords: Faroe Islands Basalt Group, Faroe-Shetland Basin, wire-line, volcaniclastic rocks, porosity, permeability.

Óluva Ellingsgaard, Department of Geology, GeoBiosphere Science Centre, Lund University, Sölvegatan 12, SE-223 62 Lund, Sweden. E-mail: oluva.ellingsgaard@gmail.com

Formationsegenskaper hos sedimentära interbasaltiska intervall från the Faroe Island Basalt Group

ÓLUVA ELLINGSGAARD

Ellingsgaard, Ó., 2009: Formationsegenskaper hos sedimentära interbasaltiska intervall från *the Faroe Islands Basalt Group*. *Examensarbeten i geologi vid Lunds universitet*, Nr. 255, 78 sid. 45 högskolepoäng.

Sammanfattning: Traditionellt anses vulkanoklastiska interbeds ha dålig reservoarpotential på grund av de vulkaniska komponenterna, som lätt kan omvandlas till olika lermineral. Publicerade arbeten från interbasaltiska sedimentära avlagringar i Faroe-Shetlands Basin tyder dock på annat. Denna studie syftar därför till att utvärdera porositets- och permeabilitetsegenskaper hos vulkanoklastiska interbeds från Faroe Islands Basalt Group (FIBG).

70 prov togs från sedimentära vulkanoklastiska horisonter, tjockare än 0,2 m, från ett vetenskapligt och 8 geotekniska borrhål tillsammans med fältprov. 43 porositets- och 30 permeabilitetsmätningar gjordes från dessa prov, vilka kommer från fyra olika formationer: Beinisvørð, Malinstindur, Sneis och Enni. Den genomsnittsliga porositeten är 17% (spännvidd: 0,1-46.4%) och permeabiliteten har ett genomsnitt på 0,86 md (spännvidd: 0,02-6,04 md).

Som jämförelse beräknades även porositetsvärden från wire-line loggar från Glyvursnes-1 borrhålet samt från offshore borrhålet 6005/15-1, som ligger vid utkanten av FIBG. Glyvursnes-1 är ~700 m djupt och är borrat genom de två basaltdominerade formationerna Malinstindur och Enni Formation. I borrhålet fanns 23 vulkanoklastiska intervall varierande i tjocklek från ~1 cm till >5 m (genomsnitt: 60 cm). Porositets- och permeabilitetsmätningar gjordes på 22 provar tagna från de tjockaste intervallen (> 0,4 m). Dessa provar hade en genomsnittslig porositet på 18,1 % (spännvidd: 9,1-46,4%) och permeabilitet på 1.13 md (spännvidd: 0,12-6,04 md).

Sex vulkanoklastiska intervall, med uppmätta porositetsvärden, valdes från borrhålet för jämförelse med porositetsvärden beräknade från Neutron-, Densitets och Sonicloggarna. De uppmätta värdena från de tre intervallen från Malinstindur formationen hade en god korrelation med porositeten från borrhåls loggarna, där det bästa utfallet blev ett R^2 värde på 0,85. Även om porositetsvärden är olika, så är trenden eller förändringen i porositeten över intervallen representativ.

Skillnaden i R^2 värdena för varje intervall är delvis orsakad av litologien, där sedimentintervallen från Malinstindur formationen domineras av sand jämfört med några av de tjockare intervallen, som t.ex. Argir beds, som visar större variabilitet i kornstorlek.

Borrhålet 6005/15-1 är 4026 m djupt och genomborrar bl.a. Kettla Member, som uppvisar intervall med vulkanoklastiskt material, och den ~1241 m sandrika Vaila formationen. Fyra sedimentära intervall undersöktes från detta borrhål nämligen, Kettla Member och tre intervall från Vaila formationen. Två av de sedimentära intervallen (Section – I och - III) från Vaila formationen är klassificerade som vulkanoklastisk sandsten i borrhålsrapporten, medan Section - II har blivit klassificerad som en icke specificerad sandsten. Från Section - II fanns uppmätt porositets och R^2 värdet för Sectionen är 0,36.

Denna studie visar att även om de vulkanoklastiska intervallen har låg permeabilitet, så visar uppmätta porositetsvärden att intervallen kan ha goda reservoaregenskaper. I de möjliga fall där det vulkanoklastiska materialet blivit uppblandat med siliciklastiskt material, som kan förväntas i de marginella delarna av basaltfältet, så torde detta kunna ytterligare öka deras potential som reservoarbergarter.

Nyckelord: Faroe Islands Basalt Group, Faroe-Shetland Basin, vulcanoclastic sten, wire-line, porositet, permeabilitet.

Óluva Ellingsgaard, Geologiska Institutionen, Centrum för GeoBiosfärsvetenskap, Lunds Universitet, Sölvegatan 12, 223 62 Lund, Sverige. E-post: oluva.ellingsgaard@gmail.com

1 Introduction and Project Outline

Basins containing abundant volcaniclastic rocks have generally been avoided during the development of hydrocarbon exploration plays, as they are perceived to have poor reservoir potential (e.g. Luo *et al.* 2005). This has slowed the research and exploration efforts in areas affected by abundant volcaniclastic rocks (e.g. passive volcanic margins). Unlike typical siliciclastic reservoirs, volcaniclastic rocks are composed of debris (glass, minerals, etc.) that are generally more reactive and unstable which can reduce primary porosity and permeability, as they commonly have complicated textures and have the potential for rapid and extensive changes during burial-thermal diagenesis (Luo *et al.* 2005). As more unconventional oil and gas reservoirs are being discovered and developed, reservoirs composed of volcaniclastic rocks are becoming more important (Sruoga & Rubinstein 2007).

Increasing our knowledge of volcaniclastic rocks in terms of sedimentology, diagenesis, petrology, lithofacies, reservoir characteristics and petrophysical characteristics can only benefit hydrocarbon exploration. Indeed, hydrocarbon basins with volcanic reservoirs have now been discovered in many parts of the world (Luo *et al.* 2005). This study aims to characterise the reservoir potential and petrophysical properties of volcaniclastic interbeds contained within the lava flow dominated Faroe Islands Basalt Group (FIBG), NE Atlantic Ocean (Passey & Bell 2007). This area was chosen because the FIBG extends offshore into the Faroe-Shetland Basin, an area of active hydrocarbon exploration with a reported interlava discovery (Helland-Hansen 2009; Varming 2009).

This study will obtain porosity and permeability measurements, laterally and vertically, for volcaniclastic interbeds from across the FIBG on the Faroe Islands. These values will be evaluated by examining the petrographies and alteration states of the volcaniclastic rocks. The study will also obtain wire-line log derived porosity values for volcaniclastic rocks in, the onshore scientific borehole, Glyvursnes-1 and comparing the results to measured values. These results will then be used to help understand the wire-line derived

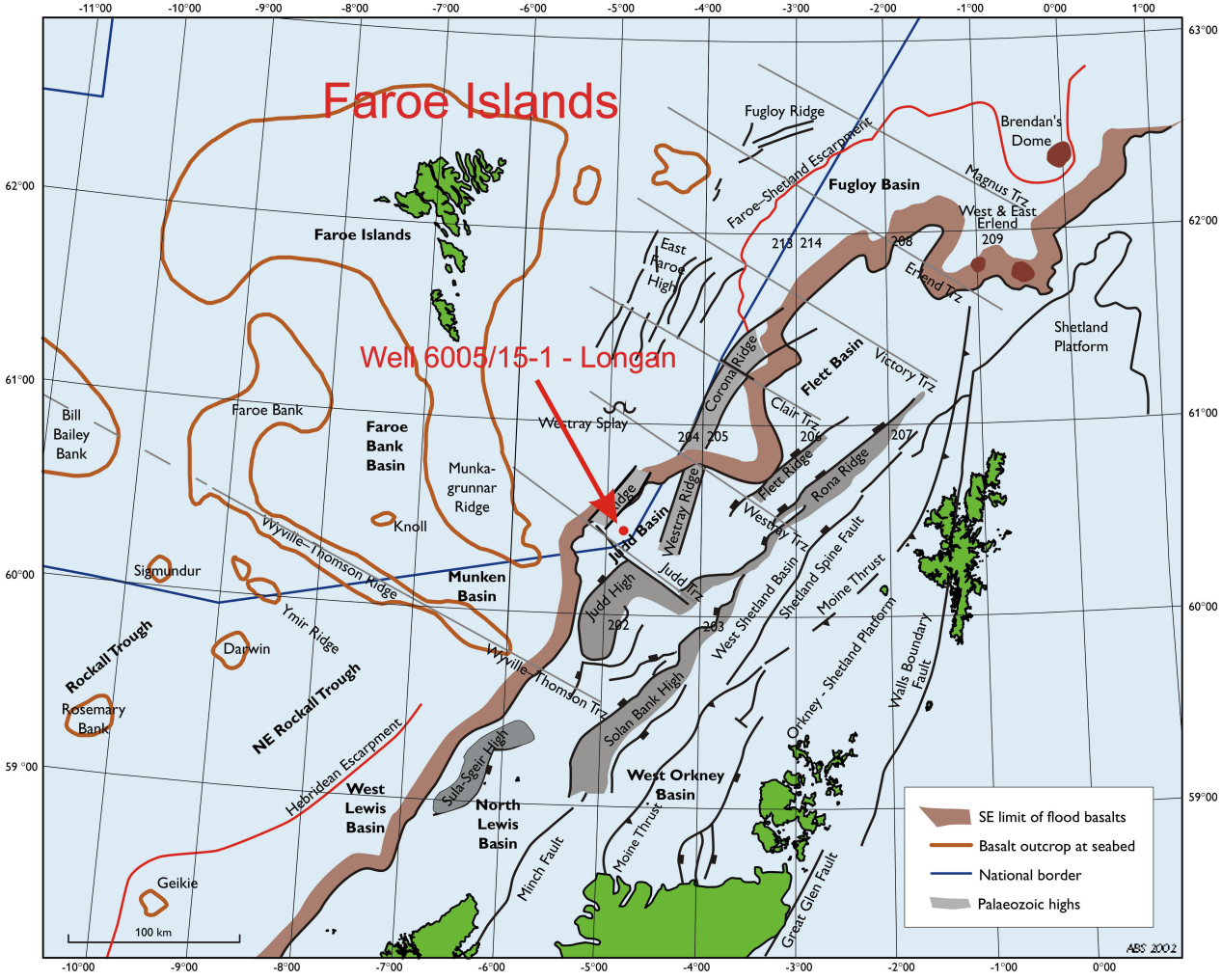

Fig. 1. Simplified geological map of the Faroe-Shetland Basin. Modified after Sørensen *et al.* 2003.

porosities from the StatoilHydro operated offshore exploration well, 6005/15-1 (Longan), drilled towards the leading edge of the FIBG lava field (Varming 2009).

1.1 Volcaniclastic Rocks

A volcaniclastic rock is a general term of a clastic rock composed of >60% volcanic debris (Shipboard Scientific Party 2002) and are classified on the basis of the dominant grain size, following the Wentworth scale (Wentworth 1922). The resulting rock name does not imply any genetic interpretation and is purely descriptive. This conforms with the original definition of Fisher (1961; 1966), subsequently reaffirmed by Fisher & Smith (1991), who stated that the term 'volcaniclastic' includes "the entire spectrum of clastic materials composed in part or entirely of volcanic fragments, formed by any particle forming mechanism (e.g. pyroclastic, hydroclastic, epiclastic and autoclastic), transported by any mechanism, deposited in any physiogenetic environment or mixed with any other volcaniclastic type or with any non-volcanic fragment types in any proportion". This descriptive scheme has previously been used by Passey (2009) for volcaniclastic interbeds from the central Faroe Islands and Passey (2004) has shown that many so-called tuffs, inferring a pyroclastic mode of emplacement, from the FIBG were re-deposited under sedimentary conditions and include fluvial and lacustrine sandstones, various mass flow deposits and palaeosols.

The volcaniclastic rocks from the Faroe Islands are typically dominated by basaltic glass at various states of alteration. Pale brown glass is typically referred to as sideromelane and is thought to have formed from rapid chilling unlike tachylyte that is generally black, but essentially opaque glass (Macdonald 1972). Sideromelane generally breaks down more quickly than tachylyte, but both produce various secondary minerals (opal, calcite, zeolites, clays) but also a reddish-brown waxy-appearing material known as palagonite (Macdonald 1972). Scoria is the basaltic equivalent of acidic pumice, characteristically highly vesicular (Macdonald 1972).

1.2 Primary and Secondary Processes in Volcaniclastic Rocks

Volcanic rocks develop both primary and secondary porosity and permeability dependent on their lithology and the formation processes they have undergone. Primary processes such as welding, deuteric crystal dissolution, gas release, flow fragmentation, and crystal shattering may lead to high porosities and permeabilities (Sruoga & Rubinstein 2007). The primary processes happen between the pre-emplacement stage and the final cooling of the volcanic rock under a closed cooling system (Scruga & Rubinstein 2007).

The alteration of volcaniclastic rocks is a secondary process that occurs during weathering, diagenesis and low-grade metamorphism which leads to mineralogical and textural changes through chemical and/or physical processes. In general, alteration typically decreases the primary porosity of the volcaniclastic rock, but certain secondary processes, such as dissolution and hydraulic fracturing, may contribute to enhance total porosity and permeability (Sruoga & Rubinstein 2007). The development of secondary porosity and permeability has been observed in volcaniclastic rocks from the Serie Tobífera unit in the Austral Basin and the Precuyano unit in the Neuquén Basin, Argentina (Sruoga *et al.* 2004; Sruoga & Rubinstein 2007).

To review the quality of volcaniclastic rocks as potential oil and gas reservoirs is achieved by identifying the different lithological types, their components and the sequence of primary and secondary processes they have undergone (Sruoga & Rubinstein 2007).

1.3 Geological Setting

The Faroe-Shetland Basin (Fig. 1) is a rift basin along the NE Atlantic margin and has a very complex geological evolution (Doré *et al.* 1999). The margin has several different phases of structural evolution, and from these, three can be seen as most important. The first event was the Caledonian orogeny in the Silurian which was followed by erosion and later extensional collapse of the mountains during the late Palaeozoic (Doré *et al.* 1999). The second was a Mesozoic-Early Cenozoic rift phase which resulted in the deposition of thick Middle Jurassic-Palaeocene sediments. The third event was the opening of the North Atlantic Ocean characterised by the eruption of vast volumes of basalt lava flows that was followed by renewed subsidence and sedimentary deposition during the Eocene (Saunders *et al.* 1997; Doré *et al.* 1999; Ritchie *et al.* 1999; Sørensen 2003). After this, three compressional phases followed in the Eocene, Oligocene and Miocene that all caused major inversion in the area (Andersen & Boldreel 1995; Sørensen 2003).

The Caledonian orogeny extends from the northern Norway south-westwards through Scotland

into southern Ireland, but also exists on the other side of the Atlantic where the east and northeast Greenland mountains are of the same Caledonian age (Doré *et al.* 1999). This orogeny was succeeded by a rifting phase in the Devonian-Carboniferous. The Palaeozoic sediments in the Faroese subsurface may partly be derived from source areas in Greenland (Sørensen 2003).

Rifting took place during late Cretaceous-Palaeocene times, prior to the final continental break-up in the Early Eocene (Saunders *et al.* 1997; Doré *et al.* 1999; Sørensen 2003). The final break-up was associated with intense volcanic activity resulting in the predominantly subaerial lava flows of East Greenland and the Faroe Islands, now separated by the Mid-Atlantic rift. Prior to the beginning of ocean floor spreading, which resulted in the opening of the NE Atlantic, the Faroe Islands and Greenland were only approximately 120 km apart. This is based upon plate reconstructions and likely geochemical correlations between the originally adjacent sequences (Saunders *et al.* 1997; Larsen *et al.* 1999). The lava flows on the eastside of the rift are known as the Faroe Islands Basalt Group (FIBG) and are Palaeogene in age (Waagstein 1988; Larsen *et al.* 1999; Passey & Bell 2007). Volcanism culminated with the eruption of vast quantities of tephra that have subsequently been reworked and are now contained in the Balder Formation which signals the onset of seafloor spreading at ~54 Ma in the Eocene (Saunders *et al.* 1997).

1.4 Faroe Island Basalt Group

A remnant of the Faroe Islands Basalt Group (FIBG) is exposed on the Faroe Islands that are located ~280 km NW of Scotland and ~400 km SE of Iceland in the NE Atlantic Ocean (Fig. 1). The islands cover an area of ~1400 km^2 and extend over a distance of ~115 km N-S by ~75 km E-W. The archipelago comprises 18 islands, where most of them are elongated in a NW-SE trend and are separated by long narrow fjords. The landscape of the Faroe Islands was sculpted by glacial action during the Quaternary Sub-period. The islands and its insular shelf (to water depths of ~150—200m) form the Faroe Platform, which has a roughly triangular shape (Fig. 1).

In the vicinity of the archipelago, the FIBG has a gross stratigraphic thickness of at least 6.6 km and is dominated by subaerial (tholeiitic basalt) lava flows (Passey & Bell 2007). The stratigraphy is subdivided into seven formations (Fig. 2) based primarily on lithology but also on geochemistry (Rasmussen & Noe-Nygaard 1969; 1970; Waagstein 1988; Passey & Bell 2007). The oldest formation is not exposed on the islands and has only been encountered in the onshore borehole, Lopra-1/1A drilled on Suðuroy to the south of the islands (Waagstein 2006; Passey & Bell 2007). The Lopra Formation is ~1.1 km thick and is dominated by a variety of volcaniclastic rocks, mainly hyaloclastites that have been intruded/invaded by sills/lava flows (Waagstein 2006; Passey & Bell 2007). The Lopra Formation is overlain by the Beinisvørð Formation that is ~3300 m (<1000 m exposed on the islands) and consists mostly of thick, laterally extensive, aphyric sheet lobes (Passey & Bell 2007). Towards the top of the Beinisvørð Formation the lava flows are commonly intercalated with volcaniclastic rocks deposited in fluvial, lacustrine and swamp environments (Passey 2004; Passey & Bell 2007). There are however, abundant saprolitic boles (weathered tops) suggesting that chemical weathering of the lava flows and volcaniclastic units must have been intense, and this could possible be associated to the warmer and wetter climate attributed to the Palaeocene-Eocene Thermal Maximum (Ellis *et al.* 2002).

The Beinisvørð Formation is overlain by the 3-15 m thick Prestfjall Formation consisting of coal, volcaniclastic mudstone, sandstone and conglomerates of swamp, lacustrine and fluvial association typical of an inter-eruption period (Lund 1983; 1989; Ellis 2002; Passey 2004). This formation represents a significant pause in the volcanic activity. The Prestfjall Formation is locally overlain by the Hvannhagi Formation composed of interbedded basaltic tuffs and volcaniclastic sedimentary lithologies deposited from high discharge debris and hyperconcentrated flow processes (Passey 2004; 2009; Passey & Bell 2007). These mass flow deposits, most likely, formed during periods of high rainfall when large amounts of pyroclastic debris covered pre-existing fluvial systems (Passey 2004; 2009).

Volcanism resumed with the emplacement of the Malinstindur Formation that is up to ~1350 m thick and is dominated by compound flows which evolve from olivine-phyric to plagioclase-phyric basalt up sequence (Noe-Nygaard & Rasmussen 1968; Rasmussen & Noe-Nygaard 1969; 1970; Waagstein 1988; Passey & Bell 2007). There is a scarcity of volcaniclastic interbeds in the Malinstindur Formation until approximately two-thirds above the base of the formation where the laterally extensive Kvívík Beds crop out (Passey 2009). The Kvívík Beds are typically a

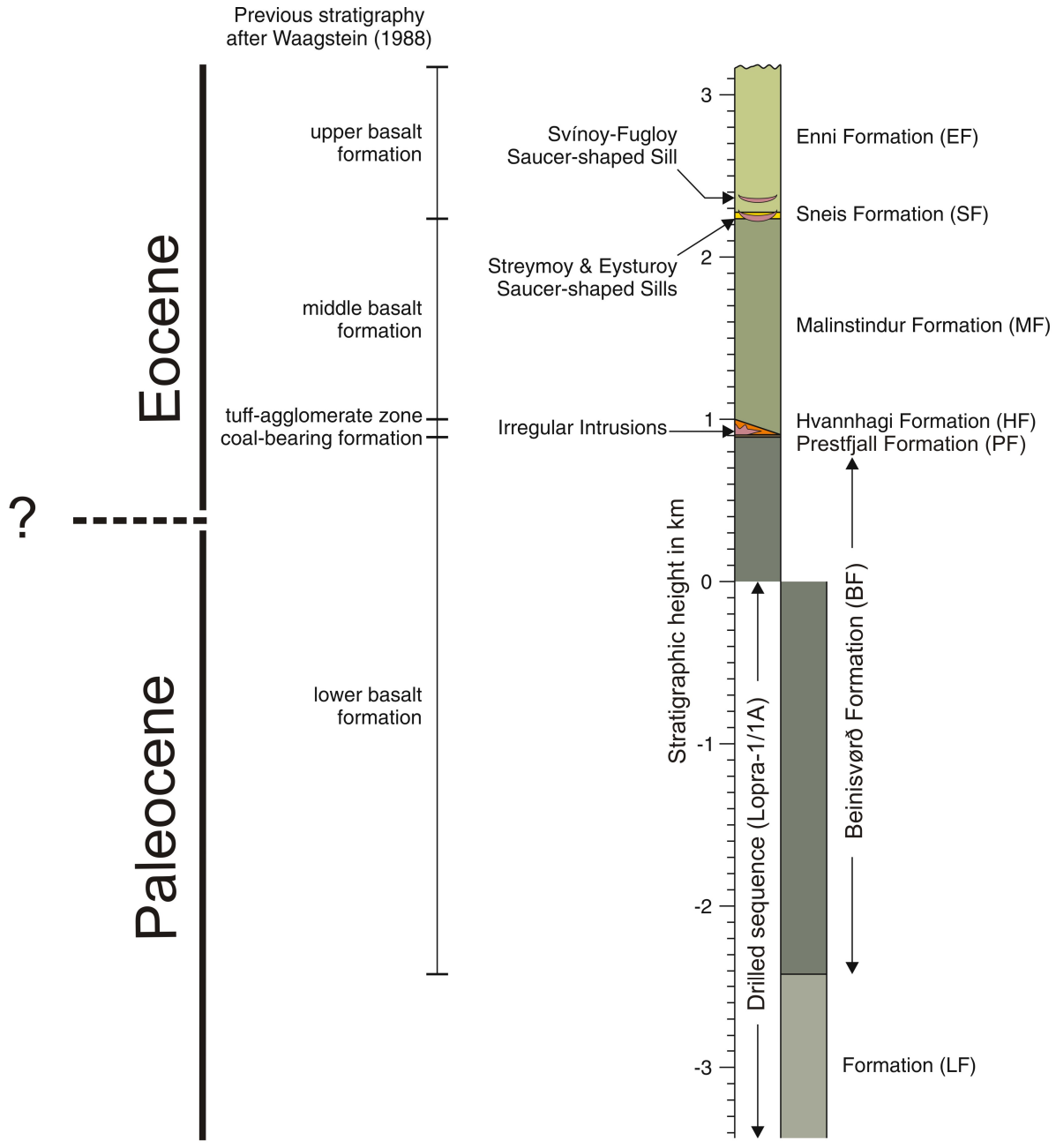

(chronostratigraphy is based on palynology after Passey & Jolley (2009

Fig. 2. The Faroese stratigraphy (Passey and Bell 2007).

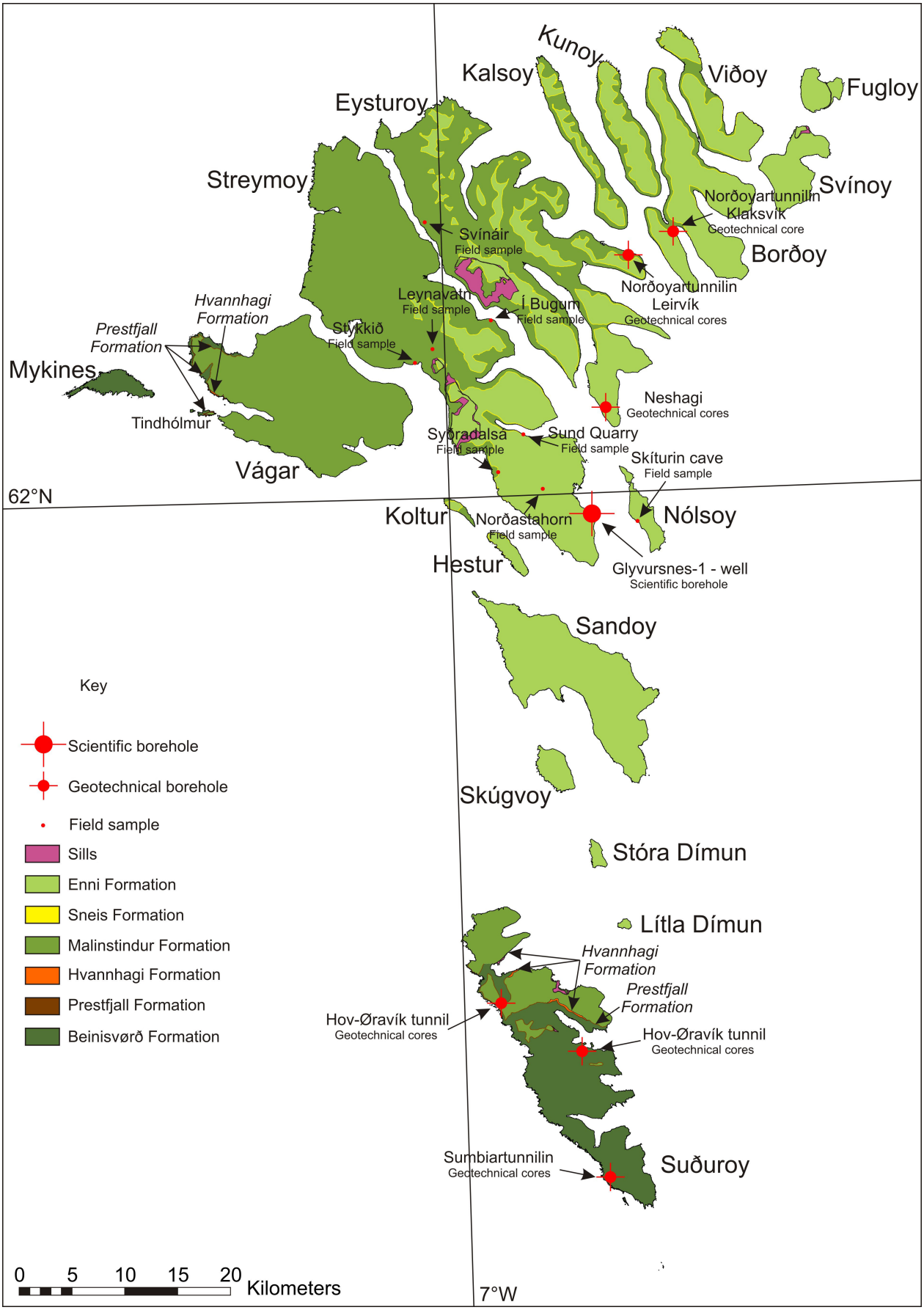

Fig. 3. Simplified geological map of the Faroe Islands showing the onshore sample locations. Modified after Passey and Bell 2007.

few metres thick and consist of bedded volcaniclastic sandstones. Volcaniclastic interbeds become much more common between the Kvívík Beds and the top of the Malinstindur Formation and consist of thin volcaniclastic sandstones composed of a variety of reworked basaltic glass at different stages of alteration (Passey 2009).

The emplacement of the Malinstindur Formation is followed by a second volcanic hiatus represented by the, albeit, thinner Sneis Formation. The Sneis Formation consists of two distinct facies; a northern, conglomerate-facies and a southern, sandstone-facies (Passey 2009). The conglomerate-facies that is up to 30 m thick consists of a basal volcaniclastic sandstone, the Sund Bed, which is overlain by volcaniclastic conglomerates, which were, most likely, deposited from hyperconcentrated and debris flow processes (Passey 2009). This contrasts with the sandstone-facies that is up to 2 m thick and consists of laminated sandstones deposited at the leading edge of the mass flow conglomerate-facies (Passey 2009).

Volcanism resumed once again with the emplacement of more lava flows of the Enni Formation. However, unlike the Beinisvørð and Malinstindur formations that comprise dominantly one morphological type, the Enni Formation consists of a mixture of interbedded sheet lobes and compound lava flows (Passey & Bell 2007). The formation is at least 900 m thick, although a few hundred metres have been estimated to have been removed through erosion (Waagstein 1988). Volcaniclastic interbeds are common in the Enni Formation due to the waning of volcanic activity and ~250 m above the base of the formation the distinctive and widespread Argir Beds crop out (Passey 2009). The Argir Beds are a <1-6 m thick bedded volcaniclastic sequence deposited in a complex fluvial-floodplain environment (Passey 2009).

The FIBG extends offshore for at least 200 km into the Faroe-Shetland Basin (Fig. 1), where the lava flows have been correlated to the Late Palaeocene

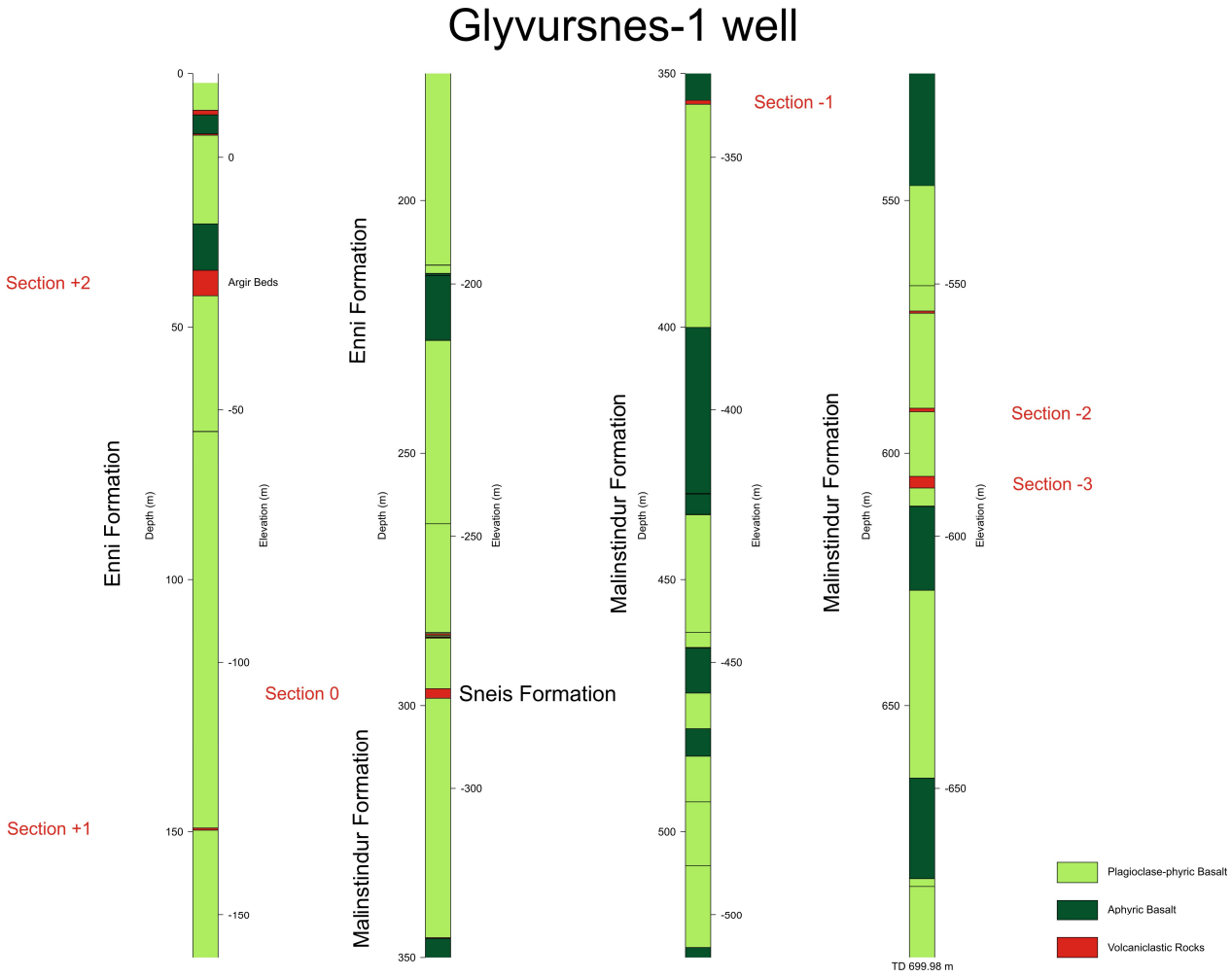

Fig. 4. A simplified lithology log from the Glyvursnes-1 well. The six investigated Sections are named relative to the Sneis Formations (Modified after Waagstein & Andersen 2003).

Flett Formation sandstones and mudstones (Ellis *et al.* 2002). Two lava flows at the leading edge of the FIBG lava field have been penetrated within the ~406 m thick Flett Formation in Well 6005/15-1 (Varming 2009) (Fig. 1). The borehole terminated at a depth of 4026 m in the Mid Palaeocene, ~1241 m thick, sand-prone Vaila Formation that has been intruded by a series of dolerite sills (Varming 2009). The Vaila Formation is overlain by the ~300 m thick mud-dominated Lamba Formation, which at the base consists of the ~36 m thick Kettla Member (Varming 2009). The Kettla Member is widespread across the Faroe-Shetland Basin and contains degraded volcanic ash with volcanogenic lithoclasts and is considered a reworked volcaniclastic rock (Jolley *et al.* 2005). The Kettla Member is thickest in the Flett Sub-Basin and thinner and often more reworked in the Judd Sub-Basin, where Well 6005/15-1 was drilled (Sørensen 2003).

2 Methodology

2.1 Measured Porosity and Permeability Analysis

2.1.1 Samples

The majority of the volcaniclastic samples analysed in this study were collected from boreholes drilled on the Faroe Islands, but additional samples were collected in the field (Fig. 3 and Appendix I). A total of 51 samples were collected from the onshore boreholes that include the deep scientific borehole Glyvursnes-1 and from 8 geotechnical boreholes (Sumbiartunnulin 1985-2, Sumbiartunnulin 1989-1, Norðoyartunnulin 2001-1, Norðoyartunnulin 2001-3, KOBH1-04 2004-1, Hov-Øravík tunnulin 2004-8, Neshagi 2005-1 and Neshagi 2005-2) that are commonly drilled in connection with tunnel building projects.

The Glyvursnes-1 borehole was drilled in 2002 as part of the SeiFaBa (Seismic and petrophysical properties of Faroes Basalt) project (Japsen *et al.* 2005). The well is located to the south of the village of Argir on the island of Streymoy and had a drill core thickness of ~700 m. The borehole penetrated the upper 400 m of the Malinstindur Formation, the ~1.8 m thick sandstone-facies of the Sneis Formation and ~300 m of the lower Enni Formation, including the ~5 m thick Argir Beds (Japsen *et al.* 2005; Passey 2009) (Fig.4). The remaining geotechnical boreholes have cores from the Beinisvørð, Prestfjall, Malinstindur and Enni formations and the only formations not sampled in this study are the Lopra and Hvannhagi formations (Fig. 2).

Samples were only collected from the boreholes if the volcaniclastic intervals had a thickness >0.2 m. The samples collected from the boreholes are all orientated perpendicular to bedding and those collected from the Glyvursnes-1 borehole had a diameter of ~25.3 mm, which contrasts to those from the geotechnical boreholes that had diameters ranging from ~40.9 mm to ~41.6 mm. The lengths of the samples were approximately 30 mm.

For later comparison between measured and derived wire-line porosities the six volcaniclastic intervals sampled from the Glyvurnes-1 borehole (Fig. 4) are numbered relative to the Sneis Formation. The Sneis Formation is therefore, referred to as Section 0 and the 3 intervals from the Malinstindur Formation are referred to, with increasing depth, as Sections -1, -2 and -3, respectively. Similarly the two intervals sampled from the Enni Formation are referred to, with increasing height, as Sections +1 and +2. Section +2 is the Argir Beds interval.

A total of 19 field samples were collected from 8 different locations that span the Malinstindur, Sneis and Enni formations (Fig. 3 and Appendix I). All the samples were collected parallel to bedding accept one sample from the Sund quarry and all had a diameter of ~37.5 mm. Four samples were collected from the Kvívík Beds at Stykkið, Streymoy and Svínáir, Eysturoy. Additional samples were collected from the upper Malinstindur Formation between the Kvívík Beds and the Sneis Formation from í Búgum and Leynavatn on Streymoy. Field samples representing the Sneis Formation on Streymoy were collected from the Sund Quarry (Sund Bed - base of conglomerate facies) and in Syðradalsá, Syðradalur (sandstone-facies). Samples from the Enni Formation were collected from the Argir Beds at Norðastahorn, Streymoy. The last field samples were collected from Skíturin on Nólsoy from above the Argir Beds in the upper part of the Enni Formation.

2.1.2 Sample Preparation

For further analysis of the samples, which had varying sizes, had to be modified to fit the Jones Porosimeter-Permeameter (see Section 2.1.3) which was built to handle sizes of 1" (25.4 mm) diameter samples up to 2" (50.8 mm) long and 1½" (38.1 mm) diameter samples up to 3" (76.2 mm) long. Due to the variability in lithology, alteration, consolidation states and clay con-

Well 6005/15-1 - Longan

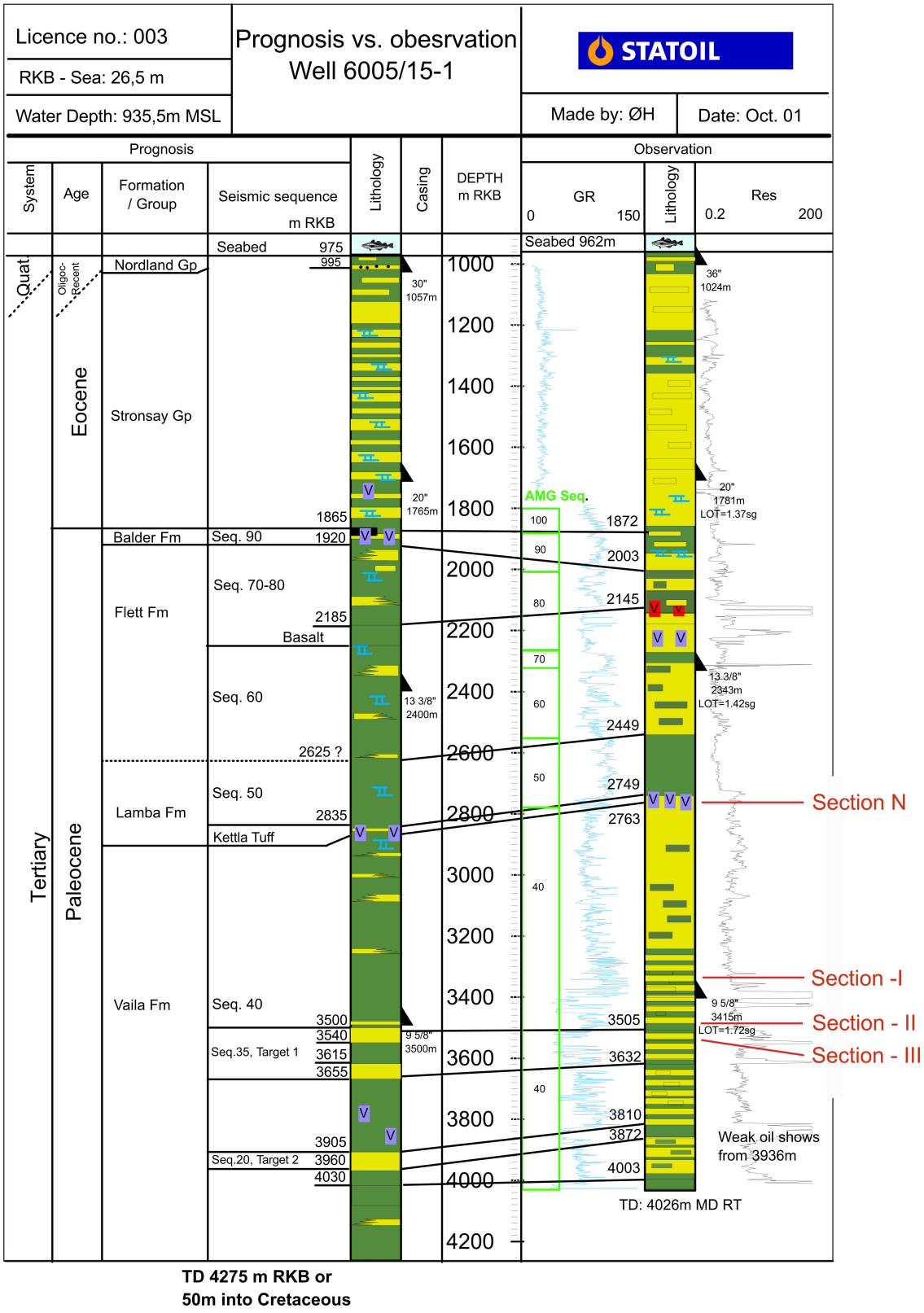

Fig. 5. Lithology log from Well 6005/15-1 - Longan with location of the four investigated Sections.

tent of the samples it was difficult to prepare the samples for further analysis. As a consequence some samples began to disintegrate and became unsuitable for analysis, but measurements from 43 samples were obtained. Out of the 43 samples, 22 samples had diameters of 25.4 mm that fitted the 25.4 cup holder, 9 samples had diameters of 37.1 mm that were able to fit the 38.1 mm cup holder, although for these samples there was a gap of ~1 mm between the sample and the edge of the cup which had to be taken into consideration (see Section 2.1.3.). The remaining 13 samples with diameters of 41.0 mm could be measured in the 38.1 mm cup holder when the sleeve was removed. The initial samples had varying lengths and therefore, billets were used to completely fill the cup holders and Table 1 outlines the specifications of these billets.

Ideally, the polished sections produced for the samples would have subsequently been impregnated with a fluorescent dye to obtain additional porosity values (e.g. Gees 1966), but due to the generally poor consolidation states of the samples they had to be saturated and hardened up to three or four times with epoxy during cutting and therefore, no additional porosities were obtained.

2.1.3 Jones Porosimeter-Permeameter

Porosity and permeability measurements have been obtained from the petrophysical laboratory at the Department of Geology and Petroleum Geology at the University of Aberdeen, Scotland. To obtain the porosity the Jones porosimeter was used and to obtain permeability both the Jones permeameter as well as a portable permeameter were used.

Table 1. Information on the billets.

	1" coreholder			
Billet	Length		Volume	Name
	(Inches)	(cm)	(cm^3)	
a	0.25	0.635	3.204	V_a
b	0.25*	0.635	3.206	V_b
c	0.50	1.270	6.418	V_c
d	1.00	2.540	12.849	V_d
1.5" coreholder				
Billet	Length		Volume	Name
	(Inches)	(cm)	(cm^3)	
a	0.25	0.635	7.359	V_a
b	0.25*	0.635	7.389	V_b
c	0.50	1.270	14.8	V_c
d	1.00	2.540	29.647	V_d
e	1.00*	2.540	29.659	V_e
sleeve			11.661	V_s

The combined porosimeter and permeameter is an instrument that has both a Coberly-Stevens Boyle's Law porosimeter and a gas permeameter situated on the same panel. The instruments operate independently.

The Coberly-Stevens porosimeter is operated by admitting helium at 100 psig (pound-force per square inch gauge) into a reference section and, by means of highly accurate digital electronic pressure gauge, reading the pressure, releasing the gas into the sample cup, followed by the reading of the resulting lower pressure. The porosity for the sample is expressed as a percentage. Due to irregularities in the core samples not fitting perfectly in the cup holders it was necessary to apply a mean loss in grain volume for all samples. This meant that samples with a diameter of 25.4 mm required a mean loss in grain volume of 5%, those samples with a diameter of 37.1 mm required a mean loss in grain volume of 1% and lastly, those samples with a diameter of 41 mm required a mean loss in grain volume of 3%.

The permeameter is equipped to regulate and measure upstream pressures over a range of 1" (25.4 mm) Meriam Unity Oil (specific gravity = 1) to 60 psig, and measure flow rates from about 0.00001 ml/sec to 3.5 ml/sec to permit very accurate measurement of permeability from about 0.1 micro-Darcys to about 2500 milli-Darcys (md). In the Jones permeameter nitrogen is used. A free standing, rugged, rapid-access Hassler sleeve core holder that is connected to the permeameter through ports on one end of the cabinet, is used and the measurements are perpendicular to bedding (Jones Porosimeter-Permeameter Instructional Manual 1995).

The portable permeameter is not as reliable as the Jones permeameter because the portable tool needs a flat surface on to which the gas injection probe is applied. Any irregularities in the surface can give higher permeabilities than the true value. The gas used in the portable permeameter is also nitrogen and the tool was used on samples that did not fit into the free standing Hassler sleeve core holder on the Jones permeameter. The results are deemed unreliable and therefore, excluded from further discussion, but for completeness the permeability values obtained from the portable permeameter are presented in Appendix IV.

2.2 Wire-line Derived Porosity Analysis

2.2.1 Wire-line Log Data

To obtain wire-line derived porosities for volcaniclastic intervals this study had access to two boreholes: Glyvursnes-1 and Well 6005/15-1 (Longan). The following wire-line logs were used from both boreholes: Caliper; Density; Gamma Ray; Neutron, Resistivity and Sonic logs. The Glyvursnes-1 borehole had two sonic compressional velocity logs: a standard log (LogTek I) and a pseudo borehole compensated log (LogTek II).

The depths for the wire-line log data from Glyvursnes-1 were measured from 16.48 m asl, whereas the corresponding lithology log was measured from 16.56 m asl. Therefore, there was a discrepancy of 8 cm between the wire-line logs and the lithology log and this had to be accounted for. The wire-line log values were measured every 10 cm and therefore, did not necessarily correspond exactly to a sample locality (see Section 2.1.1 and Appendix I). For comparison between the sample localities and wire-line logs measurements the nearest wire-line log measurement to the sample locality was used. If the sample locality was in the middle between two wire-line measurements, both wire-line log measurements were used as a comparison to the sample locality. In Well 6005/15-1 the wire-line logs have a shift of one meter deeper to the depth relative to the rotary table. Also not all the wire-line log data were measured at the same depth interval. The Caliper and Sonic logs do not have the same measuring interval as the Gamma Ray, Neutron and Density logs. It is important to obtain values from the same level for comparison and for use in the Schlumberger equations (see Section 2.2.2). Therefore, the values nearest to the desired depth were used for comparison and this generally meant discrepancies of a few centimetres in the worst cases.

Four Sections identified on the composite log for Well 6005/15-1 as containing volcaniclastic material have been investigated (Fig. 5). These include the ~36 m thick Kettla Member from the base of the Lamba Formation and will in this study be referred to as Section N. The three additional intervals are found in the underlying Vaila Formation and are referred to, with increasing depth, as Sections -I, -II and –III and are 11 m, 11.5 m and 11 m thick, respectively. Sections – I and – III have been classified as volcaniclastic sandstones by the onsite geologist but Section – II is classified as a non-specific sandstone, but is included because it has measured values for comparison.

2.2.2 Schlumberger Equations

When evaluating siliciclastic reservoirs encountered in exploration wells it is possible to apply the equations of Schlumberger (Schlumberger 1972) using wire-line log data and this study attempts to apply these equations to volcaniclastic intervals. To obtain the poros-

Table 2. The Schlumberger equations used in the porosity calculations.

	Neutron log	**Density log**	**Sonic logs**
Porosity (%)	From cross plot Chart 1979 (Schlumberger)	$\Phi = \rho_{ma}-\rho_b/\rho_{ma}-\rho_f$	$\Phi = \Delta t-\Delta t_{ma}/\Delta t_f-\Delta t_{ma}$
Volume of shale from the Gamma Ray log	$V_{sh} = 1-(PGR/GR_{max})$	$V_{sh} = 1-(PGR/GR_{max})$	$V_{sh} = 1-(PGR/GR_{max})$
Volume of shale from the Neutron log	$V_{sh}=Øn/Øn_{sh}$	$V_{sh}=Øn/Øn_{sh}$	$V_{sh}=Øn/Øn_{sh}$
Volume of shale from the Resistivity log	$V_{sh}=(R_{sh}/Rt)*1/2$	$V_{sh}=(R_{sh}/Rt)*1/2$	$V_{sh}=(R_{sh}/Rt)*1/2$
Shale correction	$\Phi_{Ncorr}=\Phi_N-V_{sh}*\Phi_{Nsh}$	$\Phi_{Dcorr}=\Phi_D-V_{sh}*\Phi_{Dsh}$	$\Phi_{Scorr}=\Phi_S-V_{sh}*\Phi_{Ssh}$
Equations used for the mineral determination plot (the M-N Plot)			
$M = (\Delta t_f-\Delta t/\rho_b-\rho_f*0.003)$		$N = ((N_\phi)_f-\phi_N/\rho_b-\rho_f)$	

M-N Plots - Glyvursnes-1 well

Malinstindur formation, Sneis Formation and Enni formation

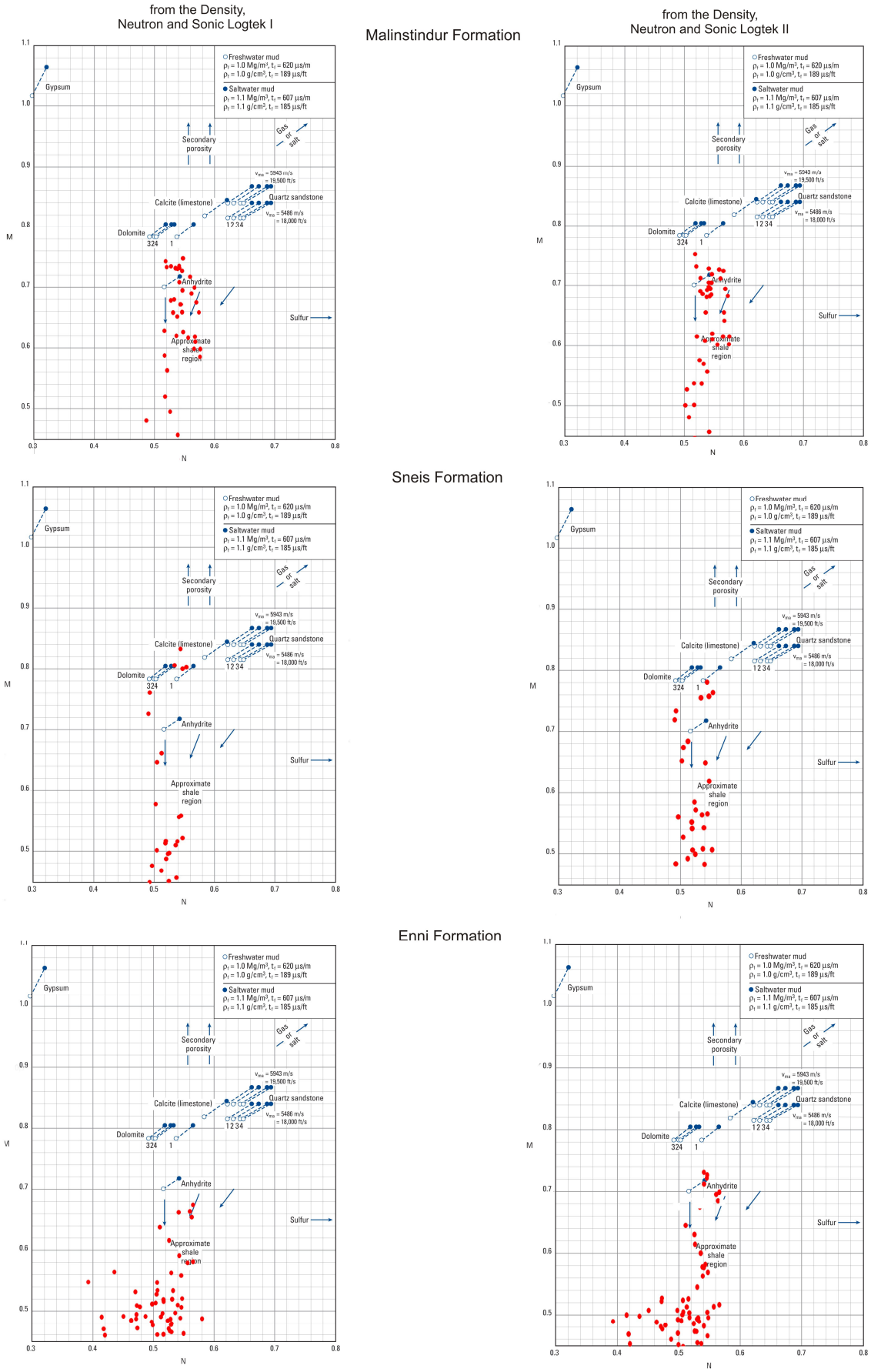

Fig. 6. M-N Plots from the Malinstindur, Sneis and Enni formations from the Glyvursnes-1 well. The three plots to the left are based on Sonic log LogTek I, and the three plots on the right are based on Sonic log LogTek II. The plots show if a Section is in the shaliness region or not.

M-N Plots - Well 6005/15-1 - Longan

Section N, -I, -II & -III

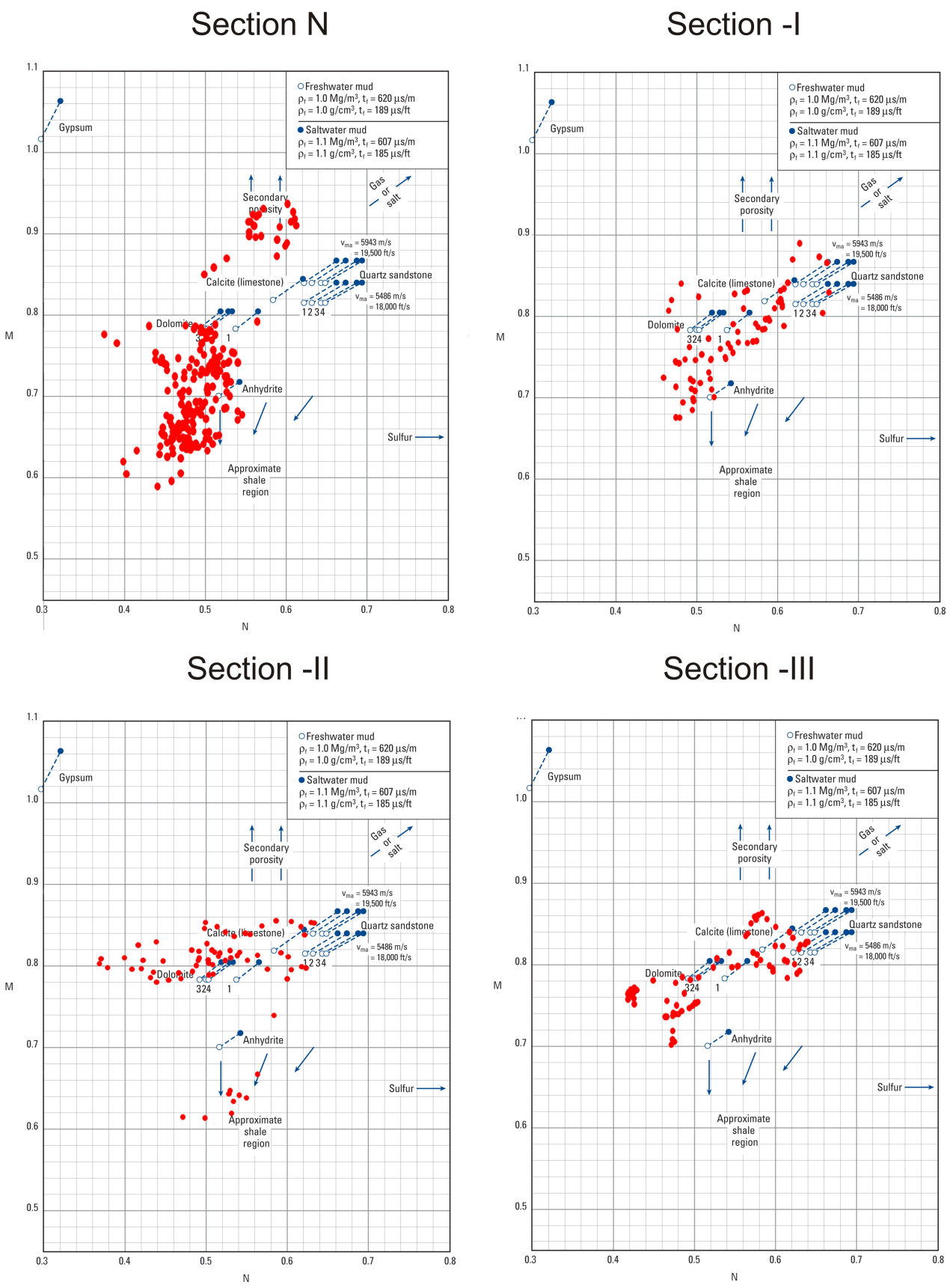

Fig 7. M-N Plots from all four Sections from Well 6005/15-1 - Longan. The plots show if a Section is in the shaliness region or not.

ities from the wire-line log data the, easily applied, equations presented in Table 2 were utilised. The equations used in this study are suitable for siliciclastic sandstones (ideal reservoir lithologies), but as no equations have been developed for volcaniclastic sandstones the usefulness of these equations are evaluated.
As the equations are lithology dependent the Schlumberger equations and cross-plots include empirical values that have been derived from different lithologies (limestone, quartz sandstone, etc.) and are therefore, principally only reliable for these specific lithologies. The equations are suitable for sandstones, but many are not pure and will contain varying amounts of clay. To determine whether and how much a sandstone is affected by clay (shale) the M-N plot (a mineral determination plot to see whether or not the Section investigated occurs in the shale region) can be used (Figs. 6 & 7). If the sandstone is affected by high volumes of shale this can be compensated for by using the, aptly named, shale correction equations. If however, the sandstones are defined as mud-rich then the reliability of these shale correction equations becomes questionable.

To apply a shale correction to the initially derived porosities it is important to determine the volume of shale (V_{sh}) in the interval studied. Different V_{sh} values can be obtained using the different wire-line logs: the Gamma Ray; the Neutron and the Resistivity logs and the equations used to obtain the different V_{sh} values can be seen in Table 2. From the different V_{sh} values obtained it is always the lowest value that is used in further equations.

The reason the different V_{sh} values are calculated is due to the different wire-line logs being more reliable in different lithologies. When using the Gamma Ray log in the shale corrections it is the highest Gamma Ray (GR_{max}) value across the specific interval that is used irrespective of detailed lithological characterisation of the interval. This is in contrast to when the Neutron and Resistivity logs are used because a mud-layer has to be identified across the interval from which the values are taken from the aforementioned logs. As these values are dependent on an exact correlation between the lithology log and the wire-line logs they are not as reliable as using the GR_{max} from the Gamma Ray log. This is particularly evident for the Glyvursnes-1 cores that have been in storage since the borehole was drilled in 2002 and during this time the cores have moved in the core boxes and to obtain a precise position of any mud layers for comparison on the wire-line logs is problematic. Therefore, the V_{sh} has consistently been determined by indentifying the GR_{max} from the Gamma Ray log for all Sections. Where a mud layer can be confidently correlated, however, the Neutron and Resistivity logs were used in addition.

Additional problems arise where wash outs have occurred in the drilling of the boreholes. The wash outs can be identified from the Caliper log and in the Glyvursnes-1 borehole can actually be observed in the core. In regions affected by wash outs the Neutron and Density logs become unreliable, but here the Sonic log is more reliable.

In order to derive the porosity (Φ) from the Neutron log, the Neutron log values and the Density log values are used in a cross plot (Schlumberger 1979). This has to be done in order to correlate for the lithology of the investigated formation, which in this study will be sandstone. When the porosity is derived from the Density and the Sonic logs the log values, ρ_b (the bulk density) and Δt (bulk transit time), respectively, are used in two porosity equations, one for the Density log and one for the Neutron log, and they are presented in Table 2. The density of the matrix (ρ_{ma}) and the transit time of the matrix material (Δt_{ma}) are empirically derived lithology dependent values, and are in this study 2.65 g/cm^3 and 182 µm/s, respectively, for sandstone. Because the investigated Sections – I and – III from Well 6005/15-1 span over more than the sedimentary section the ρ_{ma} (density of the matrix) needs to change from 2.65 g/cm^2 (sandstone) to 3.00g/cm^2 (basalt) at the lowest ~2 m of Section – I and at the top 5 m and the lowest 2.5 m of Section –III. The density of the fluid (ρ_f) and the transit time of the fluid (Δt_f) are empirically derived values dependent on the fluid in the formation. In this study the values used are 1.1 g/cm^3 and 607 µm/s, respectively, which are the values for salty mud. In the volume of shale calculations based on the Gamma Ray log values from the Gamma Ray are needed. The GR_{max} is the highest value the Gamma Ray logs shows for the investigated formation and indicates the "shale point" in the specific formation. The point values from the Gamma Ray log (PGR) for every level porosity will be calculated and is also needed in the equation. In the two volume of shale equations, one from the Neutron log and one from the Density log, the $Øn_{sh}$ and the R_{sh} values are needed and these are the values read from the Neutron log and the Resistivity log, respectively, in a mud-layer ("shale point"). The Øn and

the Rt values are read from the Neutron log and the Resistivity log for every point the porosity is calculated. To obtain the shale corrected porosity values from the three logs, the Neutron, Density and Sonic logs (Table 2) the V_{sh} that gives the lowest values is used together with the $\Phi_{Nsh,}$ the Φ_{Dsh} and the $\Phi_{Ssh,}$ which are the derived porosity values from the "shale point", the $GR_{max,}$ respectively the mud-layer (dependent on from which equation the V_{sh} used has been derived). In addition the $\Phi_{N,}$ the $\Phi_{D \text{ and the }} \Phi_S$ (the porosity values for all three logs before the shale correction) are used.

The equations used in the M-N Plot (see Section 2.2.2) are presented below in Table 2 and the plots are presented in Figure 6 & 7. For the Plot three values from three logs for every measured level in the Section will be used. The bulk density is read from the Density log (ρ_b), the Neutron log porosity is read from the Neutron log (ϕ_N) and the transit time is read from the Sonic log (Δt). N_ϕ is 1(100%) while ρ_f and the Δt_f are the fluid dependent values which in this study are 1.1 g/cm^3 and 607 µm/s for salty mud. In addition a constant of 0.003 is used in the M calculations.

3. Measured Porosity and Permeability Values

3.1 Faroe Islands Basalt Group

Seventy volcaniclastic rock samples have been collected from the Faroe Islands (Appendix I). It has not been possible, due to difficulties outlined in Section 2.1.2, to get porosities and permeability measurements from all 70 samples, but a total of 43 porosity and 30 permeability values were obtained using the Jones porosimeter-permeameter (Appendix II & III) in addition to 12 permeabilities using the portable permeameter (Appendix IV). From the seven formations that make up the FIBG on the archipelago, porosity and permeability values were obtained from the Beinisvørð, Malinstindur, Sneis and Enni formations. The lithology, petrography, porosities and permeabilities for each of the aforementioned formations will be described below from oldest to youngest, but initially the results will be presented for all the samples collected from the entire FIBG.

Table 3 presents the minimum, maximum, average and geometric mean porosity and permeability values for all the samples analysed. The average porosity and permeability for all samples from the FIBG is 17% and 0.86 md, respectively. Porosity and permeably values versus depth relative to the Malinstindur-Sneis Unconformity (MSU), base of the Sneis Formation, are presented in Figures 8a and 8b, respectively and Figure 8c presents porosity versus permeability values.

Table 3. Measured porosity and permeability values from the Faroes Islands - all samples.

	Porosity (%)	Permeability (md)
Minimum	0.1	0.02
Maximum	46.3	6.04
Average	17.0	0.86
Geometric mean	13.6	0.26
Number of samples	43	30

3.2 Beinisvørð Formation

The samples representing the Beinisvørð Formation (BF) were collected from six sedimentary Sections that range in thickness from ~0.2 m to ~3.5 m. The Sections are mainly reddish or greyish brown and vary in grain size from mudstone to fine-grained sandstone. The sections typically contain large rounded cobbles of weathered basalt derived from the underlying lava flows, suggesting that they are corestones and that the units represent saprolitic boles (i.e. palaeosols) similar to units previously described by Passey & Bell (2007). All the samples have therefore, been classified as volcaniclastic mudstones, except sample OEG-050308-G-38 that is a volcaniclastic conglomerate. At the microscopic scale the mudstones contain reddish black material too fine to be indentified. The material is, most likely, highly altered volcanic glass consisting of secondary clays, zeolites and palagonite. Locally, laths of plagioclase feldspar can be seen, but these are also

Table 4. Measured porosity from the Beinisvørð Formation.

	Porosity (%)
Minimum	6.0
Maximum	8.6
Average	7.3
Geometric mean	7.2
Number of samples	2

Porosity (%) versus depth

Faroe Islands

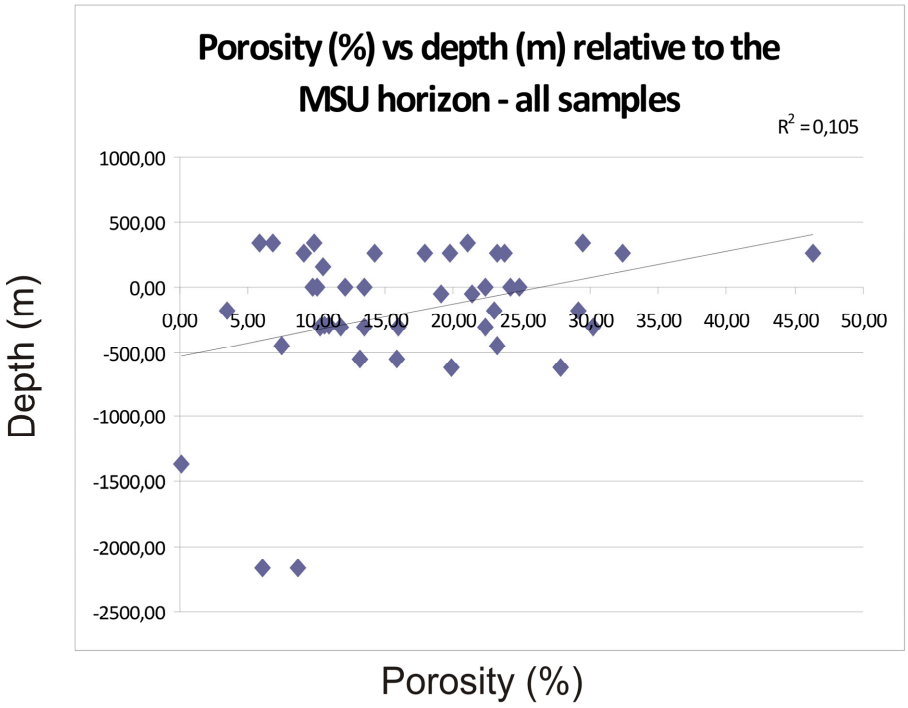

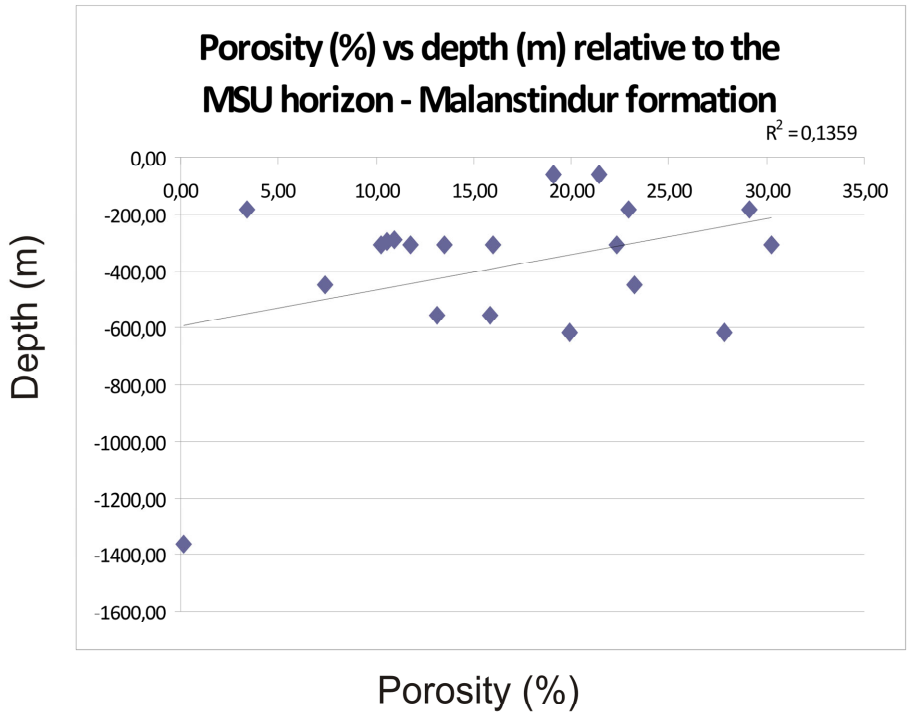

Fig. 8a. Porosity (%) versus depth (m) relative to the Malinstindur-Sneis Unconformity. Upper graph for all samples and the lower graph for Malinstindur Formation only.

Permeability (md) versus depth

Faroe Islands

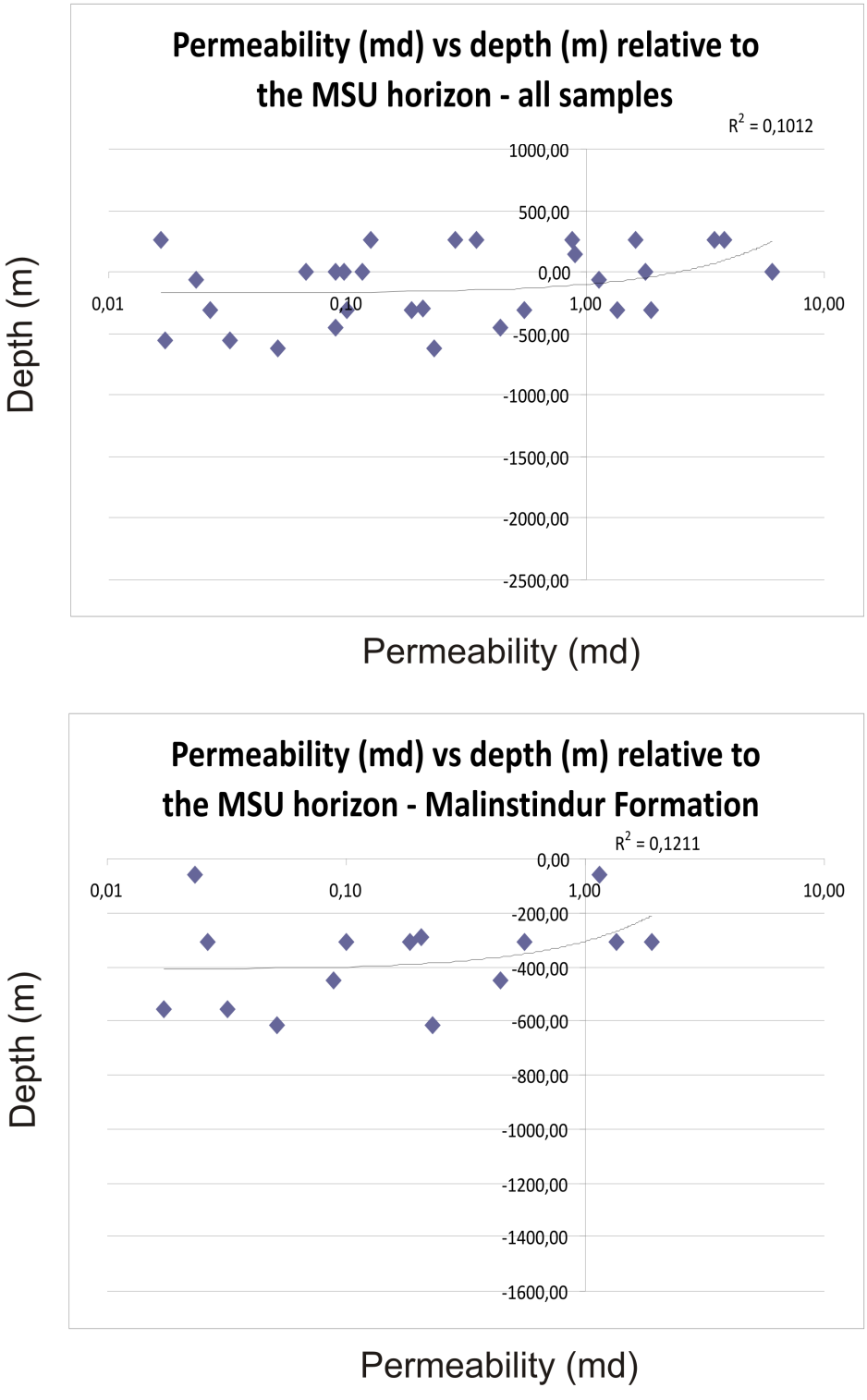

Fig. 8b. Permeability (md) versus depth (m) relative to the Malinstindur-Sneis Unconformity. Upper graph for all samples and the lower graph for Malinstindur Formation only.

Fig. 8c Porosity (%) versus permeability (md) based on all samples.

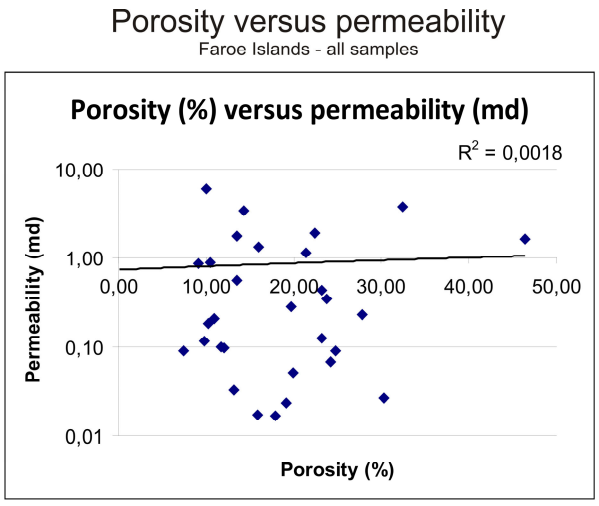

highly altered. The mudstones are typically cut by fractures that have been subsequently infilled by secondary minerals.

Due to the highly altered state of the mudstones the samples from the BF were extremely difficult to prepare for porosity and permeability analysis and out of 10 samples, only 2 porosity values were obtained for the mudstones. Negative porosity and permeability values were obtained for the conglomerate sample, OEG-050308-G-38, and consequently, is excluded from all figures and subsequent discussions. Table 4 presents the minimum, maximum, average, and geometric mean porosity and permeability values for the BF. The average porosity value for the BF mudstones is 7.3%, but as mentioned, is only based on two samples.

3.3 Malinstindur Formation

A total of 23 samples were collected from nine sedimentary Sections from the Malinstindur Formation (MF). The Sections range in thickness between ~0.65 m and ~2.3 m and vary in colour between greenish red to brownish red. In general, the units collected are fine- to coarse-grained sandstones, although some units contain granules of basalt lava. The sandstones locally contain thin (centimetre scale) mud streaks and layers. Although, the samples have been collected from different sedimentary Sections they typically have a similar petrography. The sandstones are dominated by typically rounded reworked basaltic glass at various stages of alteration. The glass varies from tachylyte to more vesicular scoria, but pale brown sideromelane is also present. (Fig. 9a-b) The glass is rarely porphyritic containing plagioclase feldspar, olivine or pyroxene phenocrysts. The glass has begun to break down to various secondary minerals, including clays, zeolites and palagonite. Locally, fractures and pore spaces (including vesicles) have been infilled by secondary minerals (Figs. 9c).

From the 23 samples collected, 20 porosity and 15 permeability measurements were obtained. Although the samples analysed are dominantly sandstones, many of the Sections also contained mud-rich layers (see Section 2.1.2). Table 5 presents the minimum, maximum, average, and geometric mean porosity and permeability values for the MF. The average porosity and permeability values for the MF samples are 16.5% and 0.42 md, respectively. It can also be mentioned that two samples analysed from the Kvívík Beds gave an average porosity of 14.5% and permeability of 0.03 md (Table 6).

Table 5. Measured porosity and permeability from the Malindstindur Formation.

	Porosity (%)	Permeability (md)
Minimum	0.1	0.02
Maximum	30.3	1.89
Average	16.5	0.42
Geometric mean	12.1	0.16
Number of samples	20	15

Table 6. Measured porosity and permeability from the Kvívíks beds.

	Porosity (%)	Permeability (md)
Minimum		0.02
Maximum	15.8	0.03
Average	14.5	0.025
Geometric mean	14.4	0.023
Number of samples	2	2

3.4 Sneis Formation

As mentioned previously, the Sneis Formation (SF) is a laterally extensive volcaniclastic sequence that can

Examples of the polished sections

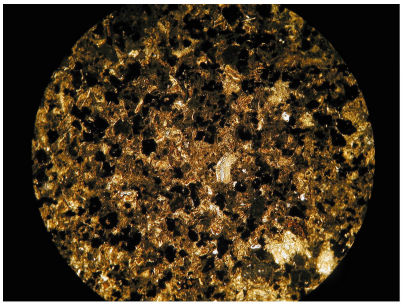

a) G-03 (MF) in plane polarized light. Sidermelande, tachylyte and vesicular scoria.

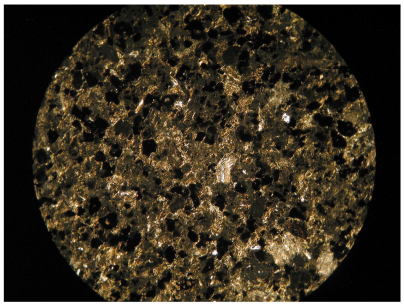

b) G-03 (MF) in cross polarized light. Sidermelande, tachylyte and vesicular scoria.

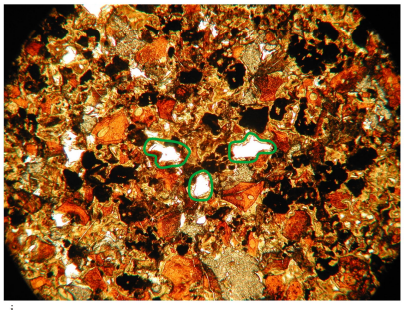

i

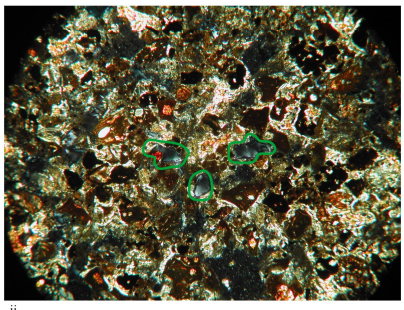

ii

c) G-08 (MF) in plane (i) and cross (ii) polorized light. Examples of secondary infilled quartz in pores.

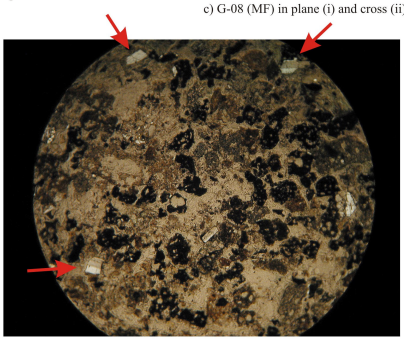

a) G- 66 (SF), in cross polarized light. Phenocrysts of plagiclase feldspar.

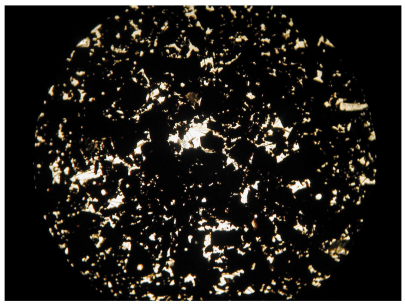

e) G- 31 (SF), in plane polarized light.The sample is almost entiraly black and opaque.

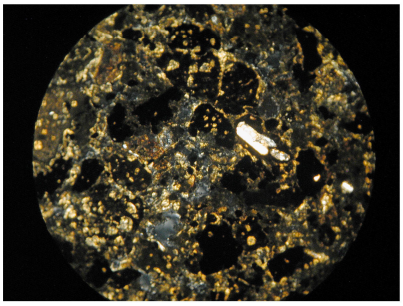

f) G-12 (SF) in cross polarized light. Infilled pores by e.g. secondary quartz.

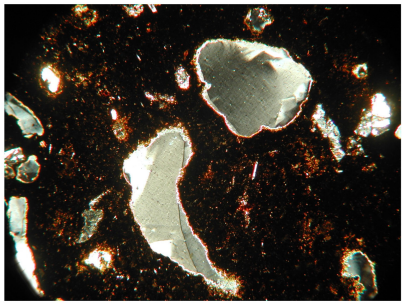

g) G-68 (EF) in cross polarized light. Secondary infilled quartz.

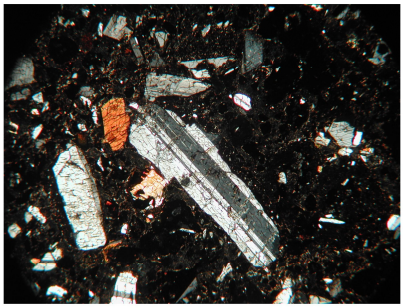

h) G-25 (EF - Argir beds) in cross polarized light. Large plagioclase.

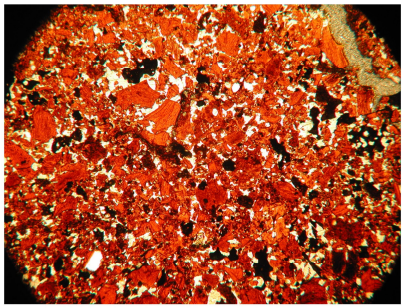

i) G-16 (EF), in plane polarized light. Example of high content of glass.

Scale:

0.5 1.0 mm

Fig. 9. Examples of polished sections from Beinisvørð, Malinstindur, Sneis and Enni formations.

be subdivided into a northern conglomerate-facies and a southern sandstone-facies. The conglomerate-facies consists of a basal sandstone unit, the Sund Bed that is overlain by conglomerates up to 25-30 m thick, whereas the sandstone-facies is exclusively composed of sandstones. Samples were only collected from the Sund Bed and the sandstone-facies. A total of 10 samples were collected from four Sections that ranged in thickness from ~0.5 m to ~1.9 m. The Sections vary in colour from greenish to reddish brown (the Sund Bed is predominantly reddish brown). The units are fine- to coarse-grained sandstones and commonly poorly sorted. The sandstones collected from the sandstone-facies are locally mud-rich at the base that coarsens upwards.

Similar to the units from the MF the SF samples are dominated by rounded reworked basaltic glass at various stages of alteration. The samples are composed of pale brown sideromelane, but tachylyte and scoria are also common. Frequently, the volcanic glass contains phenocrysts of plagioclase feldspar (Fig. 9d) and more rarely olivine and pyroxene. Sample OEG-050308-G-31 is composed almost entirely of black, near opaque tachylyte (Fig. 9e). As mentioned, the glass in all samples has begun to breakdown to various clay minerals, zeolites and palagonite. Fractures and pore spaces (including vesicles) are locally infilled with secondary minerals, including quartz (Fig. 9f), while sample OEG-060308-G-60 does not exhibit the same degree of secondary mineralisation and alteration and porosity is clearly preserved. Table 7 presents the minimum, maximum, average, and geometric mean porosity and permeability values for the SF. The average porosity and permeability values for the SF samples are 16.7% and 1.37 md, respectively.

Table 7. Measured porosity and permeability from the Sneis Formations.

	Porosity (%)	Permeability (md)
Minimum	9.7	0.07
Maximum	24.8	6.04
Average	16.7	1.37
Geometric mean	15.5	0.30
Number of samples	7	6

3.5 Enni Formation

The six sedimentary Sections, including the Argir Beds in two different localities, analysed from the Enni Formation (EF) range in thickness from ~0.4 m to >5 m. The colour of the Sections varies from yellowish green to green to reddish brown (where oxidised). The Sections, particularly the thickest ones, are heterolithic consisting of both volcaniclastic mudstones and sandstones and can be considered more mud-rich than the analysed Sections from the underlying Sneis and Malinstindur formations. The sandstones are typically fine- to coarse-grained, although locally granule-rich units can be found. Similar to the volcaniclastic sandstones from other formations they dominantly contain reworked basaltic glass at various stages of alteration (clays, zeolites and palagonite), some samples show clear secondary infilling by quartz as seen in OEG-250607-G-68 (Fig. 9g). The samples contain sideromelane, tachylyte and scoria in various proportions and sizes. The glass fragments frequently contain phenocrysts of plagioclase feldspar and more rarely olivine and pyroxene. Some samples, e.g. OEG-040308-G-25, contain conspicuous, sub-rounded, laths of plagioclase feldspar up to >3 mm long that do not appear to be contained within a glass or lava selvage

Table 8. Measured porosity and permeability from the Enni Formation.

	Porosity (%)	Permeability (md)
Minimum	9.1	0.12
Maximum	46.4	6.04
Average	18.1	1.13
Geometric mean	16.4	0.40
Number of samples	22	22

Table 9. Measured porosity and permeability from the Argir beds.

	Porosity (%)	Permeability (md)
Minimum	9.1	0.02
Maximum	46.4	3.80
Average	23.3	1.31
Geometric mean	21.0	0.50
Number of samples	9	9

(Fig. 9h). It is unclear if these crystals are derived from the erosion of lava flows, liberated from volcanic glass, or directly from a volcanic eruption or transported from outside the volcanic environment. Some of the samples from the EF still contain large amounts of unaltered glass as e.g. sample OEG-030408-G-16 (Fig. 9i). A total of 27 samples were collected, from which, 14 porosity and 9 permeability measurements were obtained. Table 8 presents the minimum, maximum, average, and geometric mean porosity and permeability values for the EF and the average porosity and permeability values are 19.3% and 1.27 md, respectively. It can also be mentioned that 14 samples were collected from the Argir Beds, where 9 were analysed and gave an average porosity of 23.4% and permeability of 1.31 md (Table 9).

4 Wire-line Derived Porosity Values

4.1 Glyvursnes-1

4.1.1 Measured Porosity Values

Six sedimentary Sections from the Malinstindur, Sneis and Enni formations were selected from the Glyvursnes-1 borehole (Fig. 4), to compare measured porosity values with those derived from the wire-line log data. The six Sections in the borehole are labelled relative to the Sneis Formation, which forms Section 0 (see Section 2.1.1) (Fig. 10). A total of 28 samples were collected, but only 22 porosity and permeability measurements were obtained, due to difficulties preparing the samples (see Section 2.1.1). Table 10 presents the minimum, maximum, average, and geometric mean porosity and permeability values for the samples analysed from the borehole and the average porosity and permeability values are 18.1% and 1.13 md, respectively. A brief description of the six Sections is given below for later comparison with the wire-line derived porosities. Lithology logs from the six sedimentary Sections together with a selection of polished sections are presented in Figures 11a-c.

Table 10. Porosity and permeability from the Gyvursnes-1 well.

	Porosity (%)	Permeability (md)
Minimum	5.8	0.02
Maximum	46.4	3.80
Average	19.3	1.27
Geometric mean	16.3	0.53
Number of samples	14	9

4.1.1.1 Malinstindur Formation

Section -3 is the deepest investigated Section from the Malinstindur Formation and is a 2.3 m thick bedded volcaniclastic sandstone unit. The Section has two small (<20 cm thick) missing intervals, most likely, due to wash outs. The units are green, brown to brownish red, medium- to coarse-grained sandstones that do not contain any noticeable mudstone layers. Some of the sandstones show apparent fining upwards. At the bottom of the Section the sandstones contain conspicuous basalt lava clasts up to 16 cm in size (Fig. 11a). The Section has an average porosity of 17.4%, but ranges from 10.3% to 30.3% based on six samples.

Section -2 is 0.67 m thick and is composed of brownish volcaniclastic sandstones varying from fine- to coarse-grained. The Section fines upwards and locally, plant fragments are found (Fig. 11a). From the Section two samples were taken but only one porosity measurement of 10.9% was obtained.

Section -1 is a 0.79 m thick volcaniclastic sequence that goes from reddish brown at the bottom to brown at the top. It is also composed of fine- to coarse-grained volcaniclastic sandstones and fines upwards (Fig. 11a). Two samples were taken and measured and had an average porosity of 20.3%.

The average porosity for all three Sections is 17.3%, ranging from 10.3% to 30.3%.

4.1.1.2 Sneis Formation

The Sneis Formation, Section 0, is a 1.9 m thick volcaniclastic sandstone sequence that varies form greenish brown at the bottom to brownish red at the top. The sandstones are mainly fine-grained but become coarse-grained towards the top of the sequence where a thin (<2 cm thick) mudstone layer is observed (Fig. 11b). From the Section four samples were taken and measured and they had an average porosity of 11.4%, ranging from 9.7% to 13.5%.

4.1.1.3 Enni Formation

Section +1 from the Enni Formation is a 0.43 m thick fining upwards volcaniclastic sandstone sequence that

All logs from the Glyvursnes-1 core
Overview of sections

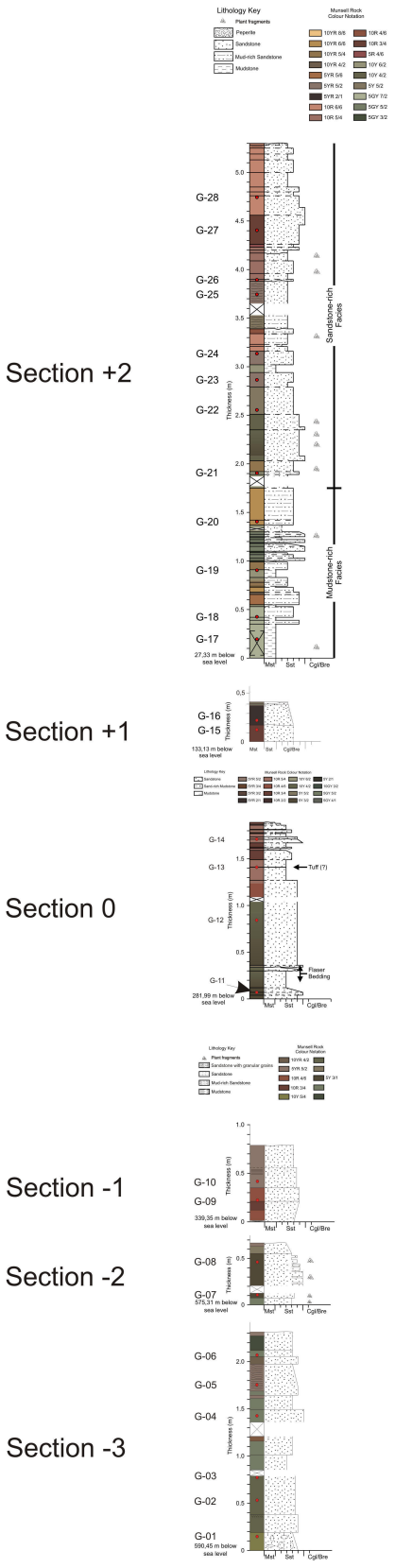

Fig 10. Overview of the six investigated Sections from the Glyvursnes-1 borehole.

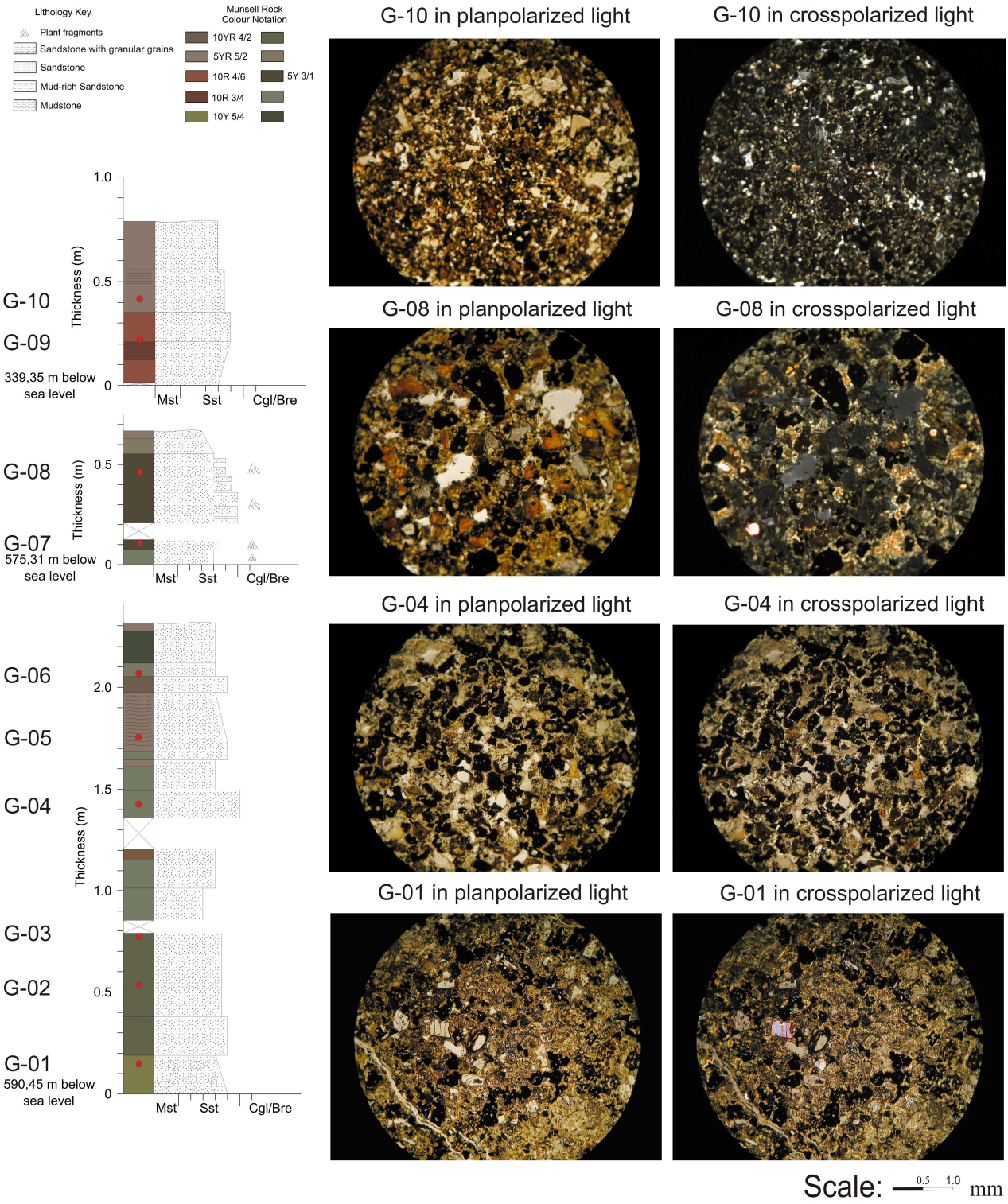

Fig 11a. A selection of polished sections from the Malinstindur Formation in the Glyvursnes-1 borehole.

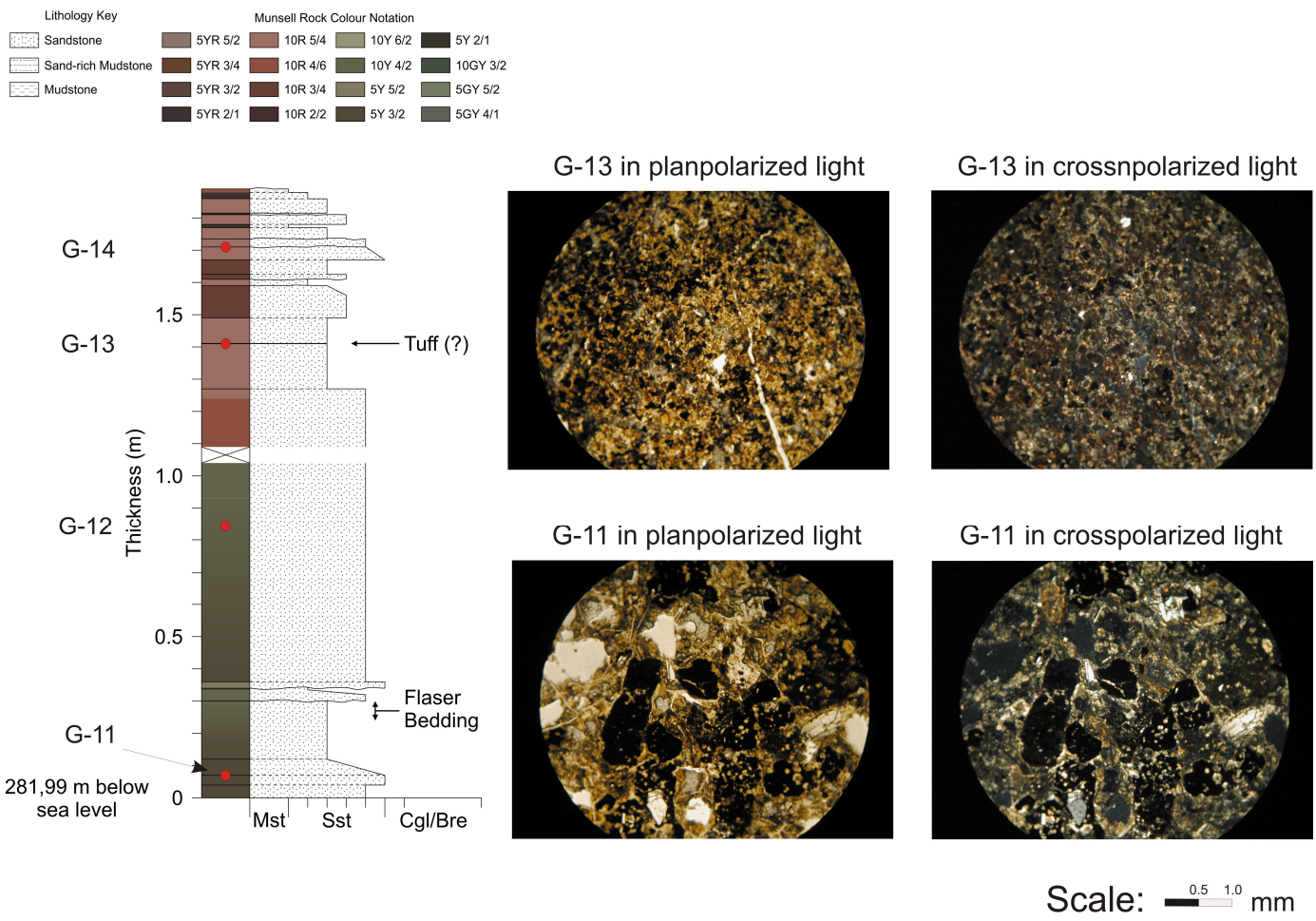

Fig 11b. A selection of polished sections from the Sneis Formation in the Glyvursnes-1 borehole.

is reddish brown at the bottom to mottled brown and olive at the top. In two places the core is missing, most likely due to wash outs (Fig. 11c). The sandstones are medium- to fine-grained. From the Section two samples were taken and one was measured, it had a porosity of 10.5%.

The Argir Beds, Section +2, is a ~5.3 m thick bedded volcaniclastic sequence that coarsens up Section from yellowish green volcaniclastic mudstones to reddish brown volcaniclastic sandstones. Locally blackened plant fragments can be found. The volcaniclastic sandstones are dominantly medium-grained, although granule-rich units are found towards the top of the unit (Fig. 11c). The Section has an average measured porosity of 23.3%, but ranges from 9.1% to 46.4% based on 8 out of 12 samples that were possible to measured from this Section..

The average porosity based on both Sections is 21.9%, ranging form 9.1% to 46.4%.

4.1.2 Wire-line Derived Porosity Values

The wire-line derived values from the Sonic logs gave unrealistic porosity values ranging from ~10% to as high as ~70%. The linear relationship between the measured and derived porosities, the R^2 value (presented in Section 5.1) only shows how good the linear relationship between the two compared values is, it does not show how close the values are. So even if the Sonic log gives a good trend it does not necessarily give the closest porosity values. A mean of how much higher the derived values are then the measured values was made and it gave an average of ~17% higher then the measured porosities (Table 11). This could possibly be used to measure the approximate porosities in formations when only the Sonic log is available or reliable, e.g. where large wash outs occur.

In this study the Sonic logs will be excluded from diagrams and discussions, but for completeness the porosity values are presented in Appendices V (Glyvursnes-1 well) and VI (Well 6005/15-1). The

Enni Formation - Section +1 & +2

Lithology log with examples of pictures in plan- and cross polarised light

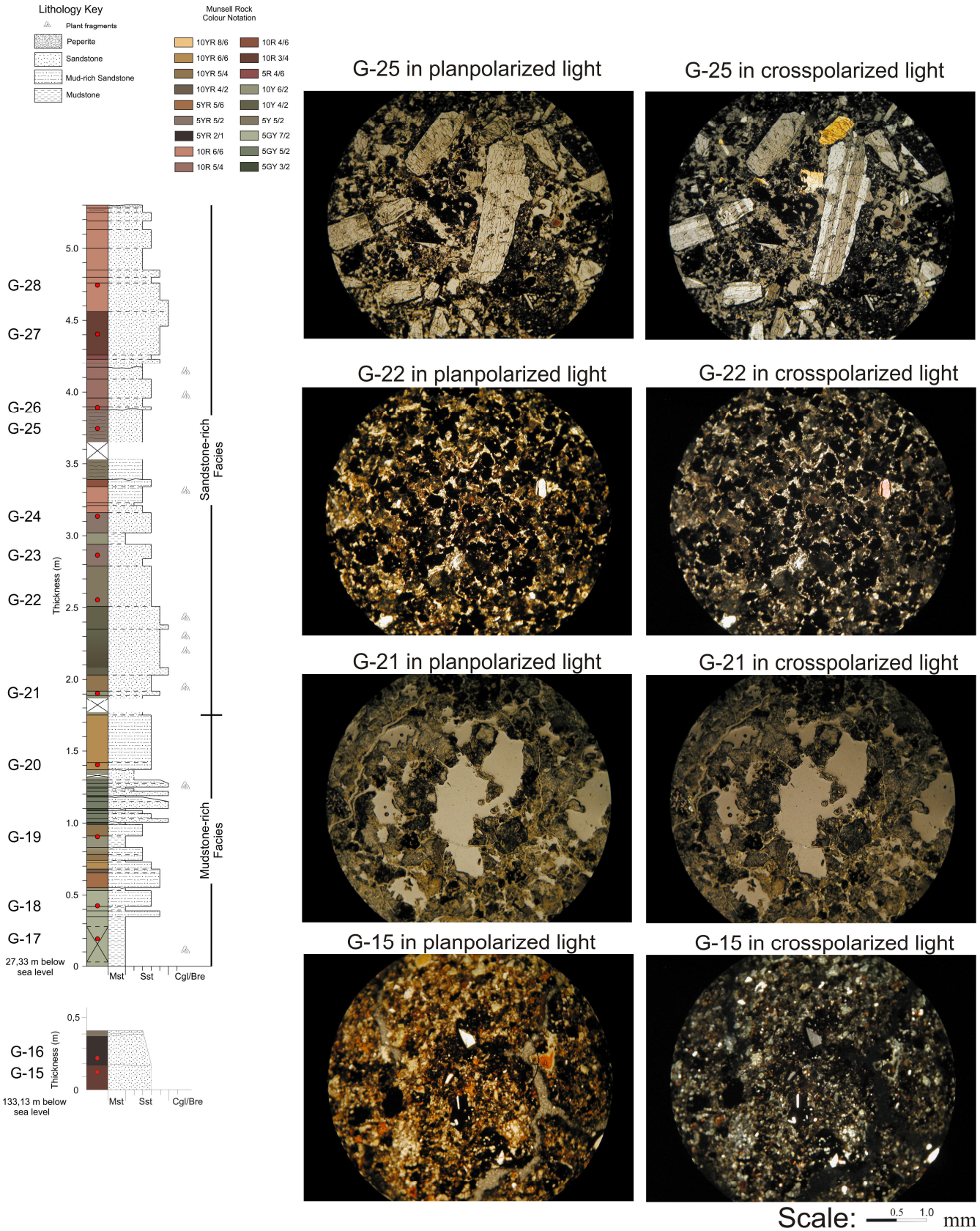

Fig 11c. A selection of polished sections from the Enni Formation in the Glyvursnes-1 borehole.

Malinstindur Formation
Lithology, Porosities and Wire lines logs
Section -3

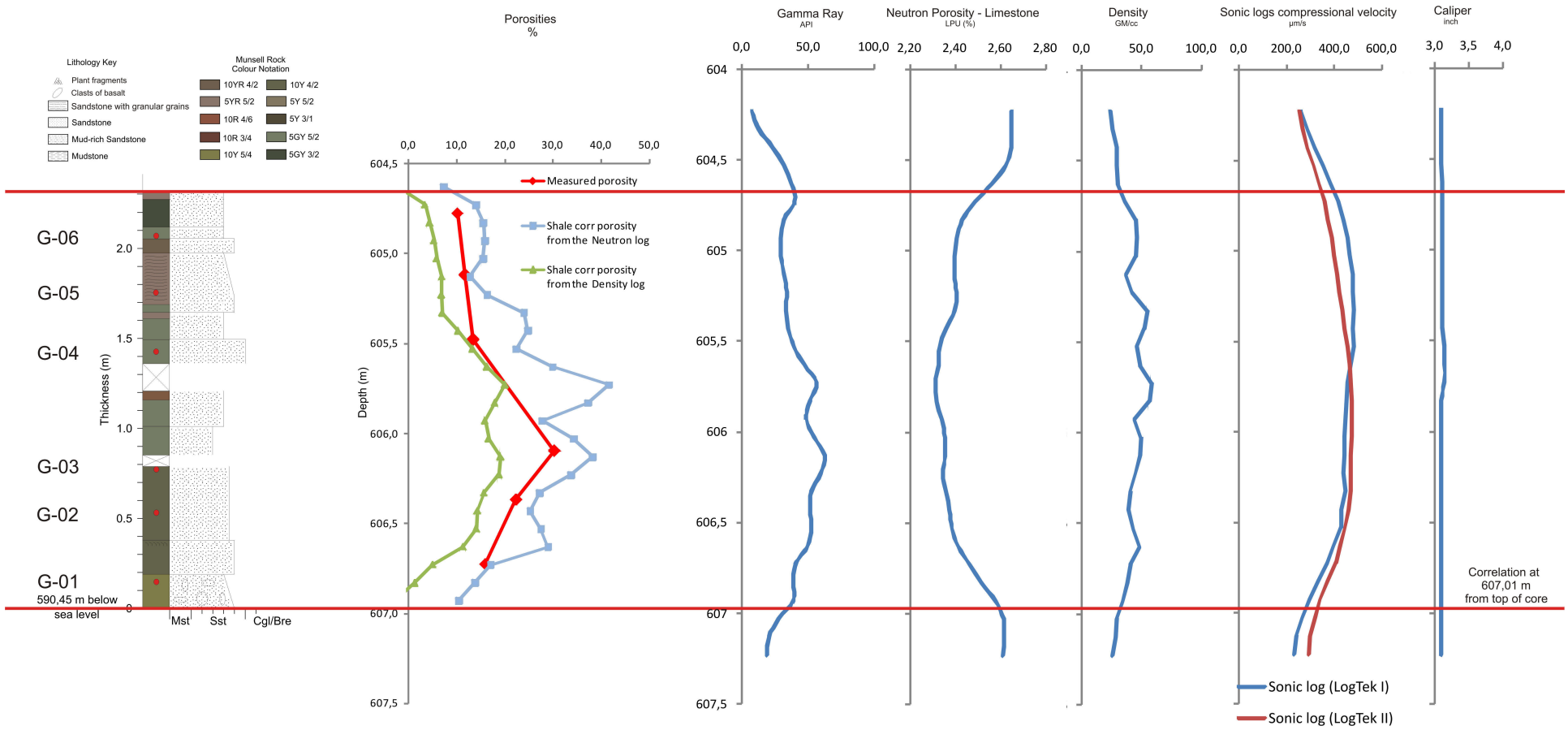

Fig 12a. A lithology log, from Section - 3 from the Malinstindur Formation together with the measured porosity and the wire-line derived porosities from the shale corrected Neutron and Density logs. Additionally all wire-line logs used in the calulations are presented together with the Caliper log.

Malinstindur Formation
Lithology, Porosities and Wire lines logs
Section -2

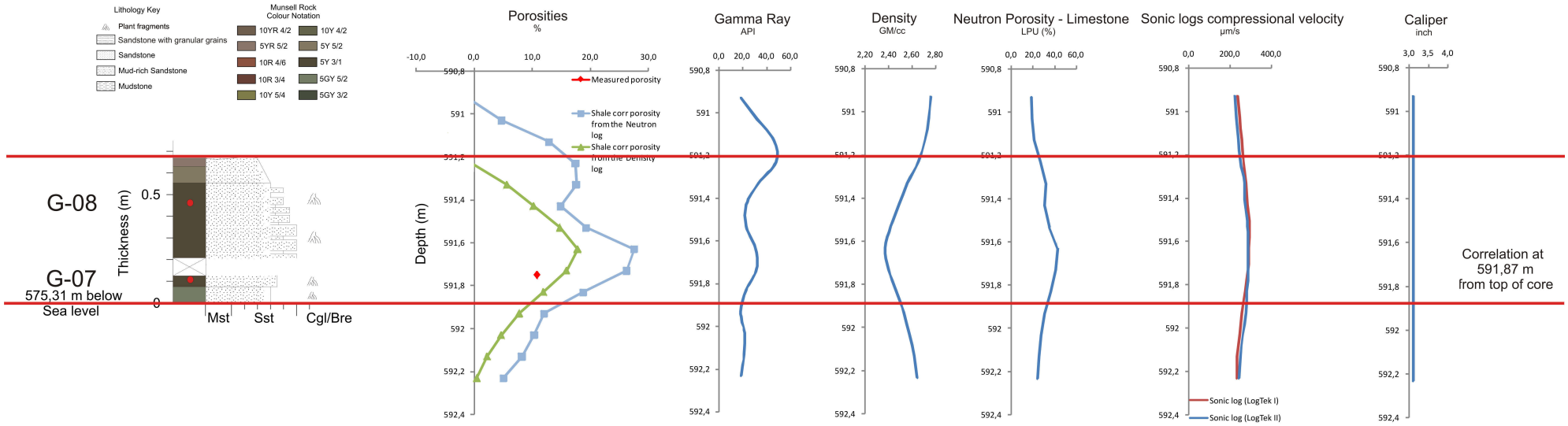

Fig 12b. A lithology log, from Section - 3 from the Malinstindur Formation together with the measured porosity and the wire-line derived porosities from the shale corrected Neutron and Density logs. Additionally all wire-line logs used in the calulations are presented together with the Caliper log.

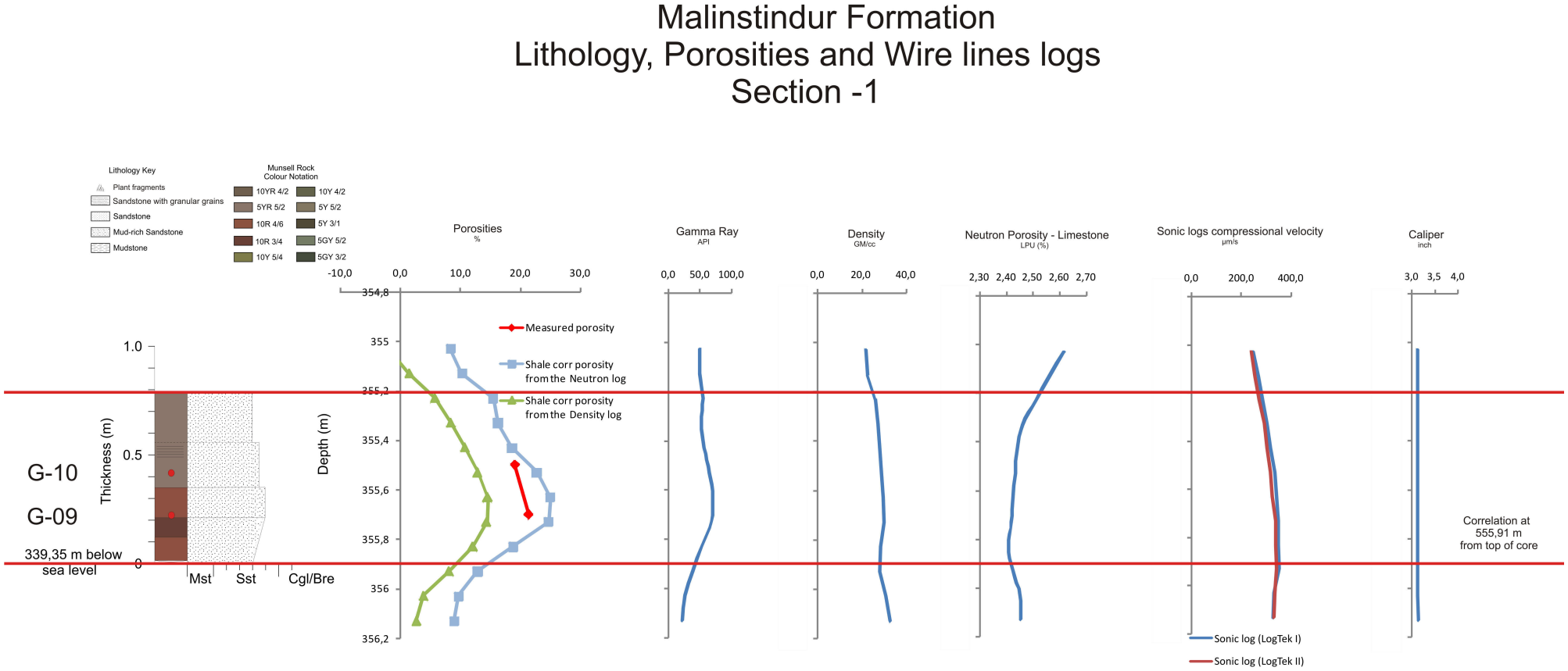

Fig 12c. A lithology log, from Section - 1 from the Malinstindur Formation together with the measured porosity and the wire-line derived porosities from the shale corrected Neutron and Density logs. Additionally all wire-line logs used in the calulations are presented together with the Caliper log.

Sneis Formation

Lithology, Porosities and Wire lines logs

Section 0

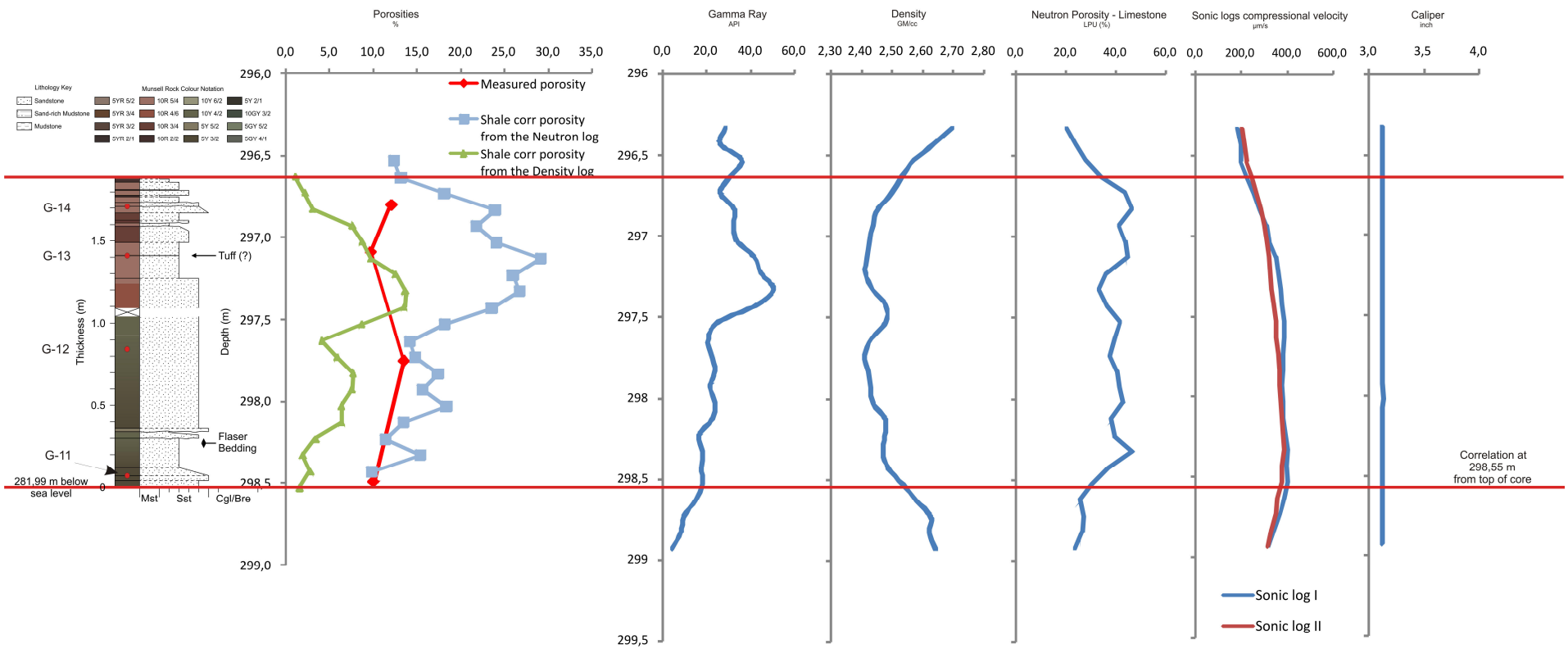

Fig 12d. A lithology log, from Section - 2 from the Malinstindur Formation together with the measured porosity and the wire-line derived porosities from the shale corrected Neutron and Density logs. Additionally all wire-line logs used in the calulations are presented together with the Caliper log.

Enni Formation

Lithology, Porosities and Wire lines logs

Section +1

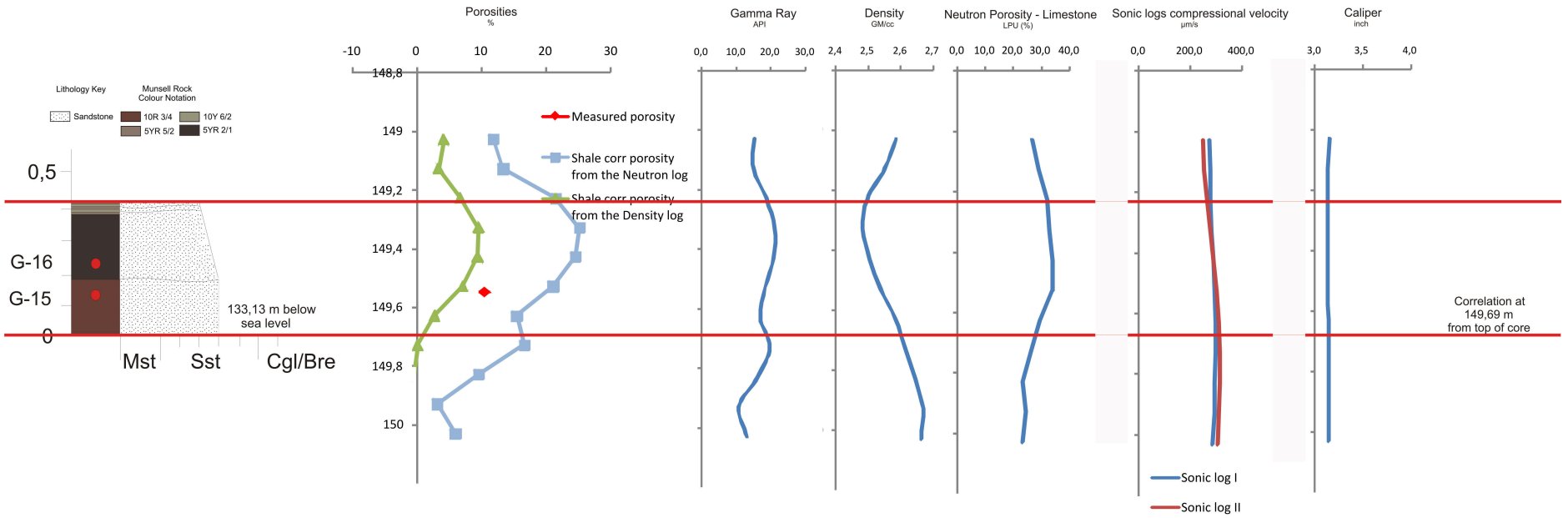

Fig 12e. A lithology log, from Section + 1 from the Malinstindur Formation together with the measured porosity and the wire-line derived porosities from the shale corrected Neutron and Density logs. Additionally all wire-line logs used in the calulations are presented together with the Caliper log.

Enni Formation - Argir beds

Lithology, Porosities and Wire lines logs

Section +2

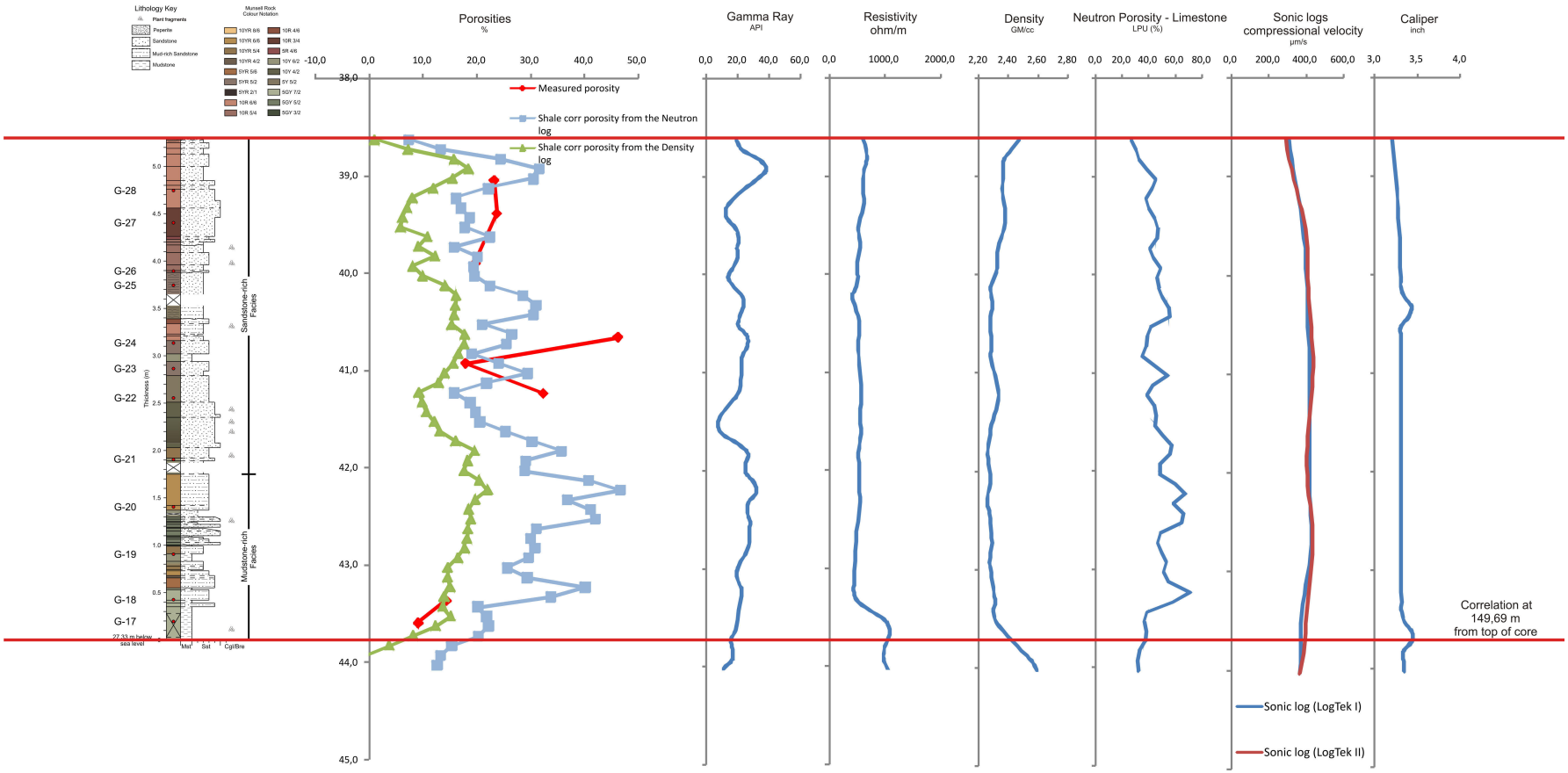

Fig 12f. A lithology log, from Section +2 from the Malinstindur Formation together with the measured porosity and the wire-line derived porosities from the shale corrected Neutron and Density logs. Additionally all wire-line logs used in the calulations are presented together with the Caliper log.

porosities derived from the shale corrected Density and Neutron logs consistently have a better correlation with the measured values and therefore, the porosities derived from the wire-line log data without shale correction will not be discussed (see appendices VII and VIII for full results). The wire-line derived porosities for the six sedimentary Sections from the Glyvursnes-1 borehole are presented in Figures 12a-f together with the measured porosity and a lithology log of each Section, for more details on how the porosities are derived see Section 2.2.2. Therefore, all porosity values derived from the wire-line log data that are mentioned in the discussion (Section 6) should be assumed to be shale corrected unless specifically stated otherwise, but to show that the shale corrected porosities give better values then the porosity values without the shale correction, both values will be presented below in Sections 4 and 5. Negative porosity values were obtained from both the Glyvursnes-1 borehole and Well 6005/15-1 close to the boundaries between the sedimentary Sections and the adjacent basalt units. The negative values have been excluded from all calculations, diagrams and discussions. This is the reason the number of values presented in Table 12 (Glyvursnes-1) and Table 13 (Well 6005/15-1) below are not always consistent.

4.1.3 Malinstindur Formation

Wire-line derived porosities from the Malinstindur Formation have an average of 10.2%, ranging from 0.6% to 20.1% for the shale corrected Density log and an average of 16.0% for the shale corrected Neutron log, ranging from 2.8% to 41.6%. For completeness all wire-line derived porosities are presented in Table 12.

4.1.4 Sneis Formation

From the Sneis Formation, the wire-line derived porosities from the shale corrected Density log have an average of 6.5%, ranging from 1.1% to 13.7% and an average of 16.4% for the Neutron log, ranging from 1.0% to 29.2% (Table 12).

4.1.5 Enni Formation

Based on the wire-line derived log data the porosities from the Enni Formation give an average of 9.6%, ranging from 0.8% to 22.0% for the shale corrected Density log while the average from the Neutron log is 20.3%, ranging from 3.3% to 46.6% (Table 12).

Table 11. Difference between the derived porosities from the Sonic logs and the measure porosity.

Porosity from the shale corrected Sonic log (%) LogTek I	Measured porosity (%)	Difference between both porosities (%) **Average difference (%)**	Porosity from the shale corrected Sonic log (%) LogTek II	Measured porosity (%)	Difference between both porosities **Average difference (%)**
12.5	16.0	3.5	19.4	16.0	3.4
48.0	22.4	25.6	52.7	22.4	30.3
57.1	30.3	26.9	63.9	30.3	33.6
60.8	30.3	30.5	67.3	30.3	37.0
48.0	13.5	34.5	39.6	13.5	26.1
42.1	11.8	30.3	25.2	11.8	13.4
30.3	10.3	20.0	12.0	10.3	1.7
10.9	10.9	0.0	15.2	10.9	4.2
29.8	21.4	8.4	28.8	21.4	7.4
37.0	21.4	15.5	35.3	21.4	13.9
36.6	19.1	17.5	33.4	19.1	14.3
32.7	19.1	13.6	29.1	19.1	10.0
		18.9			**16.3**

4.2 Well 6005/15-1 – Longan

4.2.1 Kettla Member

In Figure 13a the derived and shale corrected porosities from the Density and the Neutron logs are presented together with the wire-line logs used in the calculations and the Caliper Log. The porosities derived from the shale corrected Density log suggest that the Kettla Member has an average porosity of 15.2%, ranging from 10.2% to 22.2% and an average porosity from the shale corrected Neutron log of 25.1%, ranging from 14.3 to 39.4%. The shale corrected Neutron log indicates a higher porosity then the shale corrected Density log (Table 13).

4.2.2 Vaila Formation

The determination of the volcaniclastic sandstones from the Vaila Formation that have been investigated in this study is based on descriptions of the onsite geologist and the possibility to confirm this by examining thin sections has not been possible.

For Section – I, classified as a volcaniclastic sandstone, presented in Figure 13b, the derived porosities from the shale corrected Density log suggest an average porosity of 13.4%, ranging from 7.7% to 23.3%, while the shale corrected Neutron log suggests an average porosity of 18.5%, ranging from 0.3% to 28.4%.

Section – II, classified as a non-specified sand-

Table 12. Derived porosities from all wire-line logs from the Glyvursnes-1 well divided into formations.

Derived porosity (%) values from the Glyvursnes-1 well				
	Malinstindur Formation			
	From the Density log		From the Neutron log	
	Without shale corr.	With shale corr.	Without shale corr.	With shale corr.
Minimum	0.2	0.6	10.0	2.7
Maximum	22.0	21.1	45.0	41.6
Average	11.9	10.2	26.6	19.0
No of values	52	44	57	50
	Sneis Formation			
	From the Density log		From the Neutron log	
	Without shale corr.	With shale corr.	Without shale corr.	With shale corr.
Minimum	0.4	1.1	12.6	1.0
Maximum	15.4	13.7	33.8	29.2
Average	10.0	6.5	26.4	16.4
No of values	26	20	27	23
	Enni Formation			
	From the Density log		From the Neutron log	
	Without shale corr.	With shale corr.	Without shale corr.	With shale corr.
Minimum	0.4	0.8	15.5	3.3
Maximum	25.3	22.0	52.8	46.6
Average	13.4	9.6	28.8	20.3
No of values	64	61	66	66

stone, correlates to a conventional core from where porosities have been derived from core plug measurements. The minimum, maximum, average, and geometric mean porosity from the measured data values from Section – II are presented below in Table 14 The values are derived at 0.5 m intervals. The average porosity for the measured porosity is 10.1%, ranging from 6.0% to 15.0%. In Figure 13c the derived porosities from the shale corrected Density log suggest an average porosity of 11.2%, ranging from 7.1% to 15.2%, while the shale corrected Neutron log suggests an average porosity of 18.5%, ranging from 5.2% to 29.0%.

The derived porosities from Section – III, which has been classified as a volcaniclastic sandstone, are presented in Figure 13d and the values from

Table 13. Derived porosities from all four sedimentary Sections from Well 6005/15-1 .

Derived porosity (%) values from Section; N, -I, -II and –III				
	Section N (Kettla member)			
	From the Density log		From the Neutron log	
	Without shale corr.	With shale corr.	Without shale corr.	With shale corr.
Minimum	14.9	10.2	25.3	14.3
Maximum	27.4	22.2	46.0	39.4
Average	19.5	15.2	33.1	25.1
No of values	296	296	296	296
	Section –I			
	From the Density log		From the Neutron log	
	Without shale corr.	With shale corr.	Without shale corr.	With shale corr.
Minimum	10.9	7.7	13.0	0.3
Maximum	26.3	23.3	31.1	28.4
Average	15.6	13.4	22.8	18.8
No of values	88	88	88	80
	Section – II			
	From the Density log		From the Neutron log	
	Without shale corr.	With shale corr.	Without shale corr.	With shale corr.
Minimum	10.8	7.1	14.0	5.2
Maximum	21.1	15.2	43.0	29
Average	15.3	11.2	27.5	18.5
No of values	85	85	85	85
	Section – III			
	From the Density log		From the Neutron log	
	Without shale corr.	With shale corr.	Without shale corr.	With shale corr.
Minimum	5.4	0.1	1.1	0.4
Maximum	27.1	24.4	23.0	23.0
Average	13.4	9.3	12.5	9.8
No of values	88	85	88	61

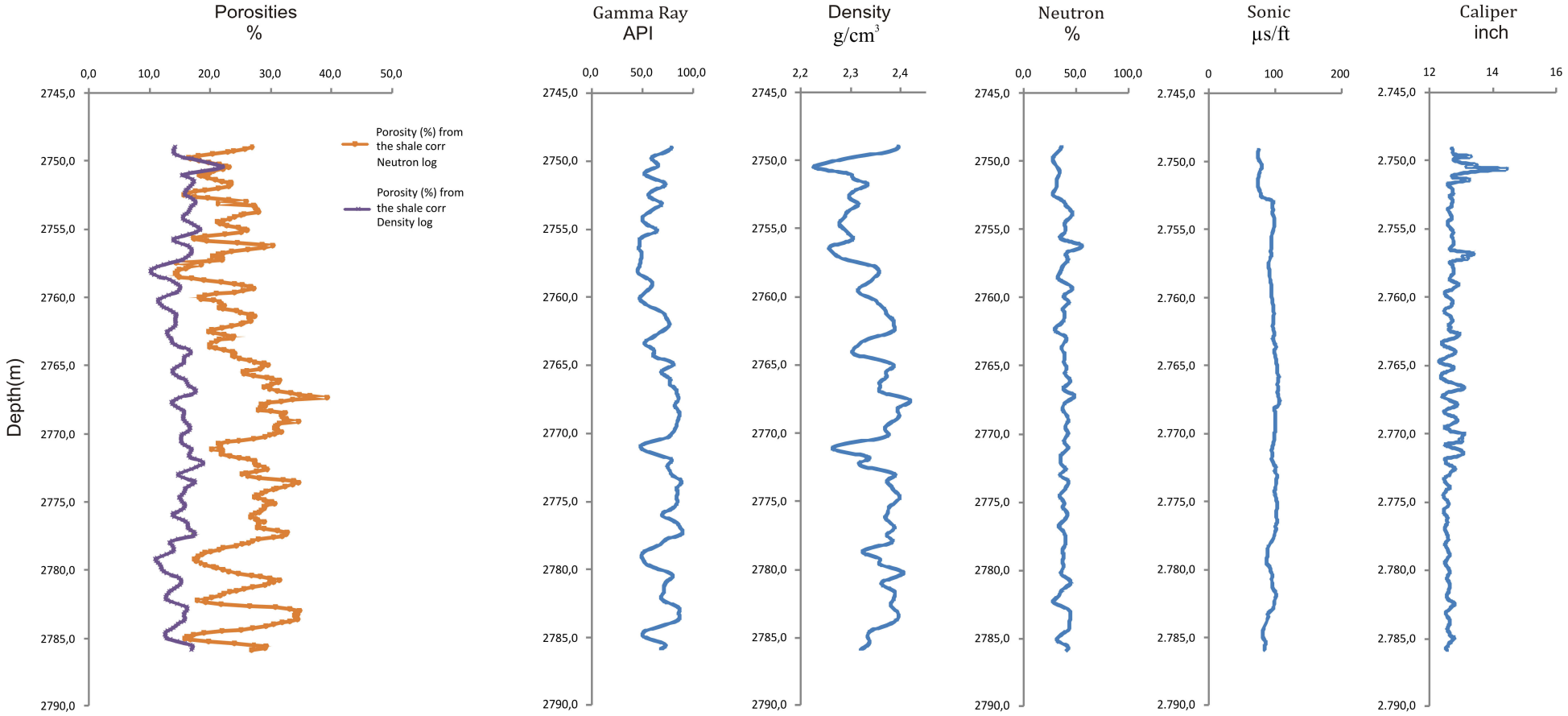

Fig 13a. The Neutron and Demsity wire-line log derived and shale corrected porosities from the Kettla Member together with all wire-line logs used in the porosity calulations and the Caliper.

Well 6005/15-1 Longan - 3360 - 3370m depth

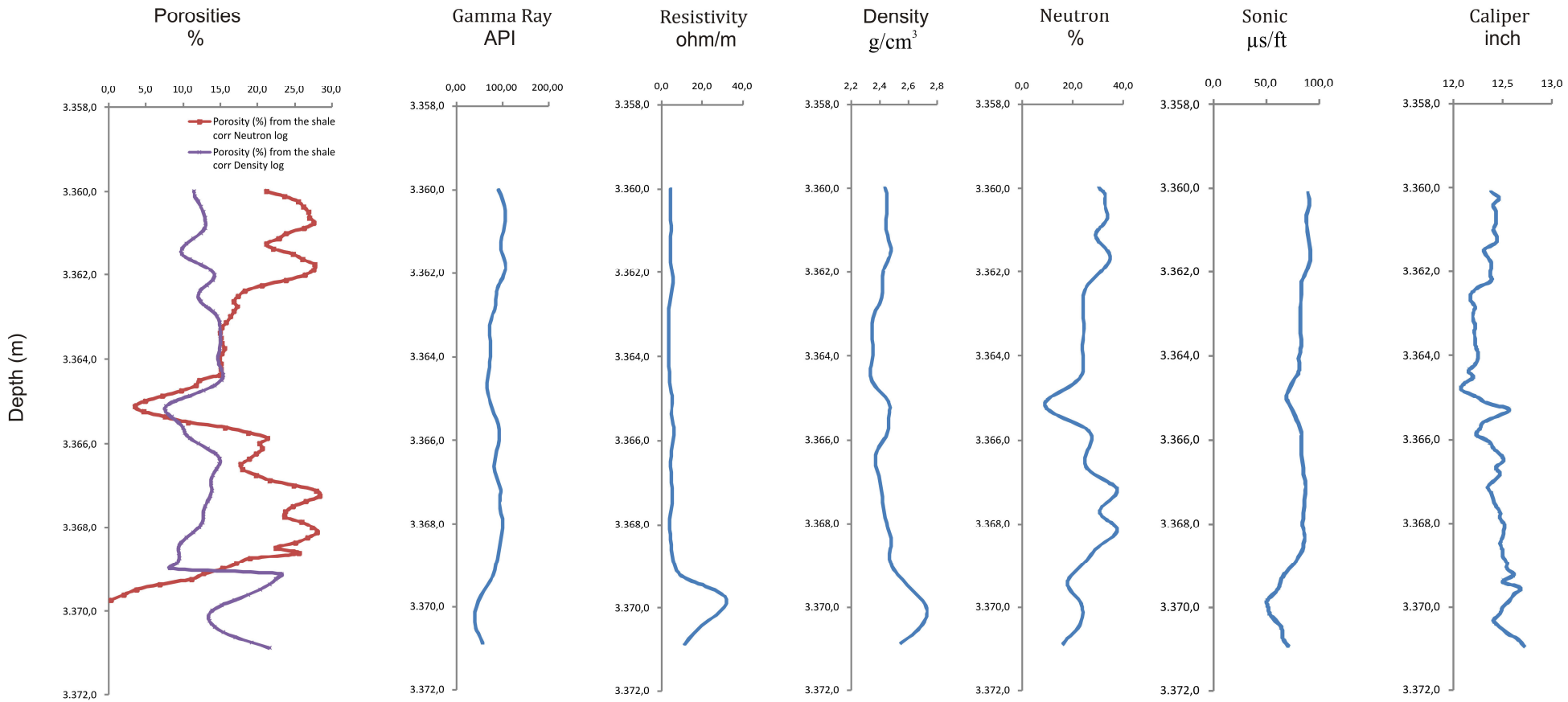

Fig 13b. The Neutron and Demsity wire-line log derived and shale corrected porosities from Section -I together with all wire-line logs used in the porosity calulations and the Caliper.

Well 6005/15-1 - Longan - correlating with the conventional core at 3507 - 3517,5m depth

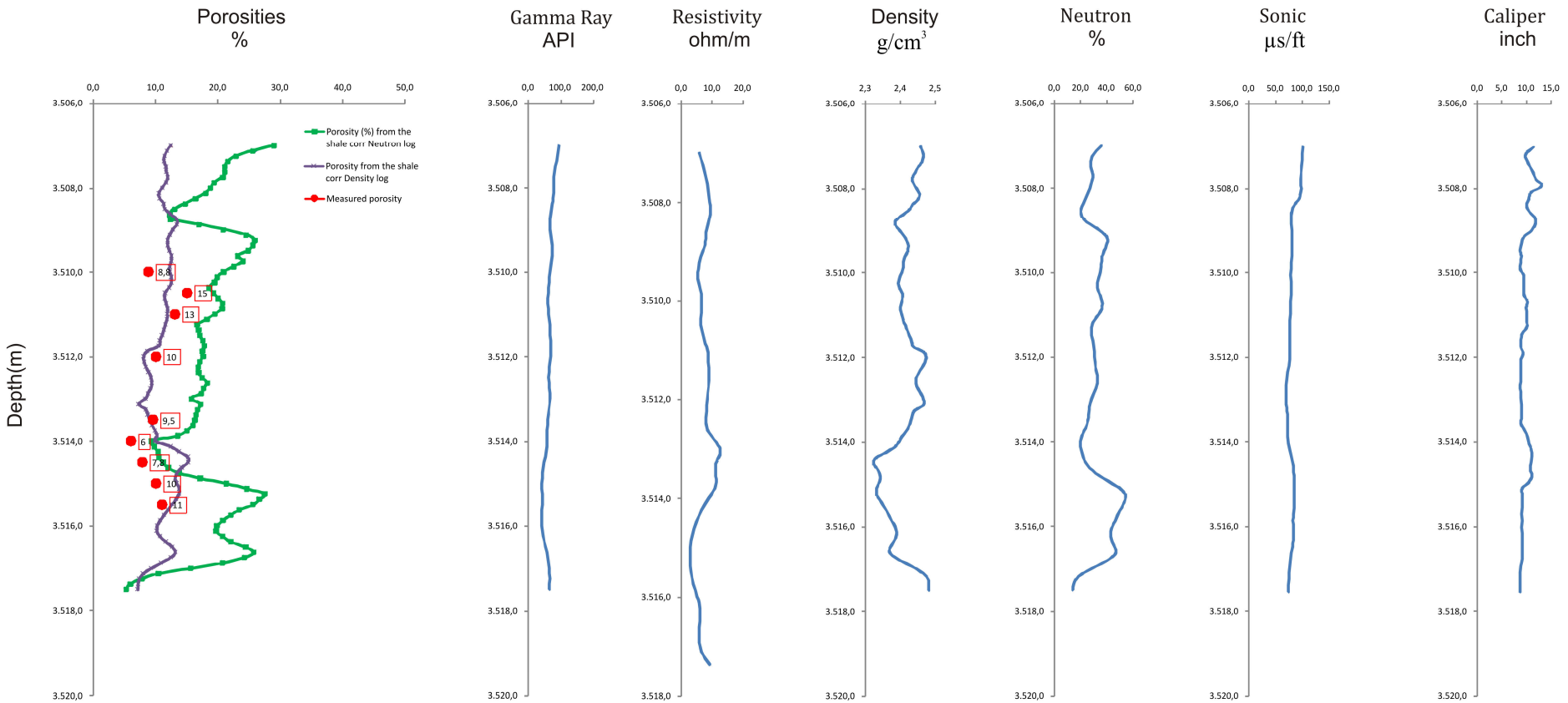

Fig 13c. Section - II. Measured porosity together with the Neutron and Demsity wire-line log derived and shale corrected porosities together with all wire-line logs used in the porosity calulations and the Caliper.

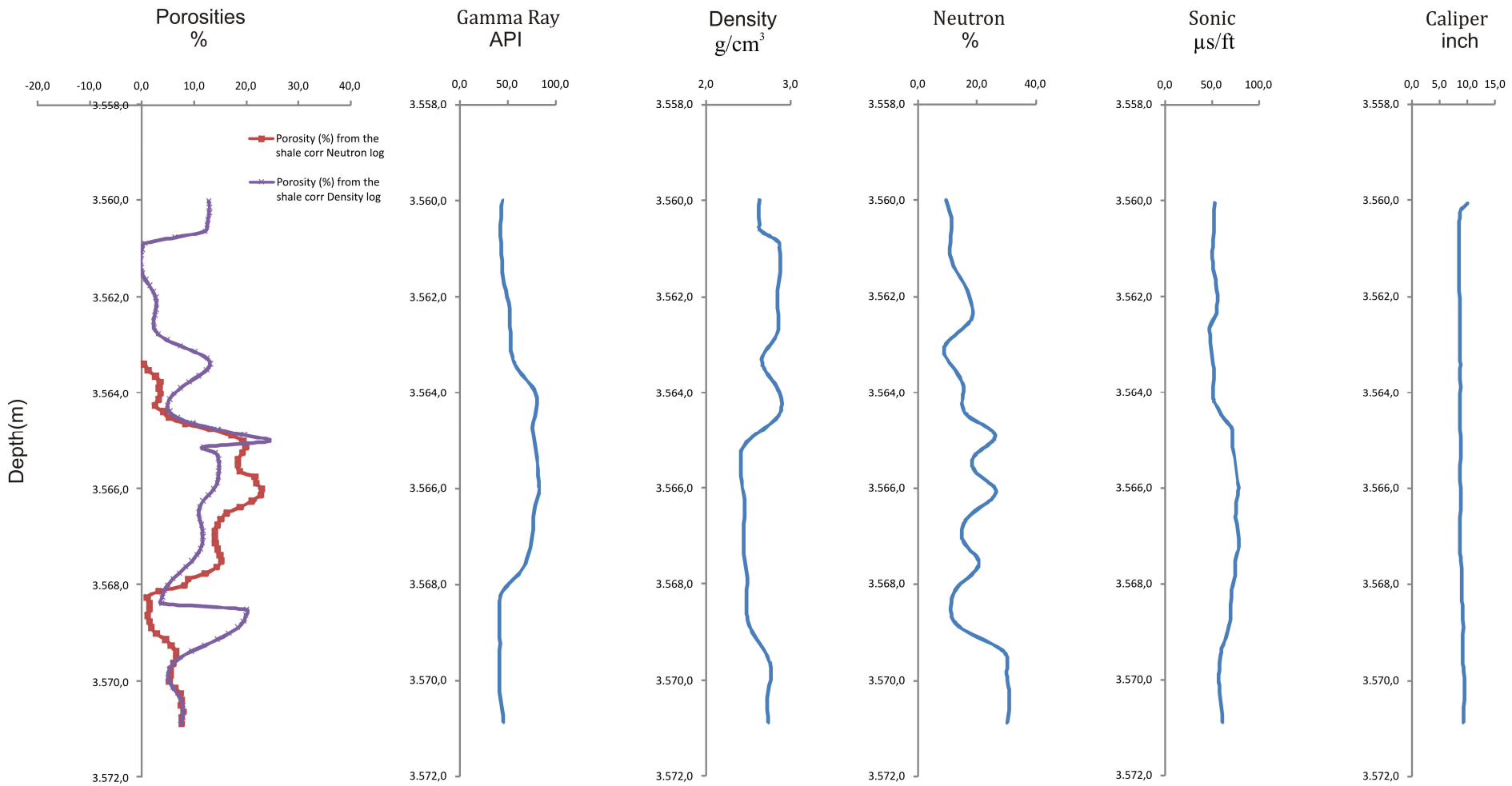

Fig 13d. The Neutron and Demsity wire-line log derived and shale corrected porosities from Section - III together with all wire-line logs used in the porosity calulations and the Caliper.

Table 14: Measured porosity from Section – II (Well 6005/15-1).

	Porosity (%)
Minimum	6.0
Maximum	15.0
Average	10.1
Geometric mean	9.8

the shale corrected Density log suggest an average porosity of 9.3%, ranging from 0.1% to 24.4%, while the shale corrected Neutron log suggests an average porosity of 9.8%, ranging from 0.4% to 23.0%.
Again, for all three Sections, the shale corrected Neutron log frequently indicates higher porosities than the shale corrected Density log. For completeness all wire-line derived porosities are presented in Table 13.

5. Comparison between measured and wire-line derived porosities

5.1 Glyvursnes-1

The six Sections investigated from the Glyvursnes-1 borehole have a number of measured porosity values that can be compared to porosities derived from the wire-line log data to test the applicability of using the Schlumberger equations in the formation analysis of volcaniclastic intervals. Figures 14 to 16 present the comparison graphs between the measured and derived porosities for the Malinstindur, Sneis and Enni formations encountered in the Glyvursnes-1 borehole. The formations are described separately below but it is worth noting that although the derived porosities are consistently either too low or too high compared to the measured values, it is the linear relationship, or trend indicated by the R^2 value, between the values that is of particular interest.

5.1.1 Malinstindur Formation

Three Sections (Sections -1, -2 and -3) were examined from the Malinstindur Formation and Figure 14a-b present the comparison between the measured porosity values and those derived from wire-line log data, the results are based on 12 and 7 sample values for all three sections and Section -3, respectively. The porosities without and with shale correction for all three Sections derived from the Neutron log have a correlation coefficient, R^2 value, of 0.05 and 0.75, respectively, with the measured porosities. Similarly, the R^2 values for the derived porosities without and with shale correction from the Density log and the measured porosities are 0.24 and 0.56, respectively. These results clearly demonstrate that the shale corrected derived porosities give the highest R^2 value when compared to the measured porosities. The strongest correlation comes from the shale corrected Neutron log (Fig 14a-b).

Six samples were collected from Section-3 and therefore, a more detailed comparison could be made between the measured and derived porosities (Fig. 14b). Again the porosities derived from the shale corrected wire-line logs give the best correlation with the measured data compared to the values without shale correction. In decreasing order the following R^2 values were obtained when the measured porosities were compared with the shale corrected logs: 0.85 for the shale corrected Neutron logs (compared to 0.23 from the Neutron log without the shale correction), 0.67 for the Density log (compared to 0.21 from the Density log without the shale correction). The strongest correlation with the measured porosities comes from the shale corrected Neutron log.

5.1.2 Sneis Formation

Figure 15 presents the comparison diagrams between the porosities measured from four samples and those derived from wire-line log data. As the dataset is only based on four samples it is difficult to make any firm interpretations. The R^2 values for the Neutron log, without and with shale correction, gave values of 0.11 and 0.001 when compared to the measured porosities. Similarly, the derived porosities without and with shale correction from the Density log gave values of 0.16 and 0.014, respectively when the derived porosities were compared to the measured values.

5.1.3 Enni Formation

The Enni Formation consists of two Sections, Sections +1 and +2 (Argir Beds), and nine samples with measured porosity values. These measured porosities are compared to those derived from the wire-line logs in Figure 16. The R^2 values from the Neutron log, without and with shale correction, give R^2 values of 0.18 and 0.08, respectively. The R^2 values from the Density log, without and with shale correction, give values of 0.27 and 0.06, respectively. In the Enni Formation, most of the R^2 values are very low and the Neutron log

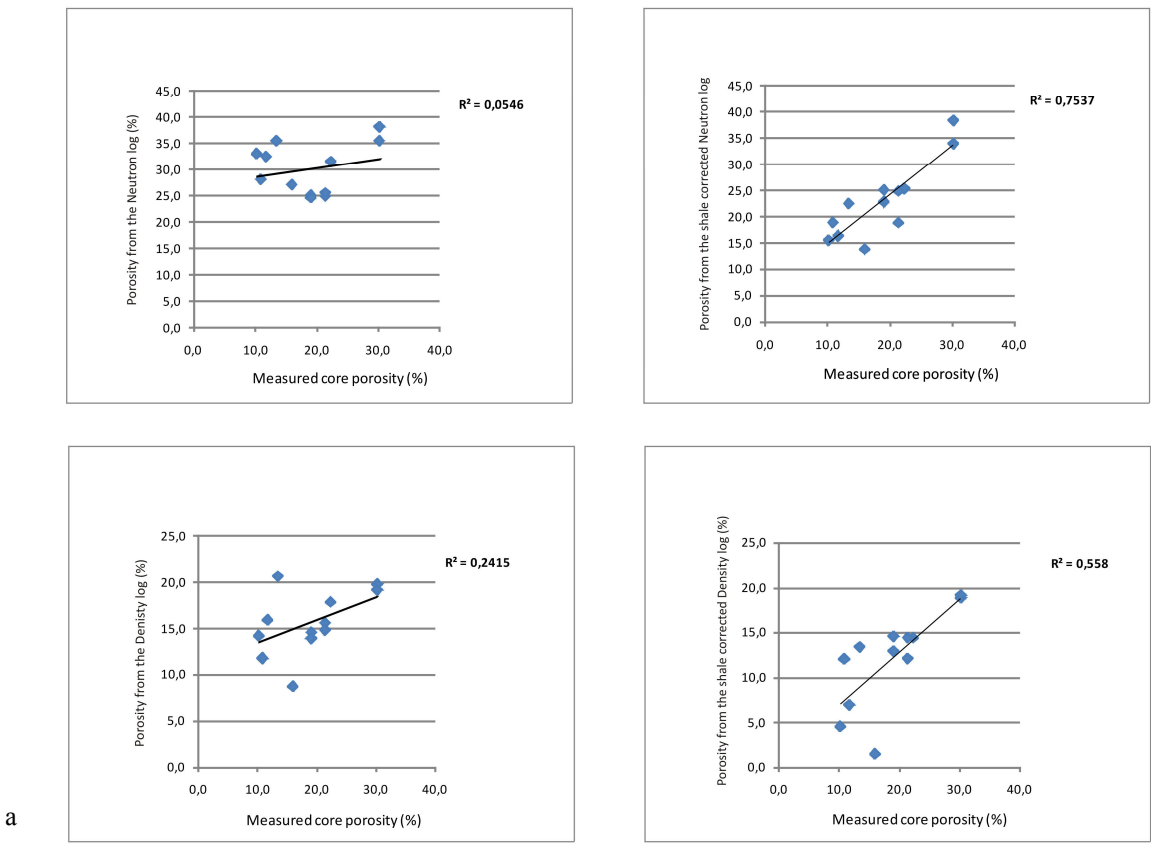

Fig.14. Correlation coefficients (R^2) between measured porosity and wire-line derived porosity from the Neutron and the Density logs a) R^2 values based on all three Sections from Malinstindur Formation. B) R^2 values based on Section - 3.

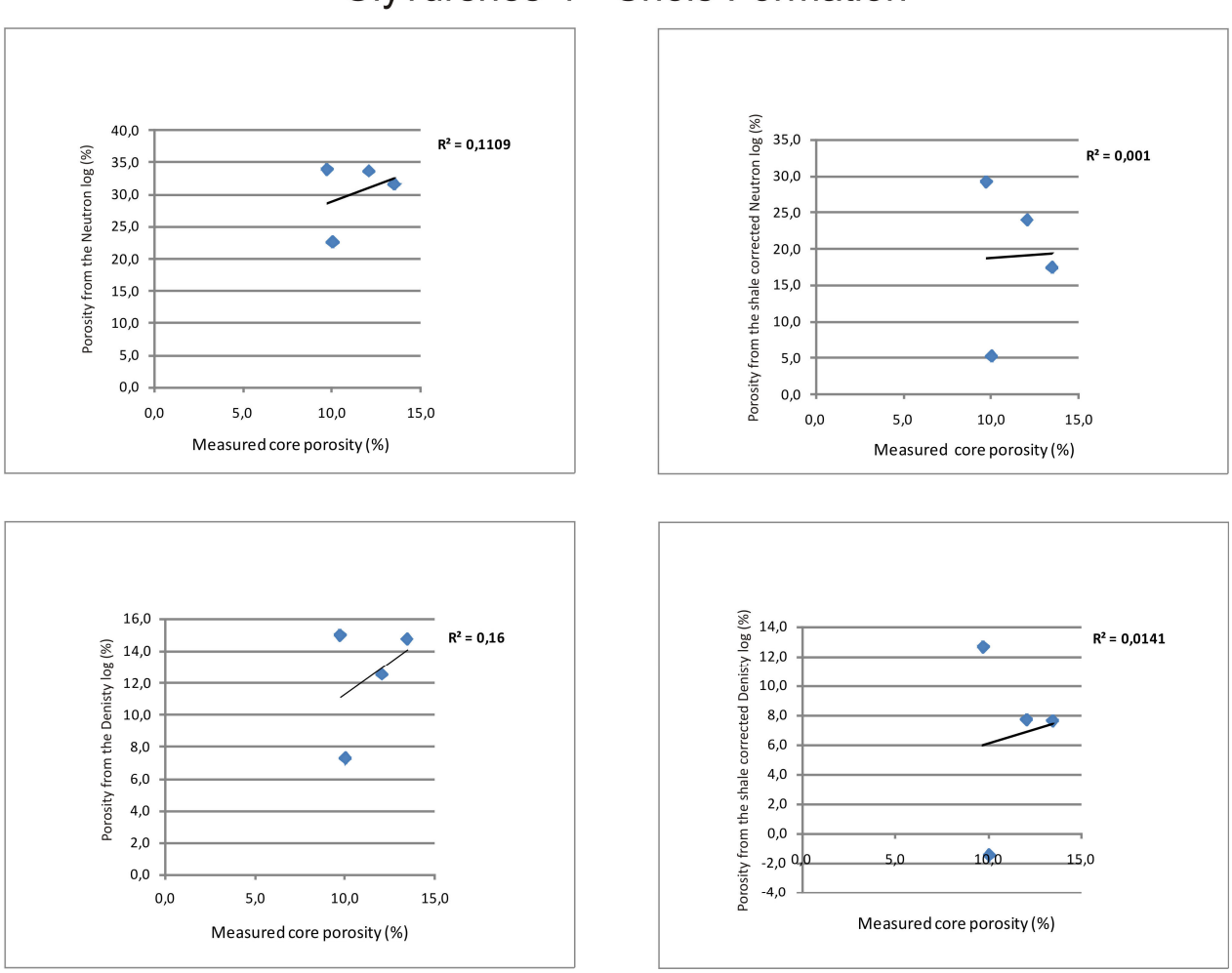

Fig.15. Correlation coefficients (R^2) between measured porosity and wire-line derived porosity from the Neutron and the Density logs from the Sneis Formation.

derived porosities that shows the best correlation are not the ones that have been shale corrected. It is important to note, that because a mud-layer was identified in the Argir beds (Section +2) it was possible to obtain additional volume of shale from the Resistivity and the Neutron logs, but the R^2 values are still consistently low and especially, for the shale corrected values.

5.1.4 Porosity Window

When looking at the porosity diagrams produced for each Section from the Glyvursnes-1 borehole (Figs. 12a-f) it appears that the measured porosities falls between the derived porosities from the shale corrected Density and Neutron logs. This pattern can be seen in Sections -3 and -1 from the Malinstindur Formation (Fig. 12a & c) and for Section 0 from the Sneis Formation. The Enni Formation, Section +2, on the contrary does not appear to fit this trend (Fig. 13f). Considering Section -2 from the Malinstindur Formation and Section +1 from the Enni Formation, there is only one measured value for each section, therefore no trend can be seen, but Section +1 falls between the logs while Section -2 falls outside.

The zone between the Density and Neutron wire-line derived porosities, where the measured porosities fall within, are referred to here as the "porosity window", where the derived porosity from the Density log represents a possible minimum value and the porosity derived from the Neutron log represents a possible maximum value.

The reason for the overall higher R^2 values from the Malinstindur Formation could be due to its lithology. The samples are all taken from sand-prone sections (Fig. 12a-c), that are homogenous unlike the heterolithic Enni Formation (e.g. Fig. 12f). The Schlumberger equations that are used in the porosity calculations in this study are lithology dependent and therefore sandstone parameters have been used (see

Comparsion of porosity values

Glyvursnes-1 - Enni Formation

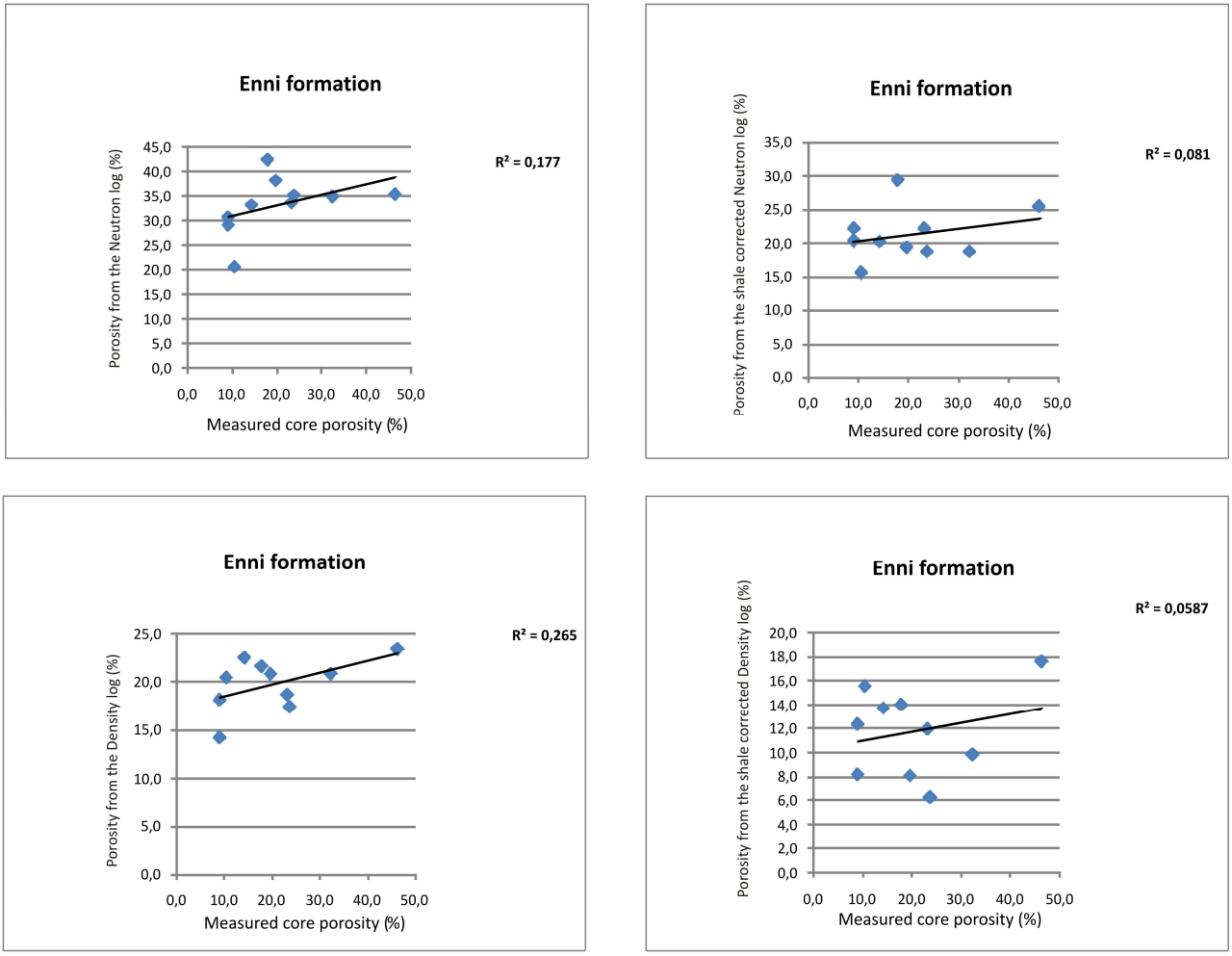

Fig.16. Correlation coefficients (R^2) between measured porosity and wire-line derived porosity from the Neutron and the Density logs from the Enni Formation.

Section 2.2.2). This could be an explanation to why the linear relationship is higher between the wire-line derived porosity and the measured porosity from the Malinsindur Formation compared to e.g. Section +2, the mud-prone Argir beds from the Enni Formation.

Results based on the linear relationship between wire-line derived porosities and measured porosity have shown that the best derived porosities come from the shale corrected Density and Neutron logs and therefore a simulated porosity based on the intermediate values was obtained in order to compare

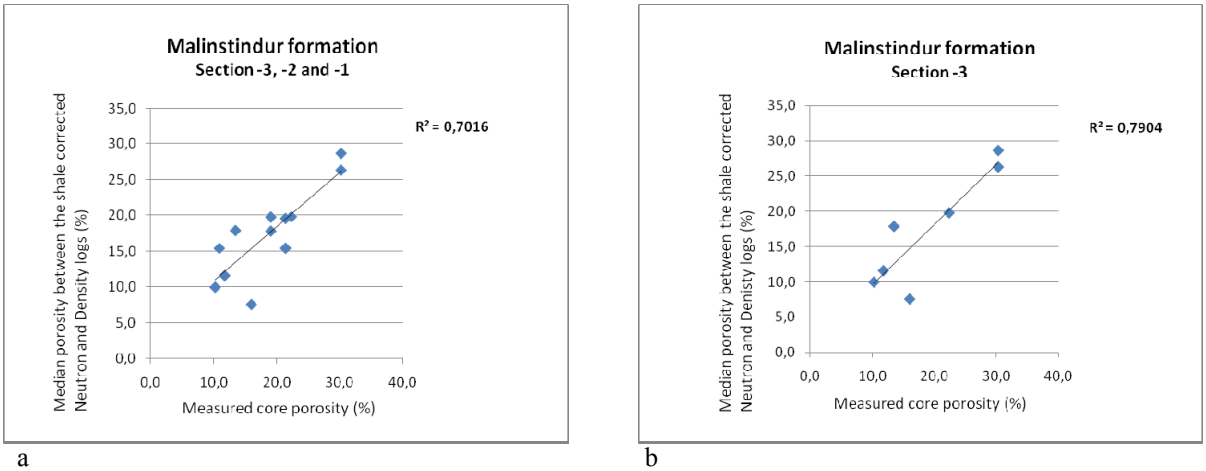

a b

Fig. 17: Simulated porosity versus measured porosity from Glyvurenes-1 well, Malinstindur Formation. a) all three Sections. b) Section -3.

Comparsion of porosity values
Well 6005/15-1 - Longan

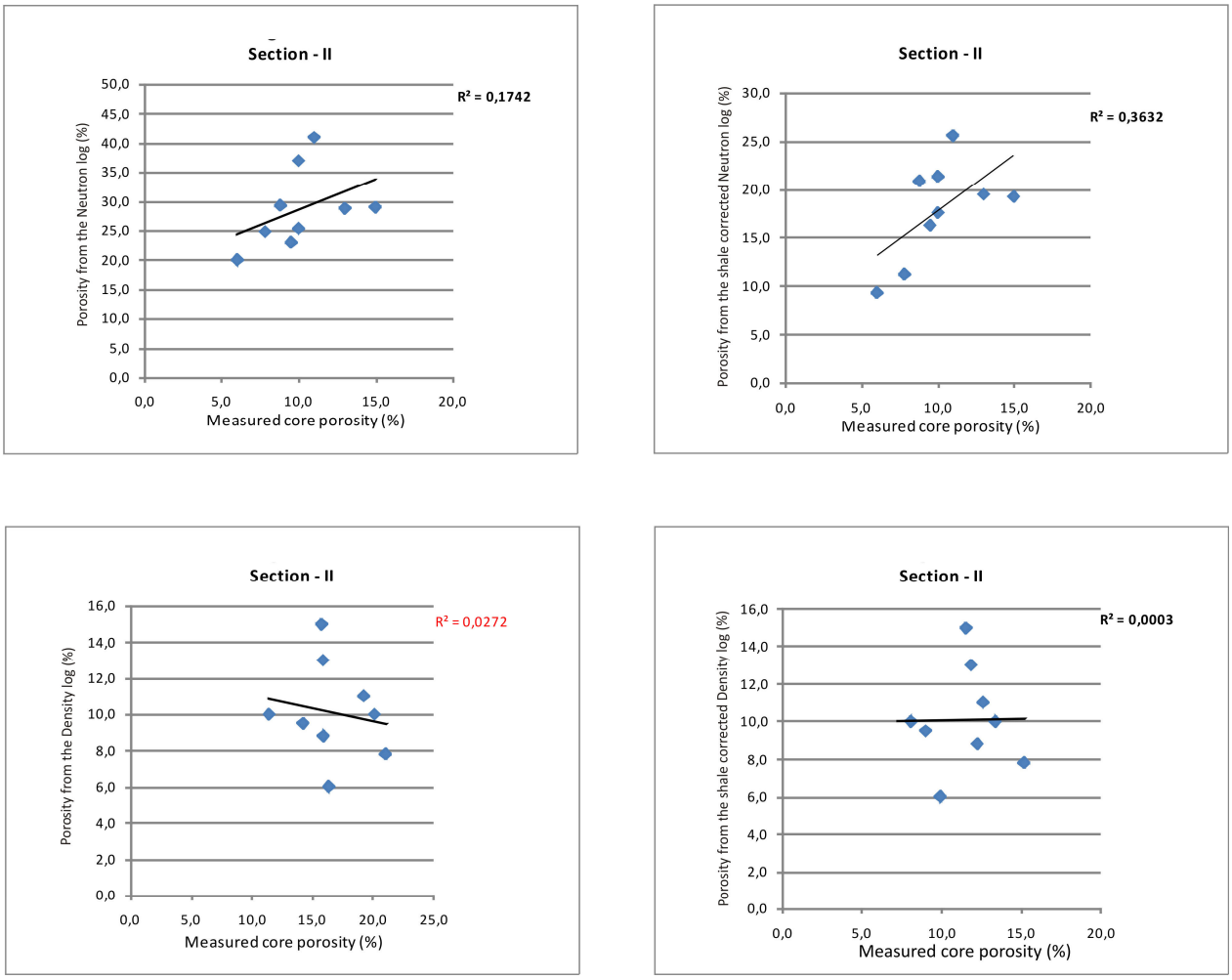

Fig 18. Correlation coefficients (R^2) between measured porosity and wire-line derived porosity from the Neutron and the Density logs from Section -II from Well 6005/15-1.

with the measured porosity for the relatively homogenous Malinstindur Formation. Two simulated porosities were made, both from the Malinstindur Formation, one based on all three Sections and one for Section -3 only, the results are presented in Figure 17. The linear relationship between the simulated porosity and the measured porosity based on all three Sections from the Malinstindur Formation has an R^2 value of 0.70 (compared to R^2 values of 0.75 for the shale corrected Neutron log and measured porosity and 0.56 for the Density log and the measured porosity) while the linear relationship between the simulated porosity and the measured porosity from Section -3 from the Malinstindur Formation has an R^2 value of 0.79 (compared to R^2

Table 15. Simulated porosity based on the median between the shale corrected Neutron and Density logs.

	Section N Porosity (%)	Section -I Porosity (%)	Section -II Porosity (%)	Section -III Porosity (%)
Average	20.2	15.0	14.8	9.0
Minimum	12.3	5.3	6.2	0.2
Maximum	27.3	21.1	20.7	21.9
Number of values	296	88	85	88

values of 0.85 for the shale corrected Neutron log and measured porosity and 0.67 for the Density log and the measured porosity).

5.2 Well 6005/15-1 – Longan

The comparison between the wire-line derived porosities and the measured porosity from control Section – II from Well 6005/15-1 are presented in Figure 18. In the figure it is possible to see that four out of nine measured porosities lie within the "porosity window" as was seen in the Malinstindur Formation (Section -3 and -1). This might suggest that it is possible to use the Schlumberger equations and the "porosity window" method on non-specified sandstones from the Vaila formation. The trend values (R^2) are not very strong, but the porosity percentage values are comparable. Therefore, the logs should be reliable and could be used for the volcaniclastic sections as well.

Based on the results presented in Section 5 porosities from Well 6005/15-1 were only derived from the Neutron log and the Density log for all four Sections. The Sonic log derived porosities have been presented in Appendix VI for completeness. The R^2 values between the aforementioned wire-line derived porosities and the measured porosity are presented in Fig. 18. The R^2 values between the measured porosity and the porosity obtained from the Density log show a reverse linear relationship of 0.023 for values without shale correction and 0.003 for the shale corrected values. The R^2 values from the Neutron log give R^2 values of 0.17 and 0.36 for the values without shale correction respectively the values with shale corrections (Fig. 18). Again the best matching results come from the shale corrected Neutron log.

Based on the identification of the "porosity window" from the volcaniclastic sandstones from the Malinstindur Formation (Section 5.1.4) a simulated porosity was obtained based on the median value between the shale corrected Density and Neutron log derived porosities. In Figure 19 the R^2 value between the simulated porosity and the measured porosity from Section -II is 0.28 (Fig. 20) which is a slight decrease compared to the R^2 value from the wire-line derived porosity from the shale corrected Neutron log and the measured porosity.

The "porosity window" method was further applied on the remaining three Sections from Well 6005/15-1 and in Table 15 average, minimum, maximum and number of values from the simulated porosity is presented while all three porosities (from the shale corrected Density and Neutron logs together with the simulated porosity) are illustrated in Figure 20.

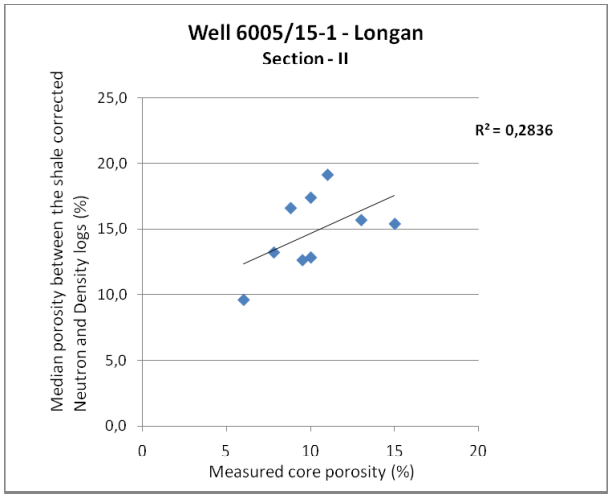

Fig. 19: The simulated porosity versus measured porosity from Section –II in Well 6005/15-1.

6. Discussion

6.1 Porosity and permeability from Measured Data

The average porosity for the onshore Faroese samples is 17% ranging from 0.1% to 46.4% based on 43 samples. Compared to the average porosities from the hydrocarbon producing Jurassic volcaniclastics from the Liaohe Basin in China, were the porosities range from 2.1% to 20.4% with averages of 8.4% – 12.2%, the porosities from the FIBG can be considered high (Luo *et al.* 2005). Other comparable examples from hydrocarbon producing volcaniclastics are found in the Austral and the Neuquén Basins in Argentina that are Mesozoic in age. In the Austral Basin the porosities range from 4.8% to 37.6% with averages from 9.1% to 30.5%. Porosities from the Neuquén Basin range from 10.7% to 23.1% with averages from 7.7% to 21.0% (Sruoga & Rubinstein 2007). In both cases the porosities compare well with the average porosity of 17% for the FIBG, especially the porosity from the Neuquén Basin which is the most productive basin of the two (Sruoga & Rubinstein 2007). Therefore, the porosities obtained for the FIBG are not unreasonable when compared to values from other volcaniclastic units in different settings (Luo *et al.* 2005; Sruoga & Rubinstein 2007).

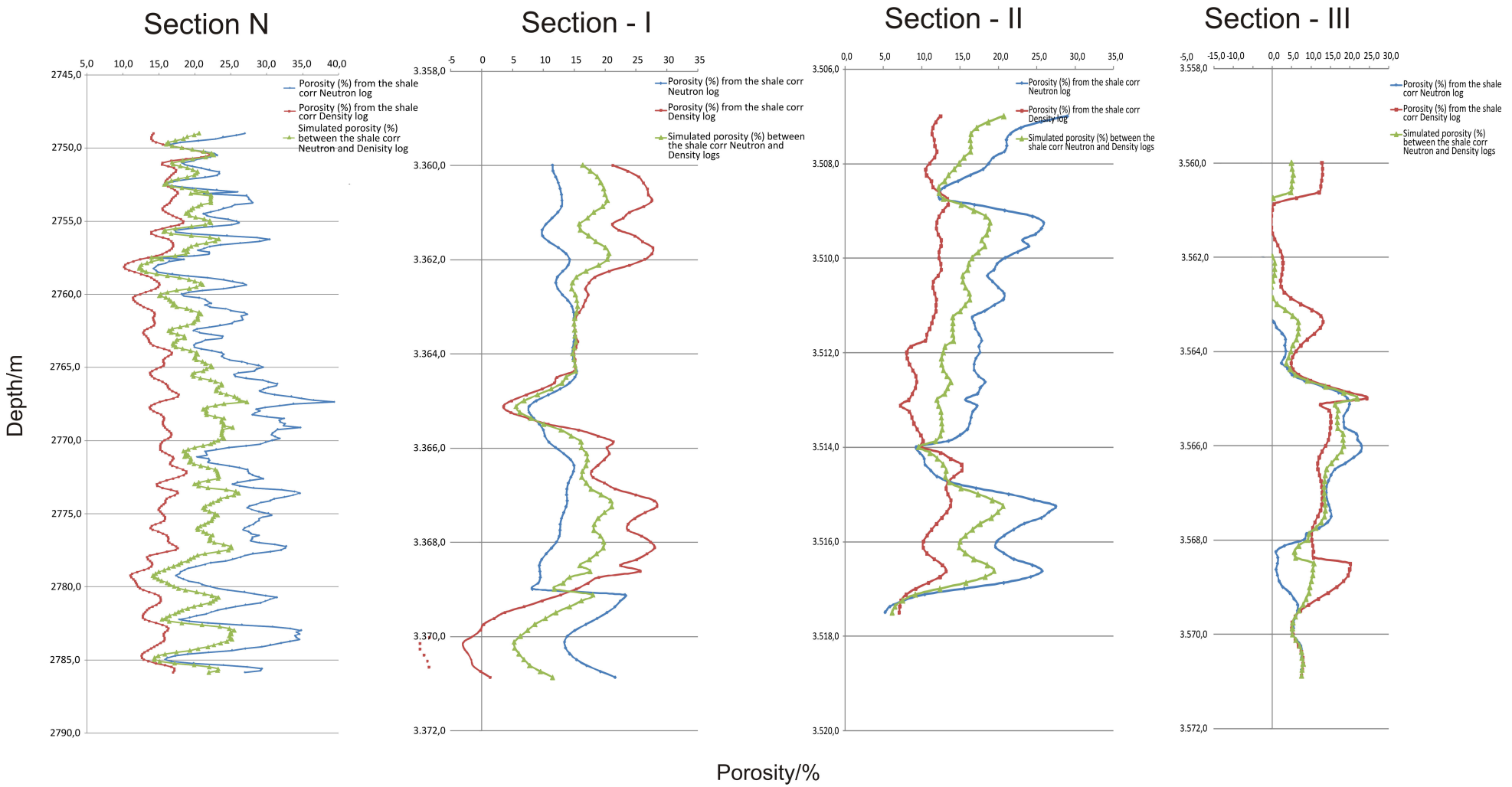

Fig 20. Simulated porosity for all four Sections from Well 6005/15-1 based on the inter median values between the shale corrected Density and Neutron logs.

When comparing the core measured porosities from onshore FIBG with the core measured porosities from offshore Well 6005/15-1 (FIBG) there is a decrease from 17% (all samples) and 16.5% (Malinstindur Formation) to 10.1% (Well 6005/15-1). This could be because the onshore volcaniclastic units have not been buried as deeply as the offshore volcaniclastic rocks. The "stratigraphically" highest measured samples from the onshore volcaniclastics have been buried by <300 m (OEG-050308-G-46, OEG-050308-G-47, OEG-050308-G-48, OEG-050308-G-50 and OEG-050308-G-51), all from the Enni Formation (Appendix I), while the lowest, which are only two (OEG-050308-G-35 and OEG-050308-G-36 from the Beinisvørð Formation), have been buried by approximately 3000 m (Jørgensen 2006). Most samples have been collected from the Malinstindur, Sneis and Enni formations which lie between 300 and 2000 meters deep in the stratigraphy and have therefore not been affected by the same pressure as the two from Beinisvørð Formation (Andersen *et al.* 2002). The measured porosities from Well 6005/15-1 have been taken from a depth of ~3500 m.

The samples from where the porosity and permeability have been measured from the Liaohe Basin in China as well as from the Austral and the Neuquén basins in Argentina vary in depth. From the Liaohe Basin the samples have been taken from depths ranging from ~2250 m to ~2750 m, while the samples from the Neuquén Basin have been taken from depths ranging from ~1000 m to ~1250 m. From the Austal Basin the samples were taken from depths between ~1200 m to ~1700 m. These depths are comparable to the FIBG.

In the case of the Liaohe Basin, the Neuquén Basin, the Austral Basin as well as Well 6005/15-1 the question remains on how much overlying material has been eroded. This is actually still a discussed problem concerning the onshore FIBG as well (Andersen et al 2002; Jørgensen 2006), but according to Waagstein (1988) an estimated few hundred metres have been eroded.

In order to see if depth of burial could have had an affect on the onshore FIBG samples two diagrams were made (Fig. 8a) showing the measured porosity versus depth based on the samples from the Faroe Islands. One diagram included all 43 samples versus depth and the other one included the 20 samples taken from Malinstindur Formation versus depth (Fig. 8a). The linear relationship between all samples versus depth gives an R^2 value of 0.1. For the samples from the Malinstindur Formation versus depth the linear relationship is 0.14. The figure indicate a slight trend in the porosity actually decreasing with depth. It should be noted that all the samples, apart from the two samples from the Beinisvørð Formation (OEG-050308-G-35 and OEG-050308-G-36), are concentrated within a 1 km depth range and this might be a reason for this rather unclear trend.

Alteration can be seen in all the polished sections. Either it can be seen by cementation, recrystallisation or when the glass has altered to various clay minerals. This has apparently had no or little effect on the porosity which in the above discussion and comparison can be considered high. The porosity, most likely, occurs within the vesicles that are often found within coria fragments, which is abundant in the investigated polished sections, or it can be found within dissolved voids and intergranular pores that are too small to observe in the polished sections. This has been seen in the volcaniclasts of the Liaohe Basin in China (Luo *et al.* 2005).

The permeability from the onshore Faroese samples have an average of 0.86 md, ranging from 0.02 md to 6.04 md. Compared to the permeabilities from the hydrocarbon producing volcaniclastic units from the Liaohe Basin in China, permeabilities range from 0.05-170.6 md, with averages between 6.6 and 25.6 md, the permeabilities from the Faroes Islands can be considered low (Luo *et al.* 2005). Compared to the Austal Basin in Argentina where permeabilities range from 0.001–762 md, with averages between 0.002 and 310.9 md, the permeability from the Faroe Islands can again be considered low. Compared to the Neuquén Basin in Argentina, where permeabilities range from 0.003 to 205.3 md, and with averages from 0.43 to 110.53 md the difference is not as great as in the other two cases, but still the permeability is higher compared to the investigated samples from onshore Faroe Islands (Sruoga & Rubinstein 2007). Although the permeability values are low the primary permeability values would have must probably been higher prior to burial and alteration.

In order to see whether or not the permeability decreases with depth two diagrams were made (Fig. 8b). One diagram based on all 30 measured samples from the onshore FIBG and one based on the 15 samples measured from the Malinstindur Formation (Fig. 8b). The R^2 values were 0.1 and 0.12 indicating the same trend that was seen in the porosity versus depth diagrams (i.e. permeability decreased slightly with

depth). Permeability was only measured on samples within a depth range of 1 km.

Permeabilities ranging from 10 to 100 md can be considered good, while permeabilities higher than 100 md are considered exceptionally high (Selley 1976). The permeability average from the onshore FIBG has an average of 0.86 md and is much lower than 10 md. One reason for this low permeability could be the alteration of the glass. In the polished sections it is visible that the glass has altered into various clay minerals and this is, most likely, reflected in the permeability values. Another reason could be the high content of volcanogenic material which is >90%. When looking at the permeability results from Luo *et al.* (2005) it can be seen that their samples classified as volcaniclastics (determined by the content of volcanogenic material) contain between 50-90% volcanogenic material. These samples have low permeability averages of 6.6 md, while the volcaniclastic units that contain less volcanilastic units (ranging from 10-50% volcanogenic material) have a permeability average of 23.5 md. The permeabilities from the Liaohe Basin are not comparable to the ones obtained from the onshore FIBG but the figures from thee Liaohe Basin show that the permeability decreases when the volcaniclasts contain more volcanogenic material suggesting that the permeabilities measured from the onshore FIBG were to be expected. From the Austal Basin in Argentina the same pattern can bee seen. Here the volcaniclastic units classified as rhyolitic tuffs range in permeability from 0.001 – 6.7 md and when the volcaniclastic material becomes mixed with other material, the permeability increases to between 0.002 and 762 md.

The sedimentary horizons that can be found on the Faroe Islands most probably extend further offshore into the Faroe-Shetland Basin and it would be interesting to investigate how porosity and permeability will change when approaching the edge of the lava field. The sediments may become mixed with siliciclastic sediments which would, most likely, increase both porosity and permeability. If this is the case it could possibly increase the reservoir potential in the basin.

6.2 Porosities Derived from Wire-Line Log Data

There is a lack of data in the literature on comparison studies between wire-line derived porosities based on Schlumberger equations and measured porosities from volcaniclastic sediments and this is why this study was undertaken. The trends (R^2) between the wire-line derived porosities and the measured porosities are good (see Section 5.1.1) between the Sections from the sand-prone Malinstindur Formation from Glyvursnes-1 borehole suggesting the wire-line derived porosities can be reliable. The average porosity based on all three Sections from the Malinstindur Formation is 19.0% (Neutron log), 10.2% (Density log) and 17.5% (simulated porosity), while the measured porosity average is 17.3%. This shows that the closest wire-line derived porosity comes from the simulated porosity, hence the "porosity window" method. Again there is a strong correlation between the wire-line derived porosities and the measured porosity.

A similar situation occurs for Section-3 where the (see Section 5.1.1) the porosity average from the Neutron log is 22.6%, from the Density log it is 11.4% while based on the simulated porosity the average is 17.4%. The porosity average from the measured values is 19.2% and the closest wire-line derived porosity average again comes from the simulated porosity, supporting the "porosity window" method.

When comparing the onshore FIBG porosities with the offshore porosities from Well 6005/15-1 porosities it is clear that the trend (R^2) between the wire-line derived porosity and the measured porosity is not as strong as what was seen from the MF in the Glyvursnes-1 borehole. For Section - II in Well 6005/15-1 the Caliper shows some smaller washouts and in some places as much as ~10 cm which could give a small uncertainty in the reliability in the derived Neutron log data.

The measured average porosity from Section - II in Well 6005/15-1 was 10.1% compared to 18.5% (Neutron log), 11.2% (Density log) and 14.8% (simulated porosity). The best comparing wire-line derived porosity average from Section –II comes from the Density log.

Compared to the measured porosity average of 10.1% the closest average value comes from the Density log but the simulated porosity average only differs from the measured porosity average by 4.7% and based on this an approach of getting the simulated porosities from the other three Sections in Well 6005/15-1 was made. The simulated average porosity from Section N (the Kettla Member), was 20.2% which could be likely and this number is not much higher than the average expected form the onshore FIBG, based on all samples from the measured cores had an average of 17.0% slightly decreasing with

depth. From Section –I the simulated porosity average was 15.0% while Section –III had a simulated average porosity of 9.0% (Table 15). These averages are a little bit lower then the porosity average from the onshore FIBG, but are comparable to averages from, for example the Liaohe Basin in China, the Neuquén and Austral Basins in Argentina (see Section 6.1) (Luo *et al.* 2005; Sruoga & Rubinstein 2007) and could indicate possibility for hydrocarbon reservoirs.

This study points towards a possibility of using the Schlumberger equations to calculate porosity for volcaniclastic units when the lithology is known. They shall be used with caution, and as much information on lithology as possible is preferable in order to be able to evaluate the reliability of the derived porosity values.

The "porosity window" method can not give an exact porosity value but it can give a good idea on where the maximum and the minimum values are and could be a quick method of getting the approximate porosity values for sand-prone volcaniclastic sandstones, even for offshore drillings, where ditch cuttings can give a fairly good idea on the lithology and mud content.

6.3 Future Research in the Area

Beyond the scope of this study, but would be interesting to investigate is a more detailed petrographic study of the onshore volcaniclastic sedimentary Sections of the Faroe Islands. Large rounded plagioclase crystals are abundant in some of the samples, as well as other feldspars. It would be interesting to ascertain the origin of these large feldspars. The following question will be, have they been eroded from volcanic areas locally or do they have a more exotic source outside the catchment area (e.g. a non-volcanic source)?

Additionally a more detailed approach to see what types of pores are dominant in the Faroese volcaniclastic rocks, are they connected to primary or to secondary processes, would be preferable.

7. Conclusion

- Porosity and permeability results were obtained from 43 and 30 samples, respectively. The porosity values are generally high with an average of 17% while permeability values are low with an average of 0.86 md.
- Comparison with hydrocarbon producing volcaniclastic units in China and Argentina suggest that the porosities from the onshore Faroe Islands are comparable and good, while permeabilities are generally lower.
- The comparison between the wire-line derived porosities and the core measured porosities from the Glyvursnes-1 borehole shows best R^2 values for the volcaniclastic sandstone samples from the Malinstindur Formation. R^2 values based on Section -3, -2 and -1 are 0.75 from the shale corrected Neutron log versus measured porosity and 0.56 from the shale corrected Density log versus measured porosity. R^2 values from Section -3, are even higher with values of 0.85 for the shale corrected Neutron log and 0.67 for the shale corrected Density log.
- Based on Figure 12a-f it is clear that the measured porosity is found in a "porosity window" between the porosities derived from the shale corrected Neutron log that define maximum values and the porosities from the shale corrected Density log defining the minimum values. Simulated porosities based on the median between the shale corrected Density and Neutron logs were made for the Malinstindur Formation, (sections -3, -2 and -1) and for Section -3 alone. R^2 values were 0.70 and 0.79, respectively, indicating that the best approximate porosity, most likely, is derived from the simulated porosity.
- The R^2 values from the Sneis and Enni formations do not indicate good derived porosity results and the reason is most likely that the samples from the Malinstindur Formation are homogeneous and contain cleaner sandstones than the sandstones from, for example, the Enni formation, where, especially the Argir Beds, contain a lot of mud and clay. The porosity calculations that were used are best suited for clean sandstones and this is, most likely, the reason the best results come from the Malinstindur Formation.
- The measured porosity average from Section – II from Well 6005/15-1 – Longan is 10.1%
- Wire-line derived porosities from Well 6005/15-1 Section – II were compared with measured porosities and the best R^2 value (0.35)

came from the shale corrected Neutron log. The simulated porosity gives an R^2 value of 0.28.

- In the polished sections it is clear that the glass has altered into various secondary minerals (clays, zeolites and calcite). Signs of cementation and crystallization can also be seen, but this does not seem to affect the porosity which is as high as 17% based on all samples from the onshore FIBG.
- Due to the high amount of volcanic debris in the Faorese samples there is a higher degree of alteration, leading to low permeability values.
- The volcanogenic material will, most likely, get mixed with siliciclastic material towards the leading edge of the lava field in the Faroe-Shetland Basin and this could most likely raise both the porosity and permeability increasing the potential for volcaniclastic reservoirs.

8 Acknowledgements

First of all I would like to show my deepest appreciations to my two supervisors, my main supervisor Professor Kent Larsson from the Geological Institution at Lund University and my external supervisor Dr Simon R. Passey from Jarðfeingi for always leaving their doors open to me, thank you so much for all your help. I would also like to show my deepest appreciation to Colin Taylor, Walter Ritchie and David Jolley at the University at Aberdeen for letting me use the laboratory and Colin, thank you for all your help with the measurements and calculations. I would also like to show my greatest gratitude to Romica Øster, John í Sjúrðagarði and Thomas Varming at Jarðfeingi for all their help, Romica and John with collecting and shipping my samples and Thomas when I had problems understanding some of the offshore material. I would also like to thank Professor Anders Lindh, at the Geological Institution at Lund University, for all his help with the microscopy and in the SEM. I would also like to use this opportunity to thank all co-workers and fellow students at the University of Lund as well as my family that has been a great support during my work. Lastly I would like to thank Jarðfeingi and StatoilHydro for providing me with material to work with and finally special thanks goes to StatoilHydro for sponsoring this project and making it possible.

9 References

Andersen, M.S. & Boldreel, L.O. 1995. Tertiary compression structures in the Faeroe-Rockall area. *In:* Scrutton, R.A., Stoker, M.S., Shimmield, G.B. & Tudhope, A.W. (eds). *The Tectonics, Sedimentation and Palaeoceanography of the North Atlantic Region*. Geological Society, London, Special Publications, **90**, 215-216.

Andersen, M.S., Sørensen, A.B., Boldreel, L.O. & Nielsen, T. 2002. Cenozoic evolution of the Faroe Platform: comparing denudation and deposition. *In:* Doré, A.G., Cartwright, J.A., Stoker, M.S., Turner, J.P. & White, N. (eds). *Exhumation of the North Atlantic Margin: Timing, Mechanisms and Implications for Petroleum Exploration*. Geological Society, London, Special Publications, **196**, 291-311.

Doré, A.G., Lundin, E.R., Jensen, L.N., Birkeland, Ø., Eliassen, P.E. & Fichler, C. 1999. Principal tectonic events in the evolution of the northwest European Atlantic margin. *In:* Fleet, A.J. & Boldy, S.A.R. (eds). *Petroleum Geology of Northwest Europe: Proceedings of the 5th Conference*. Geological Society, London, 41-61.

Ellis, D., Bell, B.R., Jolley, D.W. & O'Callaghan, M. 2002. The stratigraphy, environment of eruption and age of the Faroes Lava Group, NE Atlantic Ocean. *In:* Jolley, D.W. & Bell, B.R. (eds). *The North Atlantic Igneous Province: Stratigraphy, Tectonic, Volcanic and Magmatic Processes*. Geological Society, London, Special Publications, **197**, 253-269.

Fisher, R.V. 1961. Proposed classification of volcaniclastic sediments and rocks. *Geological Society of America Bulletin*, **72**, 1409-1414.

Fisher, R.V. 1966. Rocks composed of volcanic fragments and their classification. *Earth-Science Reviews*, **1**, 287-298.

Fisher, R.V. & Smith, G.A. 1991. Volcanism, tectonics and sedimentation. *In:* Fisher, R.V. & Smith, G.A. (eds). *Sedimentation in Volcanic Settings*. SEPM (Society for Sedimentary Geology) Special Publication, **45**, 1-5.

Gees, R.A. 1966. Porosity determination using modal analysis on thin Sections of rock and core material and simulatet well cuttings. *Geologische Rundschau*, **55**, 848-855.

Helland-Hansen, D. 2009. Rosebank - Challenges to

development from a subsurface perspective. *In:* Varming, T. & Ziska, H. (eds). *Faroe Islands Exploration Conference: Proceedings of the 2nd Conference*. Annales Societatis Scientiarum Færoensis, Tórshavn, **50**, 241-245.

Japsen, P., Andersen, C., Andersen, H.L., Andersen, M.S., Boldreel, L.O., Mavko, G., Mohammed, N.G., Pedersen, J.M., Petersen, U.K., Rasmussen, R., Shaw, F., Springer, N., Waagstein, R., White, R.S. & Worthington, M. 2005. Preliminary results from investigations of seismic and petrophysical properties of Faroes basalts in the SeiFaBa project. *In:* Doré, A.G. & Vining, B.A. (eds). *Petroleum Geology: North-West Europe and Global Perspectives - Proceedings of the 6th Petroleum Geology Conference*. Geological Society, London, 1461-1470.

Jolley, D.W., Morton, A. & Prince, I. 2005. Volcanogenic impact on phytogeography and sediment dispersal patterns in the NE Atlantic. *In:* Doré, A.G. & Vining, B.A. (eds). *Petroleum Geology: North-West Europe and Global Perspectives - Proceedings of the 6th Petroleum Geology Conference*. The Geological Society, London, 969-975.

Jørgensen, O. 2006. The regional distribution of zeolites in the basalts of the Faroe Islands and the significance of zeolites as palaeotemperature indicators. *In:* Chalmers, J.A. & Waagstein, R. (eds). *Scientific Results from the Deepened Lopra-1 Borehole, Faroe Islands*. Geological Survey of Denmark and Greenland Bulletin, Copenhagen, **9**, 123-156.

Larsen, L.M., Waagstein, R., Pedersen, A.K. & Storey, M. 1999. Trans-Atlantic correlation of the Palaeogene volcanic successions in the Faeroe Islands and East Greenland. *Journal of the Geological Society, London*, **156**, 1081-1095.

Luo, J., Morad, S., Liang, Z. & Zhu, Y. 2005. Controls on the quality of Archean metamorphic and Jurassic volcanic reservoir rocks from the Xinglongtai buried hill, western depression of Liaohe basin, China. *American Association of Petroleum Geologists Bulletin*, **89**, 1319-1346.

Lund J. 1983. Biostratigraphy of interbasaltic coals from the Faeroe Islands. In: Bott, M.H.P., Saxov, S., Talwani, M. & Thiede, J. (eds). Structure and Development of the Greenland-Scotland Ridge. New Methods and Concepts. Plenum Press, New York, 417-423.

Macdonald, G.A. 1972. *Volcanoes*. Prentice-Hall, Inc., Englewood Cliffs, New Jersey, p. 523.

Noe-Nygaard, A. & Rasmussen, J. 1968. Petrology of a 3,000 metre sequence of basaltic lavas in the Faeroe Islands. *Lithos*, **1**, 286-304.

Passey, S.R. 2004. *The Volcanic and Sedimentary Evolution of the Faeroe Plateau Lava Group, Faeroe Islands and the Faeroe-Shetland Basin, NE Atlantic*. PhD Thesis. University of Glasgow, p. 450.

Passey, S.R. & Bell, B.R. 2007. Morphologies and emplacement mechanisms of the lava flows of the Faroe Islands Basalt Group, Faroe Islands, NE Atlantic Ocean. *Bulletin of Volcanology*, **70**, 139-156.

Passey, S.R. 2009. Recognition of a faulted basalt lava flow sequence through the correlation of stratigraphic marker units, Skopunarfjørður, Faroe Islands. *In:* Varming, T. & Ziska, H. (eds). *Faroe Islands Exploration Conference: Proceedings of the 2nd Conference*. Annales Societatis Scientiarum Færoensis, Tórshavn, **50**, 174-204.

Passey, S.R. & Jolley, D.W. 2009 (for 2008). A revised lithostratigraphic nomenclature for the Palaeogene Faroe Islands Basalt Group, NE Atlantic Ocean. Earth and Environmental Science Transactions of the Royal Society of Edinburgh, 99, 127-158.

Rasmussen, J. & Noe-Nygaard, A. 1969. *Beskrivelse til Geologisk Kort over Færøerne i Målestok 1:50 000*. Danmarks Geologiske Undersøgelse, København, **1/24**, p. 370.

Rasmussen, J. & Noe-Nygaard, A. 1970 (1969). *Geology of the Faeroe Islands (Pre-Quaternary)*. *Trans:* Henderson, G., Geological Survey of Denmark, Copenhagen, **1/25**, p. 142.

Ritchie, J.D., Gatliff, R.W. & Richards, P.C. 1999. Early Tertiary magmatism in the offshore NW UK margin and surrounds. *In:* Fleet, A.J. & Boldy, S.A.R. (eds). *Petroleum Geology of Northwest Europe: Proceedings of the 5th Conference*. Geological Society, London, 573-584.

Saunders, A.D., Fitton, J.G., Kerr, A.C., Norry, M.J. & Kent, R.W. 1997. The North Atlantic Igneous

Province. *In:* Mahoney, J.J. & Coffin, M.L. (eds). *Large Igneous Provinces: Continental, Oceanic, and Planetary Flood Volcanism*. American Geophysical Union, Geophysical Monographs, **100**, 45-93.

Schlumberger 1972: *Log Interpretation Volume I – Principles*. Schlumberger Limited, New York, USA,1-113.

Schlumberger 1979: *Log Interpretation Charts*. Schlumberger Limited, New York, USA, 1-97.

Selley, R. C. 1976. *An Introduction to Sedimentology*. Academic Press Inc, London, p. 419.

Shipboard Scientific Party. 2002. Explanatory Notes. *In:* Tarduno, J.A., Duncan, R.A. & Scholl, D.W. (eds). *Proceedings of the Ocean Drilling Program, Initial Reports*. College Station, Texas (Ocean Drilling Program), **197**, 1-89.

Sørensen, A.B. 2003. Cenozoic basin development and stratigraphy of the Faroes area. *Petroleum Geoscience*, **9**, 189-207.

Sruoga, P., Rubinstein, N. & Hinterwimmer, G. 2004. Porosity and permeability in volcanic rocks: a case study on the Serie Tobífera, South Patagonia, Argentina. *Journal of Volcanology and Geothermal Research*, **132**, 31-43.

Sruoga, P. & Rubinstein, N. 2007. Processes controlling porosity and permeability in volcanic reservoirs from the Austral and Neuquén basins, Argentina. *American Association of Petroleum Geologists Bulletin*, **91**, 115-129.

Varming, T. 2009. Results from the drilling of the 1st license round wells in the Faroese part of the Judd Basin. *In:* Varming, T. & Ziska, H. (eds). *Faroe Islands Exploration Conference: Proceedings of the 2nd Conference*. Annales Societatis Scientiarum Færoensis, Tórshavn, **50**, 346-363.

Waagstein, R. 1988. Structure, composition and age of the Faeroe basalt plateau. *In:* Morton, A.C. & Parson, L.M. (eds). *Early Tertiary Volcanism and the Opening of the NE Atlantic*. Geological Society, London, Special Publications, **39**, 225-238.

Waagstein, R. & Andersen, C. 2003. *Well completion report: Glyvursnes-1 and Vestmanna-1, Faroe Islands*. Geological Survey of Denmark and Greenland, Copenhagen, **2003/99**, p. 67.

Waagstein, R. 2006. Composite log from the Lopra-1/1A well, Faroe Islands. In: Chalmers, J.A. & Waagstein, R. (eds). Scientific Results from the Deepened Lopra-1 Borehole, Faroe Islands. Geological Survey of Denmark and Greenland Bulletin, Copenhagen, 9.

Wentworth, C.K. 1922. A scale of grade and class terms for clastic sediments. *Journal of Geology*, **30**, 377-392.

Appendix I - Sample list

Samp-le No	Lithology	Geology	Location	Borehole		Depth at top from top of core	Altitud
				Project	Year		
G-01	Sandstone	Malanstindur Formation		Glyvursnes	2002	606.73	-590.17
G-02	Sandstone	Malanstindur Formation		Glyvursnes	2002	606.37	-589.81
G-03	Sandstone	Malanstindur Formation		Glyvursnes	2002	606.10	-589.54
G-04	Sandstone	Malanstindur Formation		Glyvursnes	2002	605.48	-588.92
G-05	Sandstone	Malanstindur Formation		Glyvursnes	2002	605.12	-588.56
G-06	Sandstone	Malanstindur Formation		Glyvursnes	2002	604.78	-588.22
G-07	Sandstone	Malanstindur Formation		Glyvursnes	2002	591.75	-575.19
G-08	Sandstone	Malanstindur Formation		Glyvursnes	2002	591.41	-574.85
G-09	Sandstone	Malanstindur Formation (Below the Klaksvík Flow)		Glyvursnes	2002	355.70	-339.14
G-10	Sandstone	Malanstindur Formation (Below the Klaksvík Flow)		Glyvursnes	2002	355.50	-338.94
G-11	Sandstone	Sneis Formation		Glyvursnes	2002	298.49	-281.93
G-12	Sandstone	Sneis Formation		Glyvursnes	2002	297.75	-281.19
G-13	Sandstone	Sneis Formation		Glyvursnes	2002	297.09	-280.53
G-14	Sandstone	Sneis Formation		Glyvursnes	2002	296.80	-280.24
G-15	Sandstone	Enni Formation		Glyvursnes	2002	149.55	-132.99
G-16	Sandstone	Enni Formation		Glyvursnes	2002	149.47	-132.91
G-17	Sandstone	Argir Beds, Enni Form.		Glyvursnes	2002	43.60	-27.04
G-18	Sandstone	Argir Beds, Enni Form.		Glyvursnes	2002	43.37	-26.81
G-19	Sandstone	Argir Beds, Enni From.		Glyvursnes	2002	42.89	-26.33
G-20	Sandstone	Argir Beds, Enni Form.		Glyvursnes	2002	42.39	-25.83
G-21	Sandstone	Argir Beds, Enni Form.		Glyvursnes	2002	48.89	-32.33
G-22	Sandstone	Argir Beds, Enni From.		Glyvursnes	2002	41.24	-24.68
G-23	Sandstone	Argir Beds, Enni Form.		Glyvursnes	2002	40.93	-24.37
G-24	Sandstone	Argir Beds, Enni Form.		Glyvursnes	2002	40.66	-24.10
G-25	Sandstone	Argir Beds, Enni From.		Glyvursnes	2002	40.05	-23.49

Appendix I - Sample list

G-26	Sandstone	Argir Beds, Enni Form.		Glyvursnes	2002	39.90	-23.34
G-27	Sandstone	Argir Beds, Enni Form.		Glyvursnes	2002	39.39	-22.83
G-28	Sandstone	Argir Beds, Enni From.		Glyvursnes	2002	39.05	-22.49
G-29	Sandstone	Malanstindur Formation		KOLBH1-04	2004	18.60	231.40
G-30	Sandstone	Malanstindur Formation		KOLBH1-04	2004	14.71	235.29
G-31	Sandstone	Sund Bed, Sneis Form.	Klaksvík	Norðoyartunnilin	2001	20.30	52.52
G-32	Sandstone	Malanstindur Formation	Leirvik	Norðoyartunnilin	2001	56.54	-24.54
G-33	Sandstone	Malanstindur Formation	Leirvik	Norðoyartunnilin	2001	56.20	-24.20
G-34	Sandstone	Malanstindur Formation	Leirvik	Norðoyartunnilin	2001	55.80	-23.80
G-35	Mudstone	Beinisvørð Formation		Sumbiartunnulin	1985	51.64 (63.08)	114.41
G-36	Mudstone	Beinisvørð Formation		Sumbiartunnulin	1985	51.03 (62.47)	115.02
G-37	Mudstone	Beinisvørð Formation		Sumbiartunnulin	1985	30.00	147.49
G-38	Conglomerate	Beinisvørð Formation		Sumbiartunnulin	1989	41.92	202.00
G-39	Mudstone	Beinisvørð Formation		Hov-Øravík tunnil	2004	140.15	16.92
G-40	Mudstone	Beinisvørð Formation		Hov-Øravík tunnil	2004	138.79	18.28
G-41	Mudstone	Beinisvørð Formation		Hov-Øravík tunnil	2004	97.91	59.16
G-42	Mudstone	Beinisvørð Formation		Hov-Øravík tunnil	2004	96.81	60.26
G-43	Mudstone	Beinisvørð Formation		Hov-Øravík tunnil	2004	33.87	123.20
G-44	Mudstone	Beinisvørð Formation		Hov-Øravík tunnil	2004	32.53	124.54
G-45	Sandstone	Enni Formation		Neshagi	2005	11.30	139.25
G-46	Sandstone	Enni Formation		Neshagi	2005	10.54	140.01
G-47	Sandstone	Enni Formation		Neshagi	2005	10.22	140.33
G-48	Sandstone	Enni Formation		Neshagi	2005	9.79	140.76
G-49	Sandstone	Enni Formation		Neshagi	2005	11.30	142.13
G-50	Sandstone	Enni Formation		Neshagi	2005	10.72	142.71

Appendix I - Sample list

G-51	Sandstone	Enni Formation		Neshagi	2005	10.27	143.16
G-52	Sandstone	Kvívík Beds, Malanstindur Formation	Svínáir				55.75
G-53	Sandstone	Kvívík Beds, Malanstindur Formation	Svínáir				55.97
G-54	Sandstone	Malanstindur Formation	í Bugum				70.15
G-55	Sandstone	Malanstindur Formation	í Bugum				70.80
G-56	Sandstone	Malanstindur Formation	Leynavatn				70.90
G-57	Sandstone	Malanstindur Formation	Leynavatn				71.30
G-58	Sandstone	Malanstindur Formation	Stykkið				30.50
G-59	Sandstone	Malanstindur Formation	Stykkið				30.95
G-60	Sandstone	Sund Bed, Sneis Form.	Sund Quarry				10.00
G-61	Sandstone	Sund Bed, Sneis Form.	Sund Quarry				10.00
G-62	Sandstone	Argir Beds, Enni Form.	Norðasta-horn				170.00
G-63	Sandstone	Argir Beds, Enni Form.	Norðasta-horn				171.00
G-64	Sandstone	Sneis Formation	Syðradalsá				125.25
G-65	Sandstone	Sneis Formation	Syðradalsá				125.70
G-66	Sandstone	Sneis Formation	Syðradalsá				126.20
G-67	Sandstone	Enni Formation	Skíturin				6.10
G-68	Sandstone	Enni Formation	Skíturin				7.10
G-69	Sandstone	Enni Formation	Skíturin				8.40
G-70	Sandstone	Enni Formation	Skíturin				9.60

Appendix II - Measured porosity and permeability

Sample No	Porosity (%)	Permeability (md)
OEG-040308-G-01	16.0	1.35
OEG-040308-G-02	22.4	1.89
OEG-040308-G-03	30.3	0.03
OEG-040308-G-04	13.5	0.56
OEG-040308-G-05	11.8	0.10
OEG-040308-G-06	10.3	0.19
OEG-040308-G-07	10.9	0.21
OEG-040308-G-09	21.4	1.14
OEG-040308-G-10	19.1	0.02
OEG-040308-G-11	10.1	6.04
OEG-040308-G-12	13.5	1.78
OEG-040308-G-13	9.7	0.12
OEG-040308-G-14	12.1	0.10
OEG-040308-G-15	10.5	0.90
OEG-040308-G-17	9.1	0.87
OEG-040308-G-18	14.3	3.45
OEG-040308-G-22	32.4	3.80
OEG-040308-G-23	17.9	0.02
OEG-040308-G-24	46.4	1.62
OEG-040308-G-26	19.7	0.28
OEG-040308-G-27	23.8	0.35
OEG-040308-G-28	23.3	0.13
OEG-050308-G-30	0.1	
OEG-050308-G-31	22.4	
OEG-050308-G-32	23.0	
OEG-050308-G-33	29.2	
OEG-050308-G-34	3.4	
OEG-050308-G-35	8.6	
OEG-050308-G-36	6.0	
OEG-050308-G-46	9.8	
OEG-050308-G-47	21.1	
OEG-050308-G-48	29.5	
OEG-050308-G-50	5.8	
OEG-050308-G-51	6.8	
OEG-060308-G-52	15.8	0.02
OEG-060308-G-53	13.1	0.03
OEG-060308-G-54	10.5	
OEG-060308-G-56	7.4	0.09
OEG-060308-G-57	23.2	0.44
OEG-060308-G-58	27.9	0.23
OEG-060308-G-59	19.9	0.05
OEG-060308-G-60	24.8	0.09
OEG-060308-G-61	24.2	0.07

Appendix III- Measured porosity

25.4mm **Porosity as measured using the Jones porosiometer**

Plug I.D.	Z_{i1} (psig)	P_{i1} (psig)	P_{f1} (psig)	Z_{f1} (psig)	Z_{i2} (psig)	P_{i2} (psig)	P_{f2} (psig)	Z_{f2} (psig)	Z_{i3} (psig)	P_{i3} (psig)	P_{f3} (psig)	Z_{f3} (psig)	V_a (cm^3)	V_b (cm^3)	V_c (cm^3)	V_d (cm^3)	V_{ref} (cm^3)	V_{grain} (cm^3)	Corr. V_{grain} (cm^3)
Calibration	0,46	97,58	90,55	0,46	0,46	97,43	73,87	0,46					3,204	3,206	6,418	12,85	*26,422*		
OEG-040308-G-01	0,46	97,58	90,55	0,46	0,46	97,43	73,87	0,46	0,49	97,63	81,45	0,49	0	3,206	0	12,85	*26,422*	12,836	*12,194*
OEG-040308-G-02	0,46	97,58	90,55	0,46	0,46	97,43	73,87	0,46	0,47	97,04	80,75	0,47	3,204	3,206	6,418	0	*26,422*	9,528	*9,052*
OEG-040308-G-03	0,46	97,58	90,55	0,46	0,46	97,43	73,87	0,46	0,46	97,35	83,73	0,46	3,204	3,206	0	0	*26,422*	4,150	*3,943*
OEG-040308-G-04	0,46	97,58	90,55	0,46	0,46	97,43	73,87	0,46	0,49	97,70	83,84	0,49	3,204	3,206	6,418	0	*26,422*	10,496	*9,971*
OEG-040308-G-05	0,46	97,58	90,55	0,46	0,46	97,43	73,87	0,46	0,49	97,75	83,08	0,49	0	3,206	0	12,85	*26,422*	13,424	*12,752*
OEG-040308-G-06	0,46	97,58	90,55	0,46	0,46	97,43	73,87	0,46	0,49	97,68	86,30	0,49	3,204	0	6,418	0	*26,422*	8,180	*7,771*
OEG-040308-G-07	0,46	97,58	90,55	0,46	0,46	97,43	73,87	0,46	0,49	97,71	84,13	0,49	3,204	3,206	6,418	0	*26,422*	10,600	*10,070*
OEG-040308-G-08																			
OEG-040308-G-09	0,46	97,58	90,55	0,46	0,46	97,43	73,87	0,46	0,48	97,95	80,10	0,48	3,204	3,206	6,418	0	*26,422*	8,966	*8,518*
OEG-040308-G-10	0,46	97,58	90,55	0,46	0,46	97,43	73,87	0,46	0,49	97,71	80,66	0,49	0	3,206	0	12,85	*26,422*	12,498	*11,873*
OEG-040308-G-11	0,46	97,58	90,55	0,46	0,46	97,43	73,87	0,46	0,49	97,63	87,74	0,49	3,204	3,206	0	0	*26,422*	5,477	*5,203*
OEG-040308-G-12	0,46	97,58	90,55	0,46	0,46	97,43	73,87	0,46	0,49	97,69	86,06	0,49	3,204	0	6,418	0	*26,422*	8,093	*7,688*
OEG-040308-G-13	0,46	97,58	90,55	0,46	0,46	97,43	73,87	0,46	0,49	97,67	87,75	0,49	3,204	3,206	0	0	*26,422*	5,468	*5,195*
OEG-040308-G-14	0,46	97,58	90,55	0,46	0,46	97,43	73,87	0,46	0,49	97,75	82,25	0,49	0	3,206	0	12,85	*26,422*	13,108	*12,452*
OEG-040308-G-15	0,46	97,58	90,55	0,46	0,46	97,43	73,87	0,46	0,49	97,70	85,45	0,49	3,204	3,206	6,418	0	*26,422*	11,080	*10,526*
OEG-040308-G-16																			
OEG-040308-G-17	0,46	97,58	90,55	0,46	0,46	97,43	73,87	0,46	0,49	97,67	85,44	0,49	3,204	3,206	6,418	0	*26,422*	11,086	*10,532*
OEG-040308-G-18	0,46	97,58	90,55	0,46	0,46	97,43	73,87	0,46	0,49	97,71	89,60	0,49	3,204	0	0	0	*26,422*	2,861	*2,718*
OEG-040308-G-19																			
OEG-040308-G-20																			
OEG-040308-G-21																			
OEG-040308-G-22	0,46	97,58	90,55	0,46	0,46	97,43	73,87	0,46	0,47	97,03	77,06	0,47	3,204	3,206	6,418	0	*26,422*	8,001	*7,601*
OEG-040308-G-23	0,46	97,58	90,55	0,46	0,46	97,43	73,87	0,46	0,47	97,69	82,57	0,49	3,204	3,206	6,418	0	*26,422*	10,016	*9,515*
OEG-040308-G-24	0,46	97,58	90,55	0,46	0,46	97,43	73,87	0,46	0,46	97,07	77,32	0,47	0	3,206	6,418	0	*26,422*	4,892	*4,647*
OEG-040308-G-25																			
OEG-040308-G-26	0,46	97,58	90,55	0,46	0,46	97,43	73,87	0,46	0,49	97,48	81,45	0,49	3,204	3,206	6,418	0	*26,422*	9,658	*9,175*
OEG-040308-G-27	0,46	97,58	90,55	0,46	0,46	97,43	73,87	0,46	0,48	97,83	80,52	0,49	3,204	3,206	6,418	0	*26,422*	9,172	*8,713*

Plug I.D.	V_{pore} (cm^3)	Length (cm)	Diameter (cm)	V_{plug} (cm^3)	Wt (g)	Φ (%)	Grain Den. (g/cm^3)	Rock Den. (g/cm^3)	% loss of volume Used in T (Corr grain vol)	$V_{plug\ corr}$ (cm^3)	$V_{pore\ corr}$ (cm^3)	Φ (%)
Calibration												
OEG-040308-G-01	*3,893*	3,20	2,53	16,09	31,73	*24,20*	2,47	2,08	5,00	15,28	2,45	16,01
OEG-040308-G-02	*3,866*	2,59	2,52	12,92	26,12	*29,93*	2,74	2,13	5,00	12,27	2,74	22,36
OEG-040308-G-03	*2,322*	1,25	2,53	6,26	12,20	*37,06*	2,94	2,05	5,00	5,95	1,80	30,26
OEG-040308-G-04	*2,797*	2,55	2,52	12,77	26,57	*21,91*	2,53	2,19	5,00	12,13	1,63	13,47
OEG-040308-G-05	*3,262*	3,19	2,53	16,01	34,40	*20,37*	2,56	2,26	5,00	15,21	1,79	11,76
OEG-040308-G-06	*1,823*	1,93	2,52	9,59	19,85	*19,00*	2,43	2,18	5,00	9,11	0,93	10,25
OEG-040308-G-07	*2,454*	2,51	2,52	12,52	24,46	*19,59*	2,31	2,06	5,00	11,90	1,30	10,91
OEG-040308-G-08									5,00			
OEG-040308-G-09	*3,495*	2,40	2,53	12,01	23,70	*29,09*	2,78	2,08	5,00	11,41	2,45	21,43
OEG-040308-G-10	*4,388*	3,19	2,55	16,26	33,75	*26,99*	2,84	2,18	5,00	15,45	2,95	19,10
OEG-040308-G-11	*1,207*	1,28	2,53	6,41	13,58	*18,82*	2,61	2,23	5,00	6,09	0,61	10,06
OEG-040308-G-12	*2,160*	1,96	2,53	9,85	19,72	*21,94*	2,57	2,11	5,00	9,36	1,26	13,50
OEG-040308-G-13	*1,183*	1,32	2,48	6,38	13,73	*18,54*	2,64	2,27	5,00	6,06	0,59	9,74
OEG-040308-G-14	*3,242*	3,12	2,53	15,69	34,55	*20,66*	2,77	2,32	5,00	14,91	1,80	12,09
OEG-040308-G-15	*2,509*	2,60	2,53	13,04	26,00	*19,25*	2,47	2,10	5,00	12,38	1,30	10,52
OEG-040308-G-16									5,00			
OEG-040308-G-17	*2,301*	2,57	2,52	12,83	26,13	*17,93*	2,48	2,14	5,00	12,19	1,11	9,07
OEG-040308-G-18	*0,795*	0,70	2,53	3,51	6,88	*22,64*	2,53	2,06	5,00	3,34	0,48	14,28
OEG-040308-G-19									5,00			
OEG-040308-G-20									5,00			
OEG-040308-G-21									5,00			
OEG-040308-G-22	*4,854*	2,50	2,52	12,45	24,80	*38,97*	3,26	2,10	5,00	11,83	3,83	32,38
OEG-040308-G-23	*3,324*	2,56	2,53	12,84	25,17	*25,89*	2,65	2,06	5,00	12,20	2,18	17,88
OEG-040308-G-24	*4,954*	1,92	2,53	9,60	18,74	*51,60*	4,03	2,05	5,00	9,12	4,23	46,37
OEG-040308-G-25									5,00			
OEG-040308-G-26	*3,488*	2,53	2,52	12,66	24,44	*27,55*	2,66	2,03	5,00	12,03	2,37	19,72
OEG-040308-G-27	*3,951*	2,54	2,52	12,66	24,41	*31,20*	2,80	2,03	5,00	12,03	2,86	23,76
OEG-040308-G-28	*4,942*	3,19	2,53	16,08	31,19	*30,74*	2,80	2,04	5,00	15,28	3,55	23,25

Appendix III- Measured porosity

37mm **Porosity as measured using the Jones porosiometer**

Plug I.D.	Z_{i1} (psig)	P_{i1} (psig)	P_{f1} (psig)	Z_{f1} (psig)	Z_{i2} (psig)	P_{i2} (psig)	P_{f2} (psig)	Z_{f2} (psig)	Z_{i3} (psig)	P_{i3} (psig)	P_{f3} (psig)	Z_{f3} (psig)	V_a (cm^3)	V_b (cm^3)	V_c (cm^3)	V_d (cm^3)	V_e (cm^3)	V_s (cm^3)	V_{ref} (cm^3)
Calibration	0,45	97,33	79,97	0,45	0,45	97,32	56,28	0,45					7,359	7,389	14,8	29,65	29,66	11,66	*28,639*
OEG-060308-G-52	0,45	97,33	79,97	0,45	0,45	97,32	56,28	0,45	0,48	97,31	60,9	0,48	7,359	0	14,8	29,65	0	0	*28,639*
OEG-060308-G-53	0,45	97,33	79,97	0,45	0,45	97,32	56,28	0,45	0,47	97,38	65,51	0,47	7,359	7,389	14,8	0	0	0	*28,639*
OEG-060308-G-54	0,45	97,33	79,97	0,45	0,45	97,32	56,28	0,45	0,48	97,35	69,56	0,48	7,359	7,389	14,8	0	0	0	*28,639*
OEG-060308-G-55																			
OEG-060308-G-56	0,45	97,33	79,97	0,45	0,45	97,32	56,28	0,45	0,47	97,34	65,78	0,47	7,359	7,389	14,8	29,65	0	0	*28,639*
OEG-060308-G-57	0,45	97,33	79,97	0,45	0,45	97,32	56,28	0,45	0,47	97,36	61,65	0,47	7,359	0	0	29,65	0	0	*28,639*
OEG-060308-G-58	0,45	97,33	79,97	0,45	0,45	97,32	56,28	0,45	0,47	97,34	52,15	0,47	7,359	7,389	14,8	29,65	0	0	*28,639*
OEG-060308-G-59	0,45	97,33	79,97	0,45	0,45	97,32	56,28	0,45	0,47	97,36	56,92	0,47	7,359	0	14,8	29,65	0	0	*28,639*
OEG-060308-G-60	0,45	97,33	79,97	0,45	0,45	97,32	56,28	0,45	0,48	97,37	64,73	0,48	7,359	7,389	14,8	0	0	0	*28,639*
OEG-060308-G-61	0,45	97,33	79,97	0,45	0,45	97,32	56,28	0,45	0,47	97,35	58,83	0,47	7,359	7,389	0	29,65	0	0	*28,639*

Plug I.D.	V_{grain} (cm^3)	Corr. V_{grain} (cm^3)	V_{pore} (cm^3)	Length (cm)	Diameter (cm)	V_{plug} (cm^3)	Wt (g)	Φ(%)	Grain Den. (g/cm^3)	Rock Den. (g/cm^3)	% loss of volume Used in T (Corr grain vol)	$V_{plug\ corr}$ (cm^3)	$V_{pore\ corr}$ (cm^3)	Φ(%)
Calibration														
OEG-060308-G-52	40,800	*40,392*	*8,163*	4,42	3,76	48,963	108,22	*16,81*	2,65	2,23	1,00	48,47	7,67	15,83
OEG-060308-G-53	21,767	*21,549*	*3,541*	2,30	3,74	25,308	53,72	*14,11*	2,47	2,14	1,00	25,05	3,29	13,12
OEG-060308-G-54	24,279	*24,036*	*3,134*	2,49	3,74	27,413	60,36	*11,54*	2,49	2,22	1,00	27,14	2,86	10,54
OEG-060308-G-55											1,00			
OEG-060308-G-56	51,608	*51,092*	*4,688*	5,07	3,76	56,295	125,00	*8,40*	2,42	2,24	1,00	55,73	4,12	7,40
OEG-060308-G-57	26,542	*26,277*	*8,371*	3,16	3,75	34,913	70,19	*24,16*	2,64	2,03	1,00	34,56	8,02	23,21
OEG-060308-G-58	40,405	*40,001*	*16,168*	5,10	3,76	56,573	97,85	*28,79*	2,42	1,75	1,00	56,01	15,60	27,86
OEG-060308-G-59	37,542	*37,166*	*9,813*	4,28	3,75	47,355	86,95	*20,89*	2,32	1,85	1,00	46,88	9,34	19,92
OEG-060308-G-60	21,251	*21,039*	*7,298*	2,54	3,78	28,549	59,80	*25,76*	2,81	2,12	1,00	28,26	7,01	24,81
OEG-060308-G-61	31,744	*31,427*	*10,551*	3,76	3,78	42,296	90,32	*25,14*	2,85	2,16	1,00	41,87	10,13	24,19

41mm **Porosity as measured using the Jones porosiometer**

Plug I.D.	Z_{i1} (psig)	P_{i1} (psig)	P_{f1} (psig)	Z_{f1} (psig)	Z_{i2} (psig)	P_{i2} (psig)	P_{f2} (psig)	Z_{f2} (psig)	Z_{i3} (psig)	P_{i3} (psig)	P_{f3} (psig)	Z_{f3} (psig)	V_a (cm^3)	V_b (cm^3)	V_c (cm^3)	V_d (cm^3)	V_e (cm^3)	V_s (cm^3)	V_{ref} (cm^3)	V_{grain} (cm^3)
Calibration	0,45	97,31	60,02	0,45	0,45	97,32	45,55	0,45					7,359	7,389	14,8	29,65	29,66	11,66	*50,701*	
OEG-050308-G-30	0,45	97,31	60,02	0,45	0,45	97,32	45,55	0,45	0,45	97,23	62,26	0,45	0	7,389	14,8	0	0	0	*50,701*	25,242
OEG-050308-G-31	0,45	97,31	60,02	0,45	0,45	97,32	45,55	0,45	0,48	97,38	56,79	0,48	0	7,389	0	0	29,66	0	*50,701*	32,239
OEG-050308-G-32	0,45	97,31	60,02	0,45	0,45	97,32	45,55	0,45	0,47	97,4	56,3	0,47	7,359	7,389	14,8	0	0	0	*50,701*	23,962
OEG-050308-G-33	0,45	97,31	60,02	0,45	0,45	97,32	45,55	0,45	0,44	97,34	54,84	0,44	0	7,389	0	0	29,66	0	*50,701*	29,176
OEG-050308-G-34	0,45	97,31	60,02	0,45	0,45	97,32	45,55	0,45	0,44	97,27	62,3	0,44	0	7,389	0	0	29,66	0	*50,701*	40,124
OEG-050308-G-35	0,45	97,31	60,02	0,45	0,45	97,32	45,55	0,45	0,44	97,34	59,45	0,44	0	7,389	14,8	0	0	0	*50,701*	21,372
OEG-050308-G-36	0,45	97,31	60,02	0,45	0,45	97,32	45,55	0,45	0,44	97,24	61,08	0,44	0	7,389	14,8	0	0	0	*50,701*	23,694
OEG-050308-G-37																				
OEG-050308-G-38	0,45	97,31	60,02	0,45	0,45	97,32	45,55	0,45	0,44	97,2	64,68	0,44	0	7,389	0	0	29,66	0	*50,701*	43,120
OEG-050308-G-39																				
OEG-050308-G-40																				
OEG-050308-G-41																				
OEG-050308-G-42																				
OEG-050308-G-43																				
OEG-050308-G-44																				
OEG-050308-G-45																				
OEG-050308-G-46	0,45	97,31	60,02	0,45	0,45	97,32	45,55	0,45	0,48	97,38	60,7	0,48	0	7,389	0	0	29,66	0	*50,701*	37,904
OEG-050308-G-47	0,45	97,31	60,02	0,45	0,45	97,32	45,55	0,45	0,48	97,38	56,93	0,48	0	0	0	0	29,66	0	*50,701*	25,067
OEG-050308-G-48	0,45	97,31	60,02	0,45	0,45	97,32	45,55	0,45	0,44	97,29	55,35	0,44	0	7,389	0	0	29,66	0	*50,701*	30,061
OEG-050308-G-49																				
OEG-050308-G-50	0,45	97,31	60,02	0,45	0,45	97,32	45,55	0,45	0,48	97,36	59,3	0,48	0	0	0	0	29,66	0	*50,701*	28,591
OEG-050308-G-51	0,45	97,31	60,02	0,45	0,45	97,32	45,55	0,45	0,48	97,31	60,9	0,48	0	7,389	0	0	29,66	0	*50,701*	38,233

Plug I.D.	Corr. V_{grain} (cm^3)	V_{pore} (cm^3)	Length (cm)	Diameter (cm)	V_{plug} (cm^3)	Wt (g)	Φ (%)	Grain Den. (g/cm^3)	Rock Den. (g/cm^3)	% loss of volume Used in T (Corr grain vol)	$V_{plug\ corr}$ (cm^3)	$V_{pore\ corr}$ (cm^3)	Φ (%)
Calibration													
OEG-050308-G-30	*24,485*	*0,813*	1,9290	4,1470	26,055	59,20	3,213	2,345	2,342	3,00	25,27	0,03	0,12
OEG-050308-G-31	*31,272*	*10,588*	3,1540	4,1580	42,827	84,66	25,294	2,626	2,038	3,00	41,54	9,30	*22,39*
OEG-050308-G-32	*23,243*	*8,100*	2,4320	4,0970	32,062	58,80	25,842	2,454	1,891	3,00	31,10	7,14	22,95
OEG-050308-G-33	*28,301*	*13,275*	3,1920	4,1150	42,451	85,13	31,930	2,918	2,067	3,00	41,18	12,00	29,15
OEG-050308-G-34	*38,921*	*2,702*	3,2280	4,1100	42,826	88,79	6,491	2,213	2,137	3,00	41,54	1,42	3,41
OEG-050308-G-35	*20,731*	*2,739*	1,7920	4,1390	24,111	51,44	11,670	2,407	2,199	3,00	23,39	2,02	8,62
OEG-050308-G-36	*22,983*	*2,295*	1,9400	4,1300	25,989	58,29	9,080	2,460	2,312	3,00	25,21	1,52	6,01
OEG-050308-G-37										3,00			
OEG-050308-G-38	*41,826*	*-0,669*	3,2390	4,0850	42,451	116,97	-1,626	2,713	2,841	3,00	41,18	-1,94	-4,72
OEG-050308-G-39										3,00			
OEG-050308-G-40										3,00			
OEG-050308-G-41										3,00			
OEG-050308-G-42										3,00			
OEG-050308-G-43										3,00			
OEG-050308-G-44										3,00			
OEG-050308-G-45										3,00			
OEG-050308-G-46	*36,767*	*5,433*	3,1900	4,1590	43,337	92,20	12,874	2,432	2,193	3,00	42,04	4,13	9,83
OEG-050308-G-47	*24,315*	*7,689*	2,4380	4,1360	32,756	64,91	24,025	2,589	2,043	3,00	31,77	6,71	21,11
OEG-050308-G-48	*29,159*	*13,895*	3,2170	4,1710	43,956	89,00	32,274	2,961	2,087	3,00	42,64	12,58	29,50
OEG-050308-G-49										3,00			
OEG-050308-G-50	*27,733*	*2,701*	2,3000	4,1620	31,291	71,54	8,874	2,502	2,357	3,00	30,35	1,76	5,80
OEG-050308-G-51	*37,086*	*4,078*	3,1830	4,1140	42,311	71,22	9,907	1,863	1,735	3,00	41,04	2,81	6,84

Appendix IV- Measured permeability from the Jones permeameter

Faroe Island Samples (Oluva Ellingsgaard) 06/05/08

Sample I.D.	Press. In psig	Press. Out Inch/Oil	Flow ml/sec q	Atm. Press atma B	Gas Viscosity cP u	Length cm L	Diameter cm	X Sect. Area cm^2 A	Press. In. atmg Pug	Press. out atmg Pog	Pav atma	Permeability Kapp, mD	1/Pav (1/atma)
OEG-040308-G-01	4,00	0,40	0,04	0,98	0,0176	3,20	2,53	5,03	0,272	0,001	0,273	1,46	3,67
	8,00	0,85	0,09	0,98	0,0176	3,20	2,53	5,03	0,544	0,002	0,545	1,39	1,83
	16,00	2,01	0,20	0,98	0,0176	3,20	2,53	5,03	1,089	0,005	1,091	1,35	0,92
	32,00	5,25	0,53	0,98	0,0176	3,20	2,53	5,03	2,177	0,013	2,184	1,30	0,46
	56,00	12,40	1,25	0,98	0,0176	3,20	2,53	5,03	3,811	0,030	3,826	1,25	0,26
												1,35	
OEG-040308-G-02	4,00	0,60	0,06	0,98	0,0176	2,59	2,52	4,99	0,272	0,001	0,273	1,80	3,66
	8,00	1,45	0,15	0,98	0,0176	2,59	2,52	4,99	0,544	0,004	0,546	1,93	1,83
	16,00	3,65	0,37	0,98	0,0176	2,59	2,52	4,99	1,089	0,009	1,093	2,00	0,91
	32,00	9,30	0,94	0,98	0,0176	2,59	2,52	4,99	2,177	0,023	2,189	1,88	0,46
	56,00	22,00	2,22	0,98	0,0176	2,59	2,52	4,99	3,811	0,054	3,838	1,82	0,26
												1,89	
OEG-040308-G-03	16,00	0,20	0,02	0,98	0,0176	1,25	2,53	5,02	1,089	0,000	1,089	0,05	0,92
	32,00	0,20	0,02	0,98	0,0176	1,25	2,53	5,02	2,177	0,000	2,178	0,02	0,46
	56,00	0,20	0,02	0,98	0,0176	1,25	2,53	5,02	3,811	0,000	3,811	0,01	0,26
												0,03	
OEG-040308-G-04	10,00	0,65	0,07	0,98	0,0176	2,55	2,52	5,00	0,680	0,002	0,681	0,64	1,47
	20,00	1,50	0,15	0,98	0,0176	2,55	2,52	5,00	1,361	0,004	1,363	0,59	0,73
	30,00	2,10	0,21	0,98	0,0176	2,55	2,52	5,00	2,041	0,005	2,044	0,46	0,49
	40,00	3,90	0,39	0,98	0,0176	2,55	2,52	5,00	2,722	0,010	2,727	0,54	0,37
	50,00	5,50	0,56	0,98	0,0176	2,55	2,52	5,00	3,402	0,013	3,409	0,54	0,29
												0,55	
OEG-040308-G-05	30,00	0,42	0,04	0,98	0,0176	3,19	2,53	5,02	2,041	0,001	2,042	0,11	0,49
	40,00	0,59	0,06	0,98	0,0176	3,19	2,53	5,02	2,722	0,001	2,723	0,10	0,37
	50,00	0,68	0,07	0,98	0,0176	3,19	2,53	5,02	3,402	0,002	3,403	0,08	0,29
												0,10	
OEG-040308-G-06	4,00	0,10	0,01	0,98	0,0176	1,93	2,52	4,98	0,272	0,000	0,272	0,22	3,67
	8,00	0,20	0,02	0,98	0,0176	1,93	2,52	4,98	0,544	0,000	0,545	0,20	1,84
	16,00	0,45	0,05	0,98	0,0176	1,93	2,52	4,98	1,089	0,001	1,089	0,18	0,92
	32,00	1,10	0,11	0,98	0,0176	1,93	2,52	4,98	2,177	0,003	2,179	0,16	0,46
	56,00	2,60	0,26	0,98	0,0176	1,93	2,52	4,98	3,811	0,006	3,814	0,16	0,26
												0,19	
OEG-040308-G-07	8,00	0,15	0,02	0,98	0,0176	2,51	2,52	4,98	0,544	0,000	0,545	0,19	1,84
	16,00	0,40	0,04	0,98	0,0176	2,51	2,52	4,98	1,089	0,001	1,089	0,21	0,92
	32,00	1,10	0,11	0,98	0,0176	2,51	2,52	4,98	2,177	0,003	2,179	0,21	0,46
	56,00	2,56	0,26	0,98	0,0176	2,51	2,52	4,98	3,811	0,006	3,814	0,20	0,26
												0,21	
OEG-040308-G-09	2,00	0,23	0,02	0,98	0,0176	2,40	2,53	5,01	0,136	0,001	0,136	1,34	7,33
	4,00	0,42	0,04	0,98	0,0176	2,40	2,53	5,01	0,272	0,001	0,273	1,15	3,67
	8,00	0,91	0,09	0,98	0,0176	2,40	2,53	5,01	0,544	0,002	0,545	1,12	1,83
	16,00	1,91	0,19	0,98	0,0176	2,40	2,53	5,01	1,089	0,005	1,091	0,96	0,92
												1,14	
OEG-040308-G-10	56,50	0,24	0,02	0,98	0,0176	3,19	2,55	5,09	3,845	0,001	3,845	0,02	0,26
												0,02	
OEG-040308-G-11	2,00	1,90	0,19	0,98	0,0176	1,30	2,53	5,01	0,136	0,005	0,138	6,21	7,22
	4,00	3,95	0,40	0,98	0,0176	1,30	2,53	5,01	0,272	0,010	0,277	6,05	3,61
	8,00	8,75	0,88	0,98	0,0176	1,30	2,53	5,01	0,544	0,021	0,555	5,97	1,80
	16,00	21,30	2,15	0,98	0,0176	1,30	2,53	5,01	1,089	0,052	1,115	5,98	0,90
	22,00	33,40	3,37	0,98	0,0176	1,30	2,53	5,01	1,497	0,082	1,538	6,01	0,65
												6,04	
OEG-040308-G-12	4,00	0,80	0,08	0,98	0,0176	1,96	2,53	5,03	0,272	0,002	0,273	1,80	3,66
	8,00	1,85	0,19	0,98	0,0176	1,96	2,53	5,03	0,544	0,005	0,547	1,86	1,83
	16,00	4,40	0,44	0,98	0,0176	1,96	2,53	5,03	1,089	0,011	1,094	1,81	0,91
	32,00	11,50	1,16	0,98	0,0176	1,96	2,53	5,03	2,177	0,028	2,192	1,74	0,46
	56,00	27,30	2,76	0,98	0,0176	1,96	2,53	5,03	3,811	0,067	3,844	1,70	0,26
												1,78	
OEG-040308-G-13	20,00	0,55	0,06	0,98	0,0176	1,32	2,48	4,83	1,361	0,001	1,362	0,12	0,73
	30,00	1,00	0,10	0,98	0,0176	1,32	2,48	4,83	2,041	0,002	2,043	0,12	0,49
	40,00	1,50	0,15	0,98	0,0176	1,32	2,48	4,83	2,722	0,004	2,724	0,11	0,37
	50,00	2,20	0,22	0,98	0,0176	1,32	2,48	4,83	3,402	0,005	3,405	0,11	0,29
												0,11	
OEG-040308-G-14	40,00	0,55	0,06	0,98	0,0176	3,12	2,53	5,04	2,722	0,001	2,723	0,09	0,37
	50,00	0,85	0,09	0,98	0,0176	3,12	2,53	5,04	3,402	0,002	3,403	0,10	0,29
	56,00	0,97	0,10	0,98	0,0176	3,12	2,53	5,04	3,811	0,002	3,812	0,10	0,26
												0,10	

Appendix IV- Measured permeability from the Jones permeameter

OEG-040308-G-15	8,00	0,70	0,07	0,98	0,0176	2,60	2,53	5,02	0,544	0,002	0,545	0,93	1,83
	16,00	1,70	0,17	0,98	0,0176	2,60	2,53	5,02	1,089	0,004	1,091	0,93	0,92
	32,00	4,40	0,44	0,98	0,0176	2,60	2,53	5,02	2,177	0,011	2,183	0,88	0,46
	56,00	10,40	1,05	0,98	0,0176	2,60	2,53	5,02	3,811	0,026	3,823	0,85	0,26
												0,90	
OEG-040308-G-17	4,00	0,30	0,03	0,98	0,0176	2,57	2,52	4,99	0,272	0,001	0,273	0,89	3,67
	8,00	0,70	0,07	0,98	0,0176	2,57	2,52	4,99	0,544	0,002	0,545	0,93	1,83
	16,00	1,60	0,16	0,98	0,0176	2,57	2,52	4,99	1,089	0,004	1,091	0,87	0,92
	32,00	4,30	0,43	0,98	0,0176	2,57	2,52	4,99	2,177	0,011	2,183	0,86	0,46
	56,00	10,10	1,02	0,98	0,0176	2,57	2,52	4,99	3,811	0,025	3,823	0,83	0,26
												0,87	
OEG-040308-G-18	1,00	0,70	0,07	0,98	0,0176	0,70	2,53	5,02	0,068	0,002	0,069	2,53	14,51
	2,00	1,90	0,19	0,98	0,0176	0,70	2,53	5,02	0,136	0,005	0,138	3,34	7,22
	4,00	4,20	0,42	0,98	0,0176	0,70	2,53	5,02	0,272	0,010	0,277	3,48	3,61
	8,00	10,00	1,01	0,98	0,0176	0,70	2,53	5,02	0,544	0,025	0,557	3,70	1,80
	16,00	25,00	2,53	0,98	0,0176	0,70	2,53	5,02	1,089	0,061	1,119	3,80	0,89
	18,00	29,95	3,02	0,98	0,0176	0,70	2,53	5,02	1,225	0,073	1,262	3,88	0,79
												3,45	
OEG-040308-G-22	2,00	0,65	0,07	0,98	0,0176	2,50	2,52	4,98	0,136	0,002	0,137	4,04	7,31
	4,00	1,35	0,14	0,98	0,0176	2,50	2,52	4,98	0,272	0,003	0,274	3,94	3,65
	8,00	2,90	0,29	0,98	0,0176	2,50	2,52	4,98	0,544	0,007	0,548	3,77	1,83
	16,00	6,90	0,70	0,98	0,0176	2,50	2,52	4,98	1,089	0,017	1,097	3,68	0,91
	32,00	18,20	1,84	0,98	0,0176	2,50	2,52	4,98	2,177	0,045	2,200	3,58	0,45
												3,80	
OEG-040308-G-23	40,00	0,10	0,01	0,98	0,0176	2,56	2,53	5,02	2,722	0,000	2,722	0,01	0,37
	50,00	0,20	0,02	0,98	0,0176	2,56	2,53	5,02	3,402	0,000	3,403	0,02	0,29
	56,00	0,20	0,02	0,98	0,0176	2,56	2,53	5,02	3,811	0,000	3,811	0,02	0,26
												0,02	
OEG-040308-G-24	4,00	0,80	0,08	0,98	0,0176	1,92	2,53	5,01	0,272	0,002	0,273	1,77	3,66
	8,00	1,70	0,17	0,98	0,0176	1,92	2,53	5,01	0,544	0,004	0,546	1,67	1,83
	16,00	4,00	0,40	0,98	0,0176	1,92	2,53	5,01	1,089	0,010	1,094	1,61	0,91
	32,00	10,35	1,05	0,98	0,0176	1,92	2,53	5,01	2,177	0,025	2,190	1,54	0,46
	56,00	24,65	2,49	0,98	0,0176	1,92	2,53	5,01	3,811	0,060	3,841	1,50	0,26
												1,62	
OEG-040308-G-26	20,00	0,80	0,08	0,98	0,0176	2,53	2,52	5,00	1,361	0,002	1,362	0,31	0,73
	30,00	1,30	0,13	0,98	0,0176	2,53	2,52	5,00	2,041	0,003	2,043	0,28	0,49
	40,00	2,00	0,20	0,98	0,0176	2,53	2,52	5,00	2,722	0,005	2,724	0,28	0,37
	50,00	2,90	0,29	0,98	0,0176	2,53	2,52	5,00	3,402	0,007	3,406	0,28	0,29
	60,00	3,70	0,37	0,98	0,0176	2,53	2,52	5,00	4,083	0,009	4,087	0,26	0,24
												0,28	
OEG-040308-G-27	16,00	0,70	0,07	0,98	0,0176	2,54	2,52	4,99	1,089	0,002	1,090	0,37	0,92
	32,00	1,80	0,18	0,98	0,0176	2,54	2,52	4,99	2,177	0,004	2,180	0,35	0,46
	56,00	3,95	0,40	0,98	0,0176	2,54	2,52	4,99	3,811	0,010	3,815	0,32	0,26
												0,35	
OEG-040308-G-28	40,00	0,72	0,07	0,98	0,0176	3,19	2,53	5,04	2,722	0,002	2,723	0,13	0,37
	50,00	1,03	0,10	0,98	0,0176	3,19	2,53	5,04	3,402	0,003	3,404	0,12	0,29
	56,00	1,24	0,13	0,98	0,0176	3,19	2,53	5,04	3,811	0,003	3,812	0,12	0,26
												0,12	
OEG-060308-G-52	60,00	0,31	0,03	0,98	0,0176	4,42	3,76	11,08	4,083	0,001	4,083	0,02	0,24
												0,02	
OEG-060308-G-53	30,00	0,39	0,04	0,98	0,0176	2,30	3,74	11,00	2,041	0,001	2,042	0,03	0,49
	40,00	0,62	0,06	0,98	0,0176	2,30	3,74	11,00	2,722	0,002	2,723	0,04	0,37
	60,00	0,88	0,09	0,98	0,0176	2,30	3,74	11,00	4,083	0,002	4,084	0,03	0,24
												0,03	
OEG-060308-G-56	20,00	0,30	0,03	0,98	0,0176	5,07	3,76	11,10	1,361	0,001	1,361	0,11	0,73
	40,00	0,85	0,09	0,98	0,0176	5,07	3,76	11,10	2,722	0,002	2,723	0,11	0,37
	60,00	0,85	0,09	0,98	0,0176	5,07	3,76	11,10	4,083	0,002	4,084	0,05	0,24
												0,09	
OEG-060308-G-57	10,00	1,10	0,11	0,98	0,0176	3,16	3,75	11,06	0,680	0,003	0,682	0,61	1,47
	20,00	2,26	0,23	0,98	0,0176	3,16	3,75	11,06	1,361	0,006	1,364	0,50	0,73
	30,00	2,66	0,27	0,98	0,0176	3,16	3,75	11,06	2,041	0,007	2,045	0,32	0,49
	40,00	4,18	0,42	0,98	0,0176	3,16	3,75	11,06	2,722	0,010	2,727	0,33	0,37
												0,44	
OEG-060308-G-58	40,00	1,90	0,19	0,98	0,0176	5,10	3,76	11,10	2,722	0,005	2,724	0,24	0,37
	50,00	2,60	0,26	0,98	0,0176	5,10	3,76	11,10	3,402	0,006	3,405	0,23	0,29
	60,00	3,45	0,35	0,98	0,0176	5,10	3,76	11,10	4,083	0,008	4,087	0,22	0,24
												0,23	
OEG-060308-G-59	50,00	0,59	0,06	0,98	0,0176	4,28	3,75	11,06	3,402	0,001	3,403	0,04	0,29
	60,00	1,06	0,11	0,98	0,0176	4,28	3,75	11,06	4,083	0,003	4,084	0,06	0,24
												0,05	

Appendix IV- Measured permeability from the portable permeameter

Faroe Island Samples (Oluva Ellingsgaard) **02-05-2008**

Calibration equation for the 200cc/min flow loop: K (mD) = 1,395 *Fnorm

Fnorm = (Πp - background) * (200/9.71) * (max inj P/ Pinj measured)

Results using 200cc/min flow loop.

Sample Number	Pressure Background psi	Background Flow	Pressure injected psi	Measured Flow Πp	Flow Rate Normalised Fnorm	Permeability K mD
OEG-050308-G-48	4,995	2,75	5,026	2,79	7,70	10,73
	4,997	2,73	5,019	2,71	-3,86	-5,38
	4,998	2,75	5,014	2,71	-7,72	-10,77
	5,002	2,73	5,021	2,77	7,72	10,76
	5,000	2,73	5,015	2,8	13,51	18,84
	5,001	2,77	5,014	2,8	5,79	8,08
	5,003	2,77	5,018	2,78	1,93	2,69
	4,998	2,76	5,02	2,79	5,78	8,06
						5,38
OEG-050308-G-30	5,003	2,74	5,021	2,83	17,36	24,21
	5,001	2,75	4,998	3,31	108,49	151,30
	4,999	2,74	4,974	4,81	402,79	561,73
	5,003	2,73	5,016	2,88	28,97	40,40
	5,002	2,74	5,011	2,83	17,39	24,26
	5,002	2,79	5,018	2,82	5,79	8,07
	4,998	2,77	5,008	2,82	9,66	13,47
	5,003	2,83	5,012	2,83	0,00	0,00
						102,93
OEG-050308-G-51	5,004	2,74	5,012	2,81	13,53	18,87
	5	2,75	5,018	2,82	13,50	18,83
	5,001	2,77	5,008	2,82	9,67	13,48
	4,998	2,8	5,007	2,82	3,87	5,39
	5,001	2,78	4,999	2,82	7,75	10,80
	5	2,83	4,999	2,83	0,00	0,00
	5,002	2,85	5,002	2,81	-7,74	-10,80
	5,004	2,79	5,004	2,81	3,87	5,40
						7,75
OEG-050308-G-31	5,002	2,76	5,023	2,78	3,86	5,38
	5,004	2,76	5,012	2,78	3,87	5,39
	4,998	2,8	5,003	2,81	1,93	2,70
	5,006	2,81	5,012	2,78	-5,80	-8,09
	5	2,75	5,002	2,79	7,74	10,80
	5,002	2,75	5,003	2,8	9,68	13,50
	5	2,79	5,009	2,79	0,00	0,00
	5,003	2,81	5,015	2,79	-3,86	-5,39
						3,04
OEG-050308-G-46	5,001	2,78	4,997	2,87	17,44	24,32
	5,001	2,84	5,004	2,83	-1,93	-2,70
	5	2,81	5,004	2,81	0,00	0,00
	5	2,76	4,998	2,82	11,62	16,21
	5	2,82	5	2,8	-3,87	-5,40
	5,002	2,82	5,002	2,76	-11,62	-16,20
	5	2,81	5,003	2,76	-9,67	-13,49
	5,001	2,8	5,002	2,77	-5,81	-8,10
						-0,67
OEG-050308-G-50	4,999	2,83	4,994	2,89	11,63	16,22
	5	2,8	5,003	2,74	-11,61	-16,19
	5,002	2,78	4,999	2,79	1,94	2,70
	5,003	2,76	5,004	2,73	-5,81	-8,10
	5,003	2,8	5,012	2,73	-13,53	-18,87
	4,999	2,79	5,011	2,84	9,66	13,47
	5	2,81	5,007	2,8	-1,93	-2,70
	5	2,77	5,005	2,78	1,93	2,70
						-1,35

Appendix IV- Measured permeability from the portable permeameter

OEG-050308-G-32	5,005	2,77	4,944	3,97	235,20	328,01
	5,002	2,8	4,987	3,74	182,54	254,57
	4,999	2,79	4,978	3,82	200,26	279,28
	5	2,76	4,98	3,81	204,11	284,65
	5	2,74	4,963	4,8	401,81	560,37
	5,003	2,79	4,967	4,65	362,73	505,86
	5	2,82	4,93	6,87	795,26	1109,07
	5,001	2,8	4,926	6,95	815,72	1137,60
						557,43
OEG-050308-G-47	5,004	2,78	5,005	2,93	29,04	40,49
	5	2,78	5	2,95	32,91	45,90
	5	2,78	4,99	2,87	17,46	24,35
	5,001	2,8	4,995	3,01	40,71	56,77
	5,002	2,8	5,014	2,83	5,79	8,08
	5,001	2,8	5,009	2,85	9,67	13,48
	4,999	2,78	5,01	2,86	15,45	21,55
	5,001	2,8	5,012	2,86	11,59	16,17
						28,35
OEG-050308-G-34	5,001	2,84	5,016	2,77	-13,51	-18,84
	5,002	2,78	5,015	2,79	1,93	2,69
	5,001	2,77	5,01	2,79	3,87	5,39
	5,001	2,8	5,013	2,79	-1,93	-2,69
	5,001	2,81	5,018	2,82	1,93	2,69
	4,999	2,85	5,016	2,77	-15,44	-21,53
	5,001	2,82	5,012	2,8	-3,86	-5,39
	5,002	2,88	5,016	2,78	-19,31	-26,93
						-8,08
OEG-050308-G-33	4,999	2,78	5,004	2,96	34,82	48,55
	4,998	2,83	5,003	2,9	13,54	18,88
	5,004	2,86	5,009	2,91	9,67	13,49
	5,001	2,81	4,995	2,92	21,32	29,74
	5,002	2,81	4,993	3,06	48,49	67,62
	4,998	2,83	4,981	3,34	99,08	138,17
	4,999	2,83	4,976	3,53	136,15	189,88
	5,002	2,82	4,988	3,07	48,54	67,69
						71,75
OEG-050308-G-38	4,998	2,78	4,98	2,79	1,94	2,71
	5,001	2,81	5,005	2,83	3,87	5,40
	5,002	2,84	5,01	2,82	-3,87	-5,39
	4,999	2,83	5,006	2,79	-7,73	-10,79
	5,002	2,8	5,005	2,78	-3,87	-5,40
	4,997	2,82	5	2,78	-7,74	-10,79
	5,001	2,82	5,001	2,78	-7,74	-10,80
	5,001	2,8	4,998	2,78	-3,87	-5,40
						-5,06
OEG-050308-G-36	4,998	2,83	4,99	3,01	34,91	48,68
	5,003	2,84	5,008	2,86	3,87	5,39
	5	2,85	5,017	2,8	-9,65	-13,45
	4,998	2,82	5,001	2,9	15,48	21,59
	5,001	2,85	5,006	2,82	-5,80	-8,09
	5,002	2,81	5,011	2,81	0,00	0,00
	5	2,82	5,008	2,84	3,87	5,39
	5,002	2,82	5,009	2,81	-1,93	-2,70
						7,10
OEG-050308-G-35	5,001	2,8	5,003	2,89	17,42	24,29
	4,999	2,89	5,003	2,83	-11,61	-16,19
	5,003	2,83	5,011	2,83	0,00	0,00
	5,002	2,81	5,01	2,83	3,87	5,39
	4,999	2,77	5,007	2,83	11,60	16,17
	5,001	2,83	5,009	2,84	1,93	2,70
	5,002	2,86	5,01	2,83	-5,80	-8,09
	5,001	2,8	5,011	2,82	3,86	5,39
						3,71

Appendix IV- Measured permeability from the portable permeameter

OEG-060308-G-59	4,999	2,8	5,005	2,87	13,54	18,88
	5,003	2,95	5,007	2,86	-17,41	-24,28
	5	2,92	5,008	2,86	-11,60	-16,17
	5,003	2,86	5,01	2,86	0,00	0,00
	5,005	2,85	5,015	2,86	1,93	2,69
	5	2,84	5,011	2,85	1,93	2,69
	5,001	2,86	5,007	2,85	-1,93	-2,70
	5	2,86	5,002	2,85	-1,94	-2,70
						-2,70
OEG-060308-G-54	4,998	2,85	5,003	2,79	-11,61	-16,18
	5,003	2,82	5,004	2,79	-5,81	-8,10
	4,999	2,88	5,003	2,79	-17,41	-24,28
	5,005	2,84	5,003	2,8	-7,75	-10,80
	5,002	2,88	5,006	2,79	-17,41	-24,28
	5	3	5,004	2,81	-36,76	-51,26
	4,999	2,92	5,003	2,82	-19,35	-26,98
	5	2,93	5,01	2,77	-30,92	-43,12
						-25,63
OEG-060308-G-55	4,997	2,85	4,936	6,4	695,81	970,38
	4,999	2,89	4,944	4,85	383,70	535,11
	4,997	2,83	4,995	3,1	52,30	72,93
	5,001	2,81	Stopped	readings	Stopped	readings
						526,14
OEG-040308-G-25	5,005	2,75	5,01	2,84	17,41	24,28
	5,003	2,82	5,013	2,86	7,73	10,78
	5,003	2,76	5,01	2,83	13,53	18,87
	5,001	2,76	5,004	2,84	15,48	21,59
	5,001	2,76	5,012	2,93	32,84	45,80
						24,26
OEG-040308-G-08	5	2,82	5,011	2,84	3,86	5,39
	5	2,79	5,009	2,96	32,85	45,82
	5,003	2,76	5,007	2,94	34,82	48,56
	5	2,78	4,998	3,13	67,79	94,54
	5,003	2,77	5,012	2,91	27,06	37,73
	5	2,76	4,996	3,29	102,70	143,22
	5	2,81	5,009	3	36,72	51,21
						60,92
OEG-040308-G-16	4,998	2,83	5,004	2,77	-11,60	-16,18
	5	2,82	5,011	2,79	-5,80	-8,08
	4,999	2,83	5,009	2,81	-3,86	-5,39
	5	2,82	5,011	2,78	-7,73	-10,78
	5,003	2,82	5,014	2,77	-9,66	-13,47
						-10,78
OEG-070308-G-65	5,003	2,78	5,008	2,82	7,74	10,79
	5,002	2,77	5,005	2,86	17,41	24,29
	5,002	2,76	5,01	2,79	5,80	8,09
	5,004	2,77	5,004	2,81	7,74	10,80
	5,001	2,77	5,009	2,78	1,93	2,70
	5	2,77	4,997	2,8	5,81	8,11
						10,79
OEG-040308-G-21	5	2,84	4,984	3,03	36,90	51,47
	5,003	2,78	5,009	2,92	27,07	37,76
	5,001	2,82	5,01	2,97	28,99	40,43
	5,004	2,81	5,014	3,04	44,44	61,98
	4,999	2,79	5,005	2,95	30,94	43,15
	5,002	2,79	5,008	2,98	36,74	51,24
	5,002	2,79	5,007	3	40,62	56,65
	5,004	2,78	5,002	3	42,61	59,43
						50,26
OEG-040308-G-20	5	2,85	5,012	2,81	-7,73	-10,77
	5,001	2,81	4,99	2,86	9,70	13,53
	5	2,77	4,995	2,87	19,38	27,03
	5	2,83	4,994	2,88	9,69	13,52
	4,998	2,8	5,003	2,8	0,00	0,00
	5,001	3,05	5,008	2,9	-29,00	-40,44
	4,999	2,79	5,01	2,85	11,59	16,17
						2,72
OEG-040308-G-19	5,008	2,81	5,004	3,32	98,82	137,82
	4,999	2,8	4,964	3,86	206,67	288,23
	5	2,79	4,983	3,23	85,48	119,21
	5,002	2,84	4,961	3,69	165,93	231,40
						194,16

Appendix V- Derived porosity values from the Sonic logs - Glyvursnes -1 Well

Malinstindur Formation – Section -3 (607.23-604.23m). Section -2 (592.23-590.93m) and Section -1 (356.13-355.03m)							
Porosity from the Sonic logs (%)							
LogTek I	LogTek I w/ sh corr	LogTek II	LogTek II w/ sh corr	LogTek I	LogTek I w/ sh corr	LogTek II	LogTek II w/ sh corr
11.4	-30.2	26.6	-19.9	33.4	8.4	35.1	12.3
12.9	-27.3	27.7	-17.3	34.5	12.2	36.2	15.8
19.2	-13.7	32.3	-4.5	39.2	22.9	37.4	22.5
27.1	4.4	37.7	12.3	38.6	29.7	36.8	28.8
34.8	12.5	44.3	19.4	38.0	36.9	36.3	35.3
44.3	23.3	52.2	28.7	36.6	36.6	33.4	33.4
50.5	38.2	56.9	43.1	35.2	32.7	31.4	29.1
57.7	48.4	62.1	51.7	30.7	23.8	28.2	22.0
58.4	47.9	64.4	52.6	27.9	18.5	25.9	17.3
61.9	52.3	66.8	56.0	23.6	15.5	21.3	13.9
60.0	57.1	67.0	63.8	19.8	9.2	17.0	7.4
60.7	60.7	67.2	67.2	14.7	4.3	13.7	4.2
61.2	53.8	67.5	59.2				
61.7	48.7	67.8	53.3				
63.2	52.6	67.4	55.6				
64.7	59.0	67.0	60.6				
67.3	52.9	65.6	49.5				
70.1	48.0	64.2	39.5				
69.8	43.8	61.2	32.1				
70.5	42.4	58.3	26.8				
69.3	42.0	55.7	25.1				
69.1	40.0	53.6	21.0				
66.7	35.1	51.0	15.6				
64.5	32.9	48.6	13.3				
59.8	30.2	44.9	11.9				
55.5	34.0	41.5	17.5				
47.6	23.8	36.0	9.5				
40.8	11.7	31.2	-1.3				
31.6	-5.9	25.3	-16.7				
24.6	-23.0	20.4	-32.9				
18.3	-34.2	17.1	-41.6				
11.8	-0.0	14.6	4.7				
12.4	1.5	16.1	7.1				
15.0	4.2	19.0	10.1				
17.8	5.7	22.2	12.1				
21.2	10.9	23.6	15.1				
24.9	18.3	25.1	19.7				
25.6	18.5	24.8	18.8				
26.4	16.1	24.4	15.9				
24.0	13.8	21.5	13.0				
22.1	16.1	20.8	15.8				
19.6	19.6	16.3	16.3				
17.6	17.0	14.0	13.4				
15.0	8.6	11.8	6.4				
12.5	0.5	9.7	-0.2				

Appendix V- Derived porosity values from the Sonic logs - Glyvursnes -1 Well

Sneis Formation – Section O (298.93m-296.33m)			
Porosity from the Sonic logs (%)			
LogTek I	LogTek I with shale correction	LogTek II	LogTek II with shale correction
32.3	-8.9	31.5	-0.4
38.3	0.5	35.1	5.8
45.3	8.7	39.1	10.7
48.6	16.9	41.1	16.6
52.1	23.0	45.5	22.9
50.9	21.6	45.6	22.9
51.7	22.8	48.0	25.6
49.4	18.9	46.8	23.2
47.2	22.2	45.2	25.8
47.3	23.5	44.6	26.1
46.1	20.2	43.5	23.4
46.8	23.0	42.7	24.3
47.5	22.1	42.0	22.3
48.0	21.4	40.1	19.5
48.4	26.0	39.3	21.8
46.2	39.1	36.7	31.1
45.2	45.2	35.0	35.0
42.6	37.6	33.2	29.3
40.2	32.5	32.6	26.6
32.6	17.6	29.8	18.2
30.5	14.2	28.2	15.6
22.6	6.5	23.5	11.1
16.3	-5.3	19.4	2.6
9.2	-8.1	15.1	1.6
3.7	-9.1	9.9	0
3.0	-18.7	8.0	-8.8
-0.4	-19.9	5.1	-10.0

Appendix V- Derived porosity values from the Sonic logs - Glyvursnes -1 Well

Enni Formation – Section +1 (150.03m) and +2 (44.03-38.63m)							
Porosity from the Sonic logs (%)							
LogTek I	LogTek I with shale correction	LogTek II	LogTek II with shale correction	LogTek I	LogTek I with shale correction	LogTek II	LogTek II with shale correction
24.3	13.2	29.2	18.2	53.9	42.9	57.9	47.4
25.5	20.2	30.7	25.4	53.2	37.3	56.9	41.7
26.2	24.6	31.0	29.4	52.9	37.9	55.8	41.5
26.9	22.4	31.3	26.8	52.6	39.4	54.8	42.2
26.7	23.6	30.1	27.1	52.3	38.8	54.1	41.2
26.4	26.1	28.9	28.6	52.0	33.8	53.3	36.0
24.6	24.6	25.7	25.7	51.3	22.9	53.1	22.4
22.8	20.2	22.8	20.1	50.6	21.2	52.8	21.0
22.2	15.5	19.9	13.3	50.1	33.8	52.4	36.8
21.6	15.2	17.3	11.0	49.7	23.6	52.0	23.8
21.0	21.0	15.9	15.9	48.2	32.6	50.8	35.9
43.1	29.2	42.9	27.9	46.7	28.6	49.6	19.6
44.3	29.4	45.8	29.7	45.0	19.3	47.3	19.5
44.3	29.6	47.3	31.5	43.5	19.7	45.2	19.5
44.3	30.6	48.9	34.0	41.2	17.8	42.1	16.8
44.4	31.1	49.8	35.3	39.1	26.5	39.2	27.2
44.6	29.9	50.7	34.8	36.6	31.4	35.9	30.9
45.5	25.1	51.6	29.6	34.3	34.3	32.9	32.9
46.4	31.7	52.6	38.6	32.6	28.7	30.3	26.4
48.3	34.5	53.8	40.6	31.0	17.4	27.8	14.7
50.4	34.4	55.1	39.8	29.4	5.7	26.2	0.6
52.5	35.7	56.3	40.3				
54.7	40.3	57.6	43.8				
55.9	44.7	58.1	47.4				
57.0	47.7	58.6	49.7				
57.2	47.4	58.3	48.9				
57.5	48.3	58.1	49.3				
56.7	46.0	56.8	46.6				
56.0	45.6	55.6	45.7				
55.3	49.7	54.4	49.0				
54.7	47.9	53.1	46.6				
54.6	43.0	52.4	41.3				
54.6	42.8	51.8	40.5				
55.0	44.7	52.0	42.1				
55.5	39.4	52.2	36.8				
55.5	30.2	53.1	25.7				
55.6	29.6	54.0	25.9				
55.5	29.3	55.1	26.8				
55.3	29.9	56.2	28.8				
55.2	30.0	57.2	29.9				
55.1	40.5	58.2	44.2				
55.2	40.9	59.0	45.3				
55.2	41.3	59.8	46.5				
54.9	41.3	59.3	46.3				
54.6	43.7	58.9	48.5				

Appendix VI- Derived porosity values from the Sonic log - Well 6005/15-1

Well 6005/15-1 - Longan – Section N (Kettla member) – 2749.14-2785.88m							
Porosity from the Sonic logs (%)							
Sonic log	Sonic log with shale correction	Sonic log	Sonic log with shale correction	Sonic log	Sonic log with shale correction	Sonic log	Sonic log with shale correction
15.0	11.8	30.4	19.9	32.8	20.8	35.1	30.7
14.5	11.0	30.2	20.5	31.8	20.3	34.3	30.6
14.1	10.0	30.0	21.4	32.5	21.6	33.5	29.9
14.0	8.8	29.7	22.0	33.2	23.1	33.6	29.9
14.7	8.1	29.5	22.2	34.5	25.4	33.8	30.0
15.6	7.7	29.9	22.0	35.8	27.8	33.3	29.8
17.2	8.3	30.0	20.8	34.5	27.6	32.7	29.9
18.4	9.5	29.2	18.7	33.3	27.3	32.2	30.0
18.7	10.3	28.4	16.7	33.8	28.5	31.7	29.9
18.6	10.8	27.4	15.1	34.3	29.3	31.2	29.5
17.2	10.1	26.6	14.1	34.8	30.1	30.7	29.0
16.1	9.2	26.7	14.4	35.3	30.8	30.9	29.3
15.6	7.9	26.9	14.7	35.7	31.5	31.1	29.9
15.0	6.0	27.5	15.1	36.0	32.1	31.0	29.8
14.4	4.2	28.0	15.5	36.7	32.9	30.7	29.4
14.0	3.0	28.1	15.6	37.4	33.5	31.4	29.6
13.9	3.0	28.3	16.1	37.0	32.6	32.1	30.0
14.0	3.8	28.5	16.7	36.6	31.5	33.7	31.4
14.5	5.5	28.8	17.2	37.6	31.8	35.4	33.2
15.3	7.7	29.3	17.6	38.7	32.1	34.9	33.2
16.6	10.3	29.8	17.9	38.5	31.2	34.1	32.8
17.7	12.3	29.8	17.8	38.3	30.3	35.4	34.3
17.6	12.6	29.9	17.8	37.8	29.0	36.9	36.0
19.3	13.9	29.9	17.7	37.3	27.5	36.6	35.6
26.8	20.2	29.9	17.6	37.6	27.1	36.0	34.9
32.4	24.5	30.3	17.8	38.0	27.0	35.9	34.5
31.6	22.7	30.7	18.0	37.7	27.0	35.8	34.3
31.1	21.7	30.9	18.0	37.5	27.4	35.3	33.7
31.7	21.9	31.2	18.2	38.0	28.8	34.8	33.0
32.0	22.4	31.6	18.9	38.5	30.1	34.3	32.4
31.8	22.8	32.1	20.0	39.2	31.1	33.8	31.8
31.8	23.9	32.4	21.2	39.9	31.6	34.4	32.2
32.7	25.9	32.8	22.4	39.3	30.8	35.2	32.7
33.4	27.4	33.0	23.5	38.6	30.4	35.7	32.7
33.5	27.4	33.1	24.2	35.9	29.0	36.0	32.8
33.6	26.7	32.6	23.9	33.1	27.8	36.5	32.7
33.5	25.6	32.2	23.4	34.0	30.3	37.1	32.2
33.3	24.6	32.3	23.4	35.2	32.5	37.0	30.4
33.0	23.6	32.5	23.1	35.0	32.3	36.7	28.0
32.6	22.3	32.1	22.3	34.7	31.2	36.1	25.6
31.7	20.7	31.8	21.4	34.4	29.8	35.5	23.8
30.8	19.4	32.2	21.1	34.2	28.6	35.4	23.3
30.2	18.6	32.6	20.8	34.2	28.1	35.5	23.6
29.8	18.3	33.3	21.1	34.3	28.3	36.4	25.1
30.2	19.0	33.9	21.6	34.7	29.4	37.4	27.1

Appendix VI- Derived porosity values from the Sonic log - Well 6005/15-1

Section N (Kettla member) – 2749.14-2785.88m				Section -I – 3360.12-3670.94m			
Porosity from the Sonic logs (%)				Porosity from the Sonic logs (%)			
Sonic log	Sonic log with shale correction	Sonic log	Sonic log with shale correction	Sonic log	Sonic log with shale correction	Sonic log	Sonic log with shale correction
36.6	27.8	26.4	26.1	26.2	22.9	24.1	20.7
35.3	28.2	25.9	25.9	27.0	24.8	24.8	21.8
35.3	30.0	25.1	25.0	27.3	26.1	24.3	21.5
35.6	31.8	24.1	23.2	25.8	25.3	23.9	20.9
35.0	31.9	22.9	20.5	24.8	24.7	23.5	20.1
34.1	30.8	21.8	17.9	25.5	25.4	23.1	19.2
33.5	29.7	20.7	15.7	26.1	25.9	22.7	18.4
33.0	28.7	20.2	14.6	26.6	26.1	22.5	17.6
31.7	27.3	20.0	13.9	27.2	26.1	23.3	18.3
30.3	26.1	20.0	13.2	28.0	26.2	24.0	19.4
28.7	24.9	20.1	12.2	28.3	26.2	23.2	19.2
27.2	23.6	21.2	12.0	27.3	25.1	22.3	19.1
26.2	22.8	22.9	12.7	26.0	24.3	19.5	17.2
25.4	22.5	23.3	12.2	23.6	22.8	16.7	14.5
25.5	23.3	22.8	11.2	21.7	21.5	12.5	10.0
25.9	24.6	22.4	10.5	21.6	21.6	8.3	-3.3
25.4	24.9			21.4	21.0	6.4	-5.9
24.6	24.3			21.1	19.8	4.6	-8.8
24.3	23.6			20.9	18.3	0.5	-14.7
24.0	22.8			20.8	17.1	-3.6	-18.7
25.6	23.9			20.7	16.6	-2.5	-16.7
27.9	26.1			20.9	16.6	-1.	-14.6
29.0	27.4			21.1	16.6	2.6	-9.7
29.6	28.0			21.4	16.5	6.8	-4.8
30.3	28.7			21.5	15.8	7.7	-3.0
31.1	29.4			20.5	14.1	8.4	-1.0
31.0	29.2			19.6	12.8	11.9	3.9
30.7	29.0			19.9	12.8		
30.7	29.2			19.6	12.7		
31.0	29.4			16.8	10.1		
31.2	29.4			14.1	7.6		
31.4	29.2			12.0	5.4		
32.7	30.0			10.3	3.6		
34.5	30.9			12.6	5.6		
35.4	30.7			14.8	7.6		
35.8	30.3			16.9	9.4		
35.2	29.2			19.0	11.2		
34.2	28.4			20.5	12.5		
33.7	28.9			21.9	13.9		
33.4	29.9			21.5	13.9		
33.0	30.6			21.3	14.1		
32.7	31.0			21.6	15.0		
30.4	29.2			22.0	16.1		
27.1	26.1			22.6	17.7		
26.1	25.5			23.3	19.2		

Appendix VI- Derived porosity values from the Sonic log - Well 6005/15-1

Section -II – 3507.03-3517.54m				Lection -III – 3560.06-3570.88m			
Porosity from the Sonic logs (%)				Porosity from the Sonic logs (%)			
Sonic log	Sonic log with shale correction	Sonic log	Sonic log with shale correction	Sonic log	Sonic log with shale correction	Sonic log	Sonic log with shale correction
35.6	35.6	13.9	7.2	-1.5	-9.2	18.2	18.2
35.4	34.9	15.1	4.5	-1.8	-9.7	16.7	16.7
34.9	33.5	17.0	6.9	-1.9	-9.9	14.9	14.8
33.9	31.5	19.0	8.9	-1.9	-9.9	14.8	14.3
33.3	29.7	20.8	10.3	-2.3	-10.4	14.8	14.0
33.3	28.5	22.3	11.0	-2.7	-10.8	13.6	12.5
33.3	27.7	22.7	10.6	-3.1	-11.2	12.2	10.9
33.2	27.4	23.0	10.3	-3.5	-11.5	11.7	10.4
30.4	24.6	23.0	10.0	-3.1	-11.0	11.4	10.1
23.8	17.9	23.0	9.8	-2.7	-10.6	11.2	9.8
19.7	13.4	23.0	9.9	-1.5	-9.3	11.1	9.5
19.3	11.9	22.9	9.7	-0.3	-8.1	10.0	8.0
19.3	10.6	22.0	8.5	0.2	-7.4	8.7	6.3
19.7	10.1	21.5	7.2	0.8	-6.8	6.5	3.8
20.0	9.8	22.0	6.6	0.5	-6.9	4.1	0.9
20.1	9.9	22.3	5.6	0.1	-6.9	3.2	-0.7
20.0	10.1	21.7	3.9	-2.8	-9.6	2.6	-2.4
19.6	10.3	20.8	2.2	-5.7	-12.1	2.1	-4.2
19.1	10.6	19.0	0.0	-5.3	-11.5	1.6	-5.9
18.5	10.6	17.4	-1.8	-4.9	-11.0	2.1	-6.0
18.2	10.6	16.6	-2.5	-4.4	-10.5	2.7	-5.7
18.4	10.6	15.9	-3.1	-3.9	-10.0	3.2	-5.2
18.6	9.9	15.2	-3.6	-3.0	-9.0	3.8	-4.6
18.6	9.0	14.8	-4.1	-2.0	-8.1	4.3	-4.1
18.4	8.0	14.9	-4.2	-2.3	-8.3	4.9	-3.5
17.9	7.0			-2.5	-8.5		
17.5	6.2			-2.5	-8.2		
17.3	5.7			-2.4	-7.7		
17.1	5.1			0.7	-3.8		
16.8	4.5			3.9	0.3		
16.7	4.3			8.3	5.8		
16.8	4.7			12.8	11.3		
16.7	5.2			12.7	11.9		
16.3	5.5			12.5	12.0		
15.5	5.1			13.6	13.0		
13.6	3.6			14.6	13.9		
12.1	2.3			15.4	14.4		
11.4	1.8			16.1	14.8		
11.0	1.6			16.9	15.5		
11.2	2.0			17.7	16.3		
11.8	4.0			16.9	15.8		
12.9	5.1			16.1	15.2		
13.6	5.7			15.7	15.1		
13.2	5.0			15.3	14.9		
13.1	5.4			17.8	17.6		

Appendix VII- Derived porosity values from the Density and the Neutron logs without shale corrections - Glyvursnes-1 Well

Malinstindur Formation				Sneis Formation	
Porosity (%) from the Neutron and Density logs without shale correction					
Neutron log	Neutron log	Density log	Density log	Neutron log	Density log
17,5	26,0	2,58	12,64	16,0	0,4
19,0	25,0	2,16	12,78	18,0	1,7
19,5	24,0	2,35	14,60	18,0	1,4
23,8	24,8	4,68	15,60	18,3	4,4
27,0	25,5	8,74	14,84	22,5	7,2
29,5	25,0	12,00	14,58	27,2	10,3
36,3	24,5	15,42	13,93	32,5	11,5
33,0	23,3	17,19	13,55	29,5	11,1
31,5	22,7	17,84	12,22	28,3	11,0
33,0	21,0	18,91	9,00	32,5	13,6
35,5	17,5	19,78	5,77	31,0	14,2
38,2	15,5	19,16	2,28	31,5	14,7
38,7		19,13		29,8	15,4
35,5		20,20		30,0	13,9
43,6		21,49		31,5	10,9
45,0		21,94		27,8	10,8
38,5		21,09		26,8	13,6
35,5		20,65		29,0	15,2
40,2		18,94		33,8	15,0
40,6		16,36		33,0	14,3
32,5		15,91		31,5	13,7
30,0		16,56		33,5	12,5
34,2		16,35		31,0	9,6
34,5		15,70		23,5	7,4
33,0		14,20		20,0	5,0
26,7		10,55		15,0	0,8
21,3		5,60		12,6	-3,2
20,0		1,73			
19,5		0,22			
17,0		0,00			
16,0		0,00			
15,8		0,32			
18,0		2,10			
20,0		4,52			
23,0		7,60			
28,0		11,80			
32,2		15,83			
34,0		17,75			
28,5		14,65			
24,0		10,13			
23,0		5,61			
10,0		-6,94			

Appendix VII- Derived porosity values from the Density and the Neutron logs without shale corrections - Glyvursnes-1 Well

Enni Formation			
Porosity (%) from the Neutron and Density logs without shale correction			
Neutron log	Neutron log	Density log	Density log
15,5	36,8	-0,8	23,12
15,5	31,5	-1,2	23,87
15,5	35,4	0,4	23,48
18,5	36,5	2,3	23,62
20,5	35,5	4,2	23,87
24,5	44,2	7,3	23,87
25,0	43,0	9,4	23,08
25,2	40,8	10,8	23,38
24,5	39,0	9,9	23,87
20,8	37,7	6,4	22,28
19,0	38,2	4,2	20,89
21,5	35,0	3,34	21,04
22,8	32,5	5,77	20,49
24,7	36,7	10,15	19,20
29,1	35,5	14,17	17,91
30,7	35,2	18,16	17,42
31,2	32,2	21,53	17,42
33,2	31,2	22,58	18,22
47,2	33,7	21,81	18,71
52,8	35,3	22,44	18,31
44,0	31,5	23,23	18,47
41,0	28,0	23,61	17,90
42,8	25,8	24,26	14,59
41,0	22,5	23,74	11,29
38,5		23,23	
40,0		23,61	
50,4		23,87	
50,9		24,26	
46,3		25,29	
51,8		25,03	
47,0		24,13	
39,5		23,87	
39,8		24,65	
45,2		25,16	
45,0		24,77	
41,5		24,13	
37,2		23,48	
36,5		22,05	
35,0		20,90	
32,0		20,25	
35,2		20,79	
42,5		21,68	

Appendix VIII- Derived porosity values from the Density and the Neutron logs without shale corrections - Well 6005/15-1

Section N (Kettla member) – 2749.14-2785.88m						
Porosity (%) from the Neutron log without shale correction						
Neutron log	Neutron log	Neutron log	Neutron log	Neutron log	Neutron log	Neutron log
31,0	35,1	35,5	36,0	31,2	33,0	35,2
30,2	35,5	35,0	35,0	31,5	33,3	35,7
29,2	35,5	33,0	34,0	32,4	33,5	35,0
29,5	35,4	32,2	32,5	33,5	33,0	35,0
28,8	35,0	33,0	32,5	34,5	32,9	35,2
28,0	34,0	32,5	33,3	34,8	32,2	35,9
27,7	32,5	33,6	35,5	32,5	33,0	35,7
28,0	31,9	33,6	37,0	30,5	33,1	36,0
28,8	32,9	32,5	38,4	29,5	33,1	34,7
29,5	35,2	32,3	41,0	30,0	33,3	33,0
30,5	40,0	32,0	35,2	31,0	33,0	31,8
31,5	44,1	30,5	33,5	33,7	32,8	30,7
32,8	46,0	30,0	32,0	34,5	32,0	29,8
33,5	44,8	28,5	31,3	35,0	32,0	29,3
33,5	42,1	27,5	32,0	34,5	32,3	30,2
33,7	39,0	26,7	31,1	34,0	32,5	32,0
32,0	37,0	27,2	30,2	33,2	32,8	33,8
31,5	36,0	29,0	31,7	32,8	31,7	35,5
31,0	35,2	31,5	33,7	31,2	31,0	36,0
30,5	37,0	34,0	33,0	30,5	30,1	35,0
30,0	37,2	35,0	33,2	29,6	30,0	
30,1	35,2	33,9	34,0	29,5	31,0	
29,6	29,8	34,4	34,0	30,3	31,9	
30,0	34,0	34,0	36,6	31,0	33,7	
29,8	32,2	33,5	33,6	32,2	36,0	
29,2	32,0	32,7	33,5	32,7	36,0	
28,8	31,2	32,5	33,2	31,8	36,0	
28,3	31,0	33,0	33,2	31,8	35,7	
28,0	30,3	34,0	34,0	32,4	33,8	
29,5	29,9	34,5	35,0	33,0	32,5	
31,0	29,1	34,5	34,5	34,0	31,2	
33,0	29,9	34,5	34,0	34,5	30,0	
34,5	31,0	33,6	34,0	34,5	29,2	
28,9	33,0	33,2	33,3	34,0	29,0	
35,0	35,0	32,0	33,0	33,5	28,0	
36,2	36,3	32,3	34,0	32,2	27,1	
37,5	38,0	32,9	34,8	32,0	25,3	
38,8	39,0	33,0	36,4	30,1	25,8	
40,0	38,0	34,2	37,0	29,5	27,0	
38,6	37,2	33,2	35,3	29,0	30,1	
39,0	35,1	33,2	36,2	29,8	33,0	
38,5	34,0	33,2	35,0	31,5	34,6	
38,0	33,5	33,8	33,0	32,7	35,9	
36,7	34,0	35,0	32,2	32,7	35,5	
35,3	35,8	35,0	31,5	33,1	36,0	
35,0	36,0	36,0	31,0	33,5	35,2	

Appendix VIII- Derived porosity values from the Density and the Neutron logs without shale corrections - Well 6005/15-1

Section N (Kettla member) – 2749.14-2785.88m						
Porosity (%) from the Density log without shale correction						
Density log	Density log	Density log	Density log	Density log	Density log	Density log
16,4	24,0	19,0	18,7	20,4	17,4	16,4
16,4	23,8	18,8	18,8	21,1	17,2	16,4
16,8	23,6	18,5	18,8	21,4	17,2	16,6
17,5	23,3	18,3	18,8	21,4	17,6	16,9
18,6	23,1	18,1	18,8	20,8	18,4	17,3
20,0	22,9	18,0	18,9	19,8	19,3	17,9
21,5	22,6	18,0	18,8	18,7	20,2	18,6
22,9	22,4	17,8	18,2	17,6	20,9	19,3
24,0	22,2	17,6	17,1	17,0	21,1	19,8
24,8	22,4	17,3	16,0	16,8	20,7	20,1
25,7	22,9	17,1	15,2	17,0	20,0	20,3
26,7	23,8	17,0	14,9	17,6	19,2	20,4
27,4	24,6	17,0	14,9	17,9	18,8	20,3
27,0	25,2	17,0	15,3	17,8	18,8	20,2
25,7	25,3	16,9	15,8	17,7	18,9	20,1
24,1	25,2	16,8	16,3	17,4	18,9	20,1
22,9	24,9	17,0	16,5	17,2	18,4	20,2
22,3	24,6	17,3	16,5	17,1	17,6	20,5
22,4	24,4	17,9	16,4	17,0	16,8	20,8
22,2	24,1	18,6	16,3	16,7	16,1	21,3
21,7	23,6	19,4	16,3	16,5	15,7	
20,9	22,9	20,2	16,4	16,3	15,9	
20,4	21,8	20,8	16,6	16,2	16,4	
20,4	20,7	21,2	16,9	16,3	17,0	
20,9	19,8	21,5	17,3	16,5	17,7	
21,5	19,3	21,7	17,7	16,8	18,2	
22,0	19,0	21,9	18,0	17,1	18,6	
22,3	18,9	22,1	18,1	17,4	18,6	
22,5	18,9	22,3	18,2	17,6	18,3	
22,8	19,0	22,3	18,1	17,7	17,8	
22,8	19,2	22,1	17,8	17,7	17,3	
22,6	19,5	21,4	17,7	17,7	17,0	
22,1	19,7	20,3	17,9	17,9	16,8	
21,7	20,0	19,2	18,5	18,0	16,8	
21,5	20,3	18,2	19,6	18,1	16,9	
21,7	20,6	17,5	21,1	18,0	16,9	
22,1	21,1	17,1	22,6	17,7	17,0	
22,5	21,4	17,0	23,8	17,4	17,2	
22,9	21,6	17,2	24,6	17,1	17,4	
23,1	21,6	17,6	24,9	16,9	17,4	
23,2	21,4	17,9	24,7	16,9	17,3	
23,2	21,1	18,1	23,8	17,1	17,1	
23,4	20,6	18,0	22,6	17,4	16,8	
23,6	20,0	17,9	21,3	17,7	16,6	
23,9	19,5	18,1	20,5	17,9	16,4	
24,0	19,2	18,4	20,1	17,8	16,4	

Appendix VIII- Derived porosity values from the Density and the Neutron logs without shale corrections - Well 6005/15-1

Section - I – 3360-3370 m				Section - II – 3507-3517.5 m			
Porosity (%) from the Neutron and Density logs without shale correction							
Neutron log	Neutron log	Density log	Density log	Neutron log	Neutron log	Density log	Density log
25,5	22,6	13,61	12,15	29,0	26,2	12,46	12,85
26,5	25,0	13,01	12,74	26,0	25,5	12,04	12,30
27,0	24,2	12,82	13,96	24,0	23,9	11,92	11,86
26,8	25,0	12,76	15,48	23,5	23,2	12,17	11,86
27,0	24,8	12,84	16,88	24,0	23,2	12,90	13,43
27,1	24,5	13,01	17,79	25,0	23,2	13,40	13,95
27,9	24,0	13,19	17,99	25,3	23,0	13,90	14,21
27,0	24,4	13,34	17,65	24,1	22,6	13,72	14,54
25,4	25,9	13,12	17,06	23,5	21,7	13,11	15,08
25,2	26,8	12,59	16,39	22,8	20,8	12,59	15,83
24,0	29,0	11,90	15,81	21,5	20,0	12,85	16,35
25,0	31,0	11,26	15,39	20,8	20,8	13,86	17,20
27,0	31,3	10,99	15,15	20,0	22,0	14,46	18,79
27,2	29,7	11,49	14,92	20,0	23,0	15,69	20,61
28,0	28,2	12,57	14,67	20,6	24,8	16,91	21,08
27,6	27,0	13,69	14,39	25,2	26,5	17,02	20,45
27,0	26,3	14,54	14,02	28,9	28,9	16,26	19,94
25,7	27,8	14,92	13,56	32,0	32,6	15,52	19,86
24,0	29,0	14,86	12,96	32,8	37,0	14,94	20,15
23,0	29,8	14,64	12,28	32,0	40,3	14,68	20,54
22,6	29,0	14,65	11,61	31,0	43,0	14,81	20,44
22,3	27,8	15,09	11,09	29,5	42,0	15,30	19,88
23,0	25,6	15,97	10,92	31,0	41,0	15,55	19,25
23,1	29,2	17,14	11,23	30,3	39,0	15,59	18,67
23,7	23,1	18,28	11,57	29,3	38,0	15,90	18,17
24,0	22,0	18,99	11,56	28,7	37,0	16,30	17,68
24,0	20,8	19,37	10,97	28,6	35,8	16,47	17,10
24,0	19,0	19,51	26,35	28,0	35,0	16,22	16,79
24,0	17,0	19,48	24,88	29,0	35,2	15,73	16,91
23,8	15,5	19,36	23,21	30,0	35,5	15,77	17,42
24,0	14,0	19,16	21,43	30,8	36,8	16,03	18,02
23,7	14,0	19,00	19,57	30,5	37,0	16,14	18,04
23,5	14,0	19,02	17,69	28,8	34,5	15,88	16,83
24,0	15,0	19,28	15,90	27,0	30,2	15,63	14,97
24,3	15,0	19,73	14,72	25,0	24,5	15,17	13,10
24,6	14,2	20,22	14,31	25,0	19,0	14,83	11,68
22,3	14,5	20,15	14,58	25,0	16,2	14,47	10,97
22,1	15,0	19,39	15,42	25,3	14,5	14,02	10,86
20,0	14,9	17,86	16,72	25,4	14,0	13,77	10,85
17,1	14,0	15,76	18,56	25,0		11,87	
14,1	13,8	13,50	21,04	25,3		11,38	
12,0	14,2	11,93	23,73	25,2		11,61	
12,2		11,46		25,5		12,13	
14,0		11,65		26,0		12,77	
16,0		11,99		26,7		13,23	
20,0		12,16		27,3		13,23	

Appendix VIII- Derived porosity values from the Density and the Neutron logs without shale corrections - Well 6005/15-1

Section -III – 3560-3570 m			
Porosity (%) from the Neutron and Density logs without shale correction			
Neutron log	Neutron log	Density log	Density log
7,8	19,1	19,2	15,1
8,2	19,0	19,5	15,1
9,0	19,2	19,6	15,0
8,8	22,0	19,4	14,9
8,7	22,1	19,2	14,5
8,8	23,0	18,8	13,8
5,5	23,0	13,0	12,9
2,5	21,7	7,2	12,1
1,1	20,0	6,7	11,8
1,1	17,8	6,4	11,8
2,0	17,0	6,3	12,2
3,0	16,3	6,3	12,6
3,2	15,8	6,5	12,8
4,5	15,9	6,9	12,9
5,5	16,3	7,6	12,9
5,9	17,2	8,1	12,9
7,0	18,2	8,3	12,5
7,5	18,9	8,2	11,8
7,2	18,7	7,9	11,0
7,3	17,6	7,6	10,5
6,7	15,8	7,3	10,2
5,9	17,0	7,4	10,2
4,0	13,6	8,2	10,5
4,0	12,2	9,9	10,7
3,6	13,0	12,3	10,7
4,8	13,0	15,2	27,1
6,0	12,6	17,2	26,9
7,7	13,0	17,5	26,5
7,5	13,4	16,2	25,4
7,6	14,3	13,9	23,6
7,0	16,0	11,2	21,3
5,3	17,0	8,7	18,8
4,7	18,0	6,9	16,3
4,0	18,0	5,8	14,3
3,2		5,4	
5,0		5,9	
6,5		7,6	
10,1		11,0	
15,0		15,7	
19,0		20,8	
21,0		25,4	
21,1		12,5	
20,2		14,7	

Tidigare skrifter i serien ”Examensarbeten i Geologi vid Lunds Universitet”:

206. Edvarssson, Johannes, 2006: Dendrokronologisk undersökning av tallbestånds etablering, tillväxtdynamik och degenerering orsakat av klimatrelaterade hydrologiska variationer på Viss mosse och Åbuamossen, Skåne, södra Sverige, 7300-3200 cal. BP.
207. Stenfeldt, Fredrik, 2006: Litostratigrafiska studier av en platåformad sand- och grusavlagring i Skuremåla, Blekinge.
208. Dahlenborg, Lars, 2007: A Rock Magnetic Study of the Åkerberg Gold Deposit, Northern Sweden.
209. Olsson, Johan, 2007: Två svekofenniska graniter i Bottniska bassängen; utbredning, U-Pb zirkondatering och test av olika abrasionstekniker.
210. Erlandsson, Maria, 2007: Den geologiska utvecklingen av västra Hamrångesynklinalens suprakrustalbergarter, centrala Sverige.
211. Nilsson, Pernilla, 2007: Kvidingedeltat – bildningsprocesser och arkitektonisk uppbyggnadsmodell av ett glacifluvialt Gilbertdelta.
212. Ellingsgaard, Óluva, 2007: Evaluation of wireline well logs from the borehole Kyrkheddinge-4 by comparsion to measured core data.
213. Åkerman, Jonas, 2007. Borrkärnekartering av en Zn-Ag-Pb-mineralisering vid Stenbrånet, Västerbotten.
214. Kurlovich, Dzmitry, 2007: The Polotsk-Kurzeme and the Småland-Blekinge Deformation Zones of the East European Craton: geomorphology, architecture of the sedimentary cover and the crystalline basement.
215. Mikkelsen, Angelica, 2007: Relationer mellan grundvattenmagasin och geologiska strukturer i samband med tunnelborrning genom Hallandsås, Skåne.
216. Trondman, Anna-Kari, 2007: Stratigraphic studies of a Holocene sequence from Taniente Palet bog, Isla de los Estados, South America.
217. Månsson, Carl-Henrik & Siikanen, Jonas, 2007: Measuring techniques of Induced Polarization regarding data quality with an application on a test-site in Aarhus, Denmark and the tunnel construction at the Hallandsås Horst, Sweden.
218. Ohlsson, Erika, 2007: Classification of stony meteorites from north-west Africa and the Dhofar desert region in Oman.
219. Åkesson, Maria, 2008: Mud volcanoes - a review. (15 hskp)
220. Randsalu, Linda, 2008: Holocene relative sea-level changes in the Tasiusaq area, southern Greenland, with focus on the Ta1 and Ta3 basins. (30 hskp)
221. Fredh, Daniel, 2008: Holocene relative sea-level changes in the Tasiusaq area, southern Greenland, with focus on the Ta4 basin. (30 hskp)
222. Anjar, Johanna, 2008: A sedimentological and stratigraphical study of Weichselian sediments in the Tvärkroken gravel pit, Idre, west-central Sweden. (30 hskp)
223. Stefanowicz, Sissa, 2008: Palynostratigraphy and palaeoclimatic analysis of the Lower - Middle Jurassic (Pliensbachian - Bathonian) of the Inner Hebrides, NW Scotland. (15 hskp)
224. Holm, Sanna, 2008: Variations in impactor flux to the Moon and Earth after 3.85 Ga. (15 hskp)
225. Bjärnborg, Karolina, 2008: Internal structures in detrital zircons from Hamrånge: a study of cathodoluminescence and back-scattered electron images. (15 hskp)
226. Noresten, Barbro, 2008: A reconstruction of subglacial processes based on a classification of erosional forms at Ramsvikslandet, SW Sweden. (30 hskp)
227. Mehlqvist, Kristina, 2008: En mellanjurassisk flora från Bagå-formationen, Bornholm. (15 hskp)
228. Lindvall, Hanna, 2008: Kortvariga effekter av tefranedfall i lakustrin och terrestrisk miljö. (15 hskp)
229. Löfroth, Elin, 2008: Are solar activity and cosmic rays important factors behind climate change? (15 hskp)
230. Damberg, Lisa, 2008: Pyrit som källa för spårämnen – kalkstenar från övre och mellersta Danien, Skåne. (15 hskp)
331. Cegrell, Miriam & Mårtensson, Jimmy, 2008: Resistivity and IP measurements at the Bolmen Tunnel and Ådalsbanan, Sweden. (30 hskp)

232. Vang, Ina, 2008: Skarn minerals and geological structures at Kalkheia, Kristiansand, southern Norway. (15 hskp)
233. Arvidsson, Kristina, 2008: Vegetationen i Skandinavien under Eem och Weichsel samt fallstudie i submoräna organiska avlagringar från Nybygget, Småland. (15 hskp)
234. Persson, Jonas, 2008: An environmental magnetic study of a marine sediment core from Disko Bugt, West Greenland: implications for ocean current variability. (30 hskp)
235. Holm, Sanna, 2008: Titanium- and chromium-rich opaque minerals in condensed sediments: chondritic, lunar and terrestrial origins. (30 hskp)
236. Bohlin, Erik & Landen, Ludvig, 2008: Geofysiska mätmetoder för prospektering till ballastmaterial. (30 hskp)
237. Brodén, Olof, 2008: Primär och sekundär migration av hydrokarboner. (15 hskp)
238. Bergman, Bo, 2009: Geofysiska analyser (stångslingram, CVES och IP) av lagerföljd och lakvattenrörelser vid Albäcksdeponin, Trelleborg. (30 hskp)
239. Mehlqvist, Kristina, 2009: The spore record of early land plants from upper Silurian strata in Klinta 1 well, Skåne, Sweden. (45 hskp)
239. Mehlqvist, Kristina, 2009: The spore record of early land plants from upper Silurian strata in Klinta 1 well, Skåne, Sweden. (45 hskp)
240. Bjärnborg, Karolina, 2009: The copper sulphide mineralization of the Zinkgruvan deposit, Bergslagen, Sweden. (45 hskp)
241. Stenberg, Li, 2009: Historiska kartor som hjälp vid jordartsgeologisk kartering – en pilotstudie från Vångs by i Blekinge. (15 hskp)
242. Nilsson, Mimmi, 2009: Robust U-Pb baddeleyite ages of mafic dykes and intrusions in southern West Greenland: constraints on the coherency of crustal blocks of the North Atlantic Craton. (30 hskp)
243. Hult, Elin, 2009: Oligocene to middle Miocene sediments from ODP leg 159, site 959 offshore Ivory Coast, equatorial West Africa. (15 hskp)
244. Olsson, Håkan, 2009: Climate archives and the Late Ordovician Boda Event. (15 hskp)
245. Wollein Waldetoft, Kristofer, 2009: Svekofennisk granit från olika metamorfa miljöer. (15 hskp)
246. Månsby, Urban, 2009: Late Cretaceous coprolites from the Kristianstad Basin, southern Sweden. (15 hskp)
247. MacGimpsey, I., 2008: Petroleum Geology of the Barents Sea. (15 hskp)
248. Jäckel, O., 2009: Comparison between two sediment X-ray Fluorescence records of the Late Holocene from Disko Bugt, West Greenland; Paleoclimatic and methodological implications. (45 hskp)
249. Andersen, Christine, 2009: The mineral composition of the Burkland Cu-sulphide deposit at Zinkgruvan, Sweden – a supplementary study. (15 hskp)
250. Riebe, My, 2009: Spinel group minerals in carbonaceous and ordinary chondrites. (15 hskp)
251. Nilsson, Filip, 2009: Föroreningsspridning och geologi vid Filborna i Helsingborg. (30 hskp)
252. Peetz, Romina, 2009: A geochemical characterization of the lower part of the Miocene shield-building lavas on Gran Canaria. (45 hskp)
253. Maria Åkesson, 2010: Mass movements as contamination carriers in surface water systems – Swedish experiences and risks.
254. Elin Löfroth, 2010: Elin Löfroth, 2010: A Greeland ice core perspective on the dating of the Late Bronze Age Santorini eruption. (45 hskp)
255. Óluva Ellingsgaard, 2009: Formation Evaluation of Interlava Volcaniclastic Rocks from the Faroe Islands and the Faroe-Shetland Basin. (45 hskp)

LUNDS UNIVERSITET

Geologiska institutionen
Centrum för GeoBiosfärsvetenskap
Sölvegatan 12, 223 62 Lund